universität wien

DISSERTATION / DOCTORAL THESIS

Titel der Dissertation /Title of the Doctoral Thesis

„Investigating the role of bilirubin in vivo and in vitro: effects on ageing, telomere length and other age-related biomarkers“

verfasst von / submitted by

Anela Tosevska

angestrebter akademischer Grad / in partial fulfilment of the requirements for the degree of

Doktorin der Naturwissenschaften (Dr. rer. nat.)

Wien, 2016 / Vienna, 2016

Studienkennzahl lt. Studienblatt / degree programme code as it appears on the student record sheet:	A 796 610 449
Dissertationsgebiet lt. Studienblatt / field of study as it appears on the student record sheet:	NAWI aus d. Bereich Lebenswissenschaften UG2002 (Dissertationsgebiet: Pharmazie)
Betreut von / Supervisors:	Univ.-Prof. Dr. Karl-Heinz Wagner Univ.-Prof. Dr. Verena Dirsch

INVESTIGATING THE ROLE OF BILIRUBIN *IN VIVO* AND *IN VITRO*: EFFECTS ON AGEING, TELOMERE LENGTH AND OTHER AGE-RELATED BIOMARKERS

ANELA TOSEVSKA

Anela Tosevska: *Investigating the role of bilirubin* in vivo *and* in vitro*: effects on ageing, telomere length and other age-related biomarkers*

A thesis submitted in partial fulfillment of the requirements for the degree of:

Ph.D.

at the

Research Platform Active Aging
Fakultät für Lebenswissenschaften
Universität Wien

© Juli 2016

ABSTRACT

Unconjugated bilirubin (UCB) is a product of haem metabolism, normally present in the bloodstream of healthy individuals at low concentrations. Mildly increased UCB has been implicated to be involved in human ageing and disease protection. Telomere attrition, on the other hand, is a well-established hallmark of ageing, commonly associated with the outbreak of age-related diseases.

The aim of this work is identifying a relationship between bilirubin and telomere length as a potential mechanism for the positive effects of increased UCB. To this end, we utilized samples and data from two human studies (original publications provided as chapters 3 and 5), as well as cultured primary human lymphocytes (chapter 4). The central method used in this work is a qPCR method for absolute telomere length measurement, whose optimization is described in detail in chapter 2.

The first publication encompasses a human study on age- and gender-matched cases with Gilbert's syndrome (GS) (n = 60) and healthy controls (n = 60). Gilbert's Syndrome is a condition of mild unconjugated hyperbilirubinaemia, convenient for studying the effects of UCB in humans. We could clearly observe an occurrence of longer telomeres in GS cases (mean difference = 0.78 kb, p = 0.031, paired samples t-test), potentially related to the antioxidant and immune-modulatory effects of UCB. Preliminary results from cultured human PBMCs could partly confirm these observations, as the extent of H_2O_2-induced oxidized guanine lesions in telomeres was reduced upon treatment with UCB.

The second publication in this work deals with a population of institutionalized elderly individuals from the Vienna Active Ageing Study (VAAS) where the relationship between UCB, circulating cell-free DNA and telomere length was investigated. Here we could again observe a trend for longer telomeres in individuals with higher UCB (Pearson r = 0.238, p = 0.051).

Cumulatively, this work reveals a novel possibility for the involvement of bilirubin in telomere dynamics and telomere biology, setting the grounds for further in-depth mechanistic studies.

ZUSAMMENFASSUNG

Unkonjugiertes Bilirubin (UCB) ist ein potenziell neurotoxisches Produkt des Häm Metabolismus, das bei einem Großteil der Bevölkerung in geringer Konzentration im Blut vorhanden ist. Trotz der neurotoxischen Eigenschaften von UCB in sehr hohen Konzentrationen, kann eine moderat erhöhte UCB Konzentration im Blut positive Effekte auf den Alterungsprozess und altersbedingte Erkrankungen haben. Als Indikator für die Zellalterung wird eine kurze Telomerlänge beschrieben. Diese Dissertation beschäftigt sich mit dem potentiellen Zusammenhang zwischen UCB und der Telomerlänge in Lymphozyten, um eine Erklärung für die alterspräventiven Eigenschaften von UCB zu finden. Grundlage dieser Arbeit sind die Ergebnisse von zwei Humanstudien (Kapitel 3 und 5) sowie die Ergebnisse der in-vitro Untersuchungen an primären, humanen Lymphozyten (Kapitel 4).

In Kapitel 2 dieser Arbeit wird die zentrale Methode zur Bestimmung der Telomerlänge mithilfe der qPCR detailliert beschrieben. Kapitel 3 beschäftigt sich mit der ersten Publikation, welche Daten einer Humanstudie an je 60 alters- und geschlechtsgematchten Personen mit und ohne Gilbert's Syndrome (GS) berücksichtigte. GS zeichnet sich durch einen leicht erhöhten UCB Spiegel im Blut aus, ein Effekt der in unserer Studie deutlich mit erhöhter Telomerlänge korrelierte (Mittelwert-Differenz: 0.78kb, p = 0.031).

In Kapitel 4 wird untersucht wie sich die antioxidativen und immunmodulatorischen Effekte von UCB auswirken könnten. Vorläufige Resultate von humane PBMCs in Zellkultur zeigen, dass Zellen die mit H_2O_2 behandelt wurden eine geringere Anzahl an oxidierten Guaninen in Telomeren aufweisen, sofern sie auch mit UCB behandelt wurden.

Die zweite Publikation in Kapitel 5 beschreibt Daten von Senioren der Vienna Active Ageing Study (VAAS) bei der Zusammenhänge zwischen UCB, extrazellulärer DNA und der Telomerlänge untersucht wurden. Auch hier konnte ein Trend nachgewiesen werden, dass Personen mit hohen UCB-Gehalten im Blut längere Telomere ausweisen (Pearson r = 0.238, p = 0.051).

Zusammenfassend konnte mit dieser Dissertation eine Rolle von Bilirubin in Telomerdynamik und Telomerbiologie sowohl in vitro als auch in vivo gezeigt werden, was als Basis für weitere Studien zu detaillierten molekularen Zusammenhängen genutzt werden kann.

PUBLICATIONS

Manuscripts and publications that are not subject of this thesis.

Bernhard Franzke, Barbara Schober-Halper, Marlene Hofmann, Stefan Oesen, Anela Tosevska, Trine Henriksen, Henrik E. Poulsen, Eva-Maria Strasser, Barbara Wessner, Karl-Heinz Wagner, and Vienna Active Ageing Study Group. **Age and the effect of exercise, nutrition and cognitive training on oxidative stress – the vienna active aging study (vaas), a randomised controlled trial**. Under review in *Plos One*, 2016.

Annemarie Grindel, Helmut Brath, Bianca Guggenberger, Lukas Eichberger, Christina Pöppelmeyer, Michaela Gschaider, Anela Tosevska, and Karl-Heinz Wagner. **Oxidative stress, dna damage and dna repair in female patients with diabetes mellitus type 2**. Under review in *Plos One*, 2016.

Christine Moelzer, Marlies Wallner, Carina Kern, Anela Tosevska, Ursula Schwarz, Rene Zadnikar, Daniel Doberer, Rodrig Marculescu, and Karl-Heinz Wagner. **All engines go: Features of an altered ampk metabolic pathway in Gilbert's Syndrome, and its role in energy turnover and metabolic health**. accepted for publication in *Scientific Reports*, 2016.

Bernhard Franzke, Barbara Halper, Marlene Hofmann, Stefan Oesen, Béatrice Pierson, Ariane Cremer, Evelyn Bacher, Birgit Fuchs, Andreas Baierl, Anela Tosevska, et al. **The effect of six months of elastic band resistance training, nutritional supplementation or cognitive training on chromosomal damage in institutionalized elderly**. *Experimental gerontology*, 65:16–22, 2015.

Bernhard Franzke, Barbara Halper, Marlene Hofmann, Stefan Oesen, Waltraud Jandrasits, Andreas Baierl, Anela Tosevska, Eva-Maria Strasser, Barbara Wessner, Karl-Heinz Wagner, et al. **The impact of six months strength training, nutritional supplementation or cognitive training on dna damage in institutionalised elderly**. *Mutagenesis*, 30(1):147–153, 2015.

Bernhard Franzke, Barbara Halper, Marlene Hofmann, Stefan Oesen, Heidemarie Peherstorfer, Klemens Krejci, Birgit Koller, Karin Geider, Andreas Baierl, Anela Tosevska, et al. **The influence of age and aerobic fitness on chromosomal damage in austrian institutionalised elderly**. *Mutagenesis*, 29(6):441–445, 2014.

ACKNOWLEDGMENTS

First and foremost, I would like to thank my supervisor, *Karl-Heinz Wagner*, for all the trust and support he provided me with during my PhD studies. He gave me the freedom to explore and build my own path, supported my decisions and gave me great advice on how to deal with challenges.

I would like to thank my co-supervisor *Verena Dirsch*, for always asking the right questions and making me think about everything more deeply. She offered her support whenever I needed it.

Some very important people for my reasearch and personal growth are all the trainees I had worked with. I want to thank *Izabela Goscianska, Milan Janosec, Ursula Schwarz, Immina Vierheilig and Nazlisadat Seyed Khoei* for helping me improve as a teacher and mentor.

This work would not have been possible without collaboration from the General Hospital in Vienna, as well as the Curatorship of Viennese Retirement Homes and its residents for taking part in the Vienna Active Ageing Study.

My group(s) and all the people I worked with had a very special role in my life during all these years. I want to thank *Christine Mölzer* who has shared all her knowledge and passion about bilirubin research with me in the long days of culturing cells and all the failed imaging experiments; *Annemarie Grindel*, who is not only great to work with, but is also a great friend and partner in crime in the hot July days when the Danube is much more enjoyable than the office; and thanks to *Dongdong Wang and Atanas Atanasov* for all the great work that came out from a single idea. It was great working with all past and present members of the Wagner lab, Dirsch lab and the Active Ageing Platform members. I additionally want to thank everyone at my two departments, pharmacognosy and nutritional sciences, for the relaxed and friendly working athmosphere.

I am very happy I had the opportunity to spend 6 weeks in *Michael Fenech*'s lab at CSIRO in Adelaide, where I learnt almost everything I know about working with DNA (special thanks to *Tina McCarthy*), and I met some wonderful people.

One of my greatest achievments is having good friends, from both my home countries, that make my life so much more diverse and full of memories.

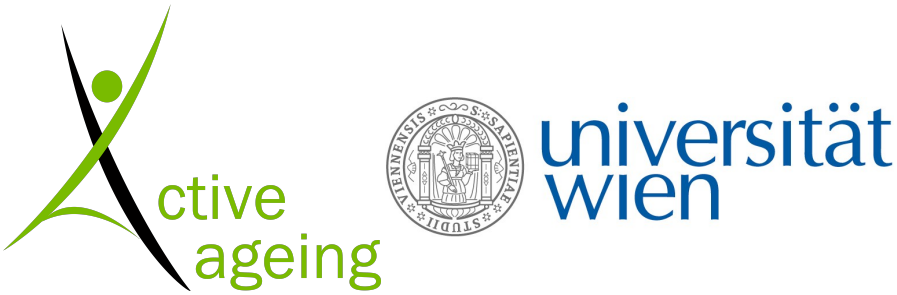
A very big thank you goes to my extended family, the people who had always believed in me and made me think I am smart enough to do this in the first place. Especially my closest ones: my mother *Marika Tosevska* who always encouraged me to fight my way through and my brother *Nikola Tosevski* who helped me whenever I needed help. And as in all big moments, I greatly miss my father *Mitko Tosevski* who

had left us way too early. I want to thank my Viennese family, especially *Doris Badelt and Walter Karban* for always taking care that things are running smoothly.

The greatest acknowledgement goes to the most important person in my life, who is at the same time giving me the harshest critique and the greatest laugh, *Stefan Badelt*. I have learned a lot from him; he has helped me immensely not only with this work, but with everything I do. *I dedicate this thesis to him.*

FUNDING

This work has been funded by the Research Platform Active Ageing at the University of Vienna.



CONTENTS

i INTRODUCTION 1

1 INTRODUCTION 3
- 1.1 Ageing . . . 3
- 1.2 Telomeres, telomerase and shelterin . . . 5
  - 1.2.1 Telomeres in ageing and disease . . . 6
- 1.3 Bilirubin . . . 8
  - 1.3.1 Haem metabolism and bilirubin . . . 8
  - 1.3.2 Bilirubin-related diseases . . . 9
  - 1.3.3 Bilirubin: the bad vs. the good . . . 10
- 1.4 Aims of the thesis . . . 13

2 METHOD OPTIMIZATION FOR ABSOLUTE TELOMERE LENGTH MEASUREMENT BY QPCR 15
- 2.1 Choosing a method for telomere length measurement . . . 17
- 2.2 DNA extraction . . . 19
  - 2.2.1 Qiagen DNeasy blood and tissue kit . . . 19
  - 2.2.2 PeqGOLD Blood DNA Mini Kit Plus . . . 20
  - 2.2.3 Bio&Sell . . . 20
- 2.3 DNA yield and quality assessment . . . 20
  - 2.3.1 Nanodrop 2000c . . . 20
  - 2.3.2 QuantiFluor®dsDNA System . . . 21
  - 2.3.3 Gel electrophoresis for quality assessment . . . 22
- 2.4 Results – DNA extraction . . . 23
- 2.5 qPCR analyses of telomere length . . . 24
  - 2.5.1 qPCR reagents, master mix and primers . . . 25
  - 2.5.2 Standards design and preparation . . . 26
  - 2.5.3 Calculation of telomere length . . . 28

ii PRELIMINARY, SUBMITTED AND PUBLISHED RESULTS 31

3 ORIGINAL ARTICLE 1 33
- 3.1 Supplementary material . . . 46

4 IN VITRO 59
- 4.1 In vitro experiments using primary PBMCs and bilirubin . . . 59
- 4.2 Oxidative damage in telomeres . . . 59
- 4.3 Methods . . . 60
  - 4.3.1 Solubilisation of Unconjugated Bilirubin . . . 60
  - 4.3.2 HPLC method for bilirubin concentration measurement . . . 60

4.3.3 PBMCs isolation and cultivation . . . 61
4.3.4 Storage of viable PBMC . . . 61
4.3.5 Cell count and viability . . . 62
4.3.6 Cultivation of human primary PBMCs . . . 62
4.3.7 Cellular uptake of UCB in PBMCs . . . 63
4.3.8 Cellular and nuclear uptake of UCB measured by *flow cytometry* 63
4.3.9 Oxidative stress and cell cycle analysis by flow cytometry . . . 64
4.3.10 An extended qPCR telomere assay for measuring oxidized guanine lesions in the telomere . . . 64
4.4 Results . . . 65
4.4.1 UCB solubility in different cell culture media . . . 65
4.4.2 UCB uptake, oxidative stress and cell cycle changes measured by flow cytometry . . . 66
4.4.3 Oxidized guanine lesions in the telomeric sequence . . . 68
4.5 Discussion and conclusions . . . 69
4.6 Acknowledgements . . . 71
5 ORIGINAL ARTICLE 2 75
5.1 Supplementary material . . . 107

iii CONCLUSION 115
6 CONCLUDING REMARKS 117
6.1 Future prospects . . . 118

BIBLIOGRAPHY 121

LIST OF FIGURES

Figure 1 The mammalian telomeric complex . . . 6
Figure 2 Haem matabolism . . . 9
Figure 3 DNA integrity . . . 22
Figure 4 Amplification plot Power SYBR . . . 26
Figure 5 Amplification plot SYBR Select . . . 27
Figure 6 Amplification plot telomere standards . . . 28
Figure 7 Amplification plot 36b4 standards . . . 29
Figure 8 Cellullar uptake of UCB, HPLC . . . 66
Figure 9 FBS-supplemented media, HPLC . . . 67
Figure 10 Serum free media, HPLC . . . 68
Figure 11 Cell viability . . . 69
Figure 12 Cellular uptake of UCB, flow cytometry . . . 70
Figure 13 Cell cycle analysis after treatment with UCB and H_2O_2 . . . 71
Figure 14 Fpg-sensitive lesions in the telomere, UCB and H_2O_2 . . . 72
Figure 15 Fpg-sensitive lesions in the telomere, UCB and H_2O_2 co-treatment 73

LIST OF TABLES

Table 1 Conjugated hyperbilirubinaemias . . . 10
Table 2 Unconjugated hyperbilirubinaemias . . . 11
Table 3 Methods for telomere length measurement . . . 16
Table 4 Dilution scheme . . . 22
Table 5 DNA extraction kits . . . 23
Table 6 Starting material for DNA extraction . . . 24

ACRONYMS

8-oxo-dG 8-oxo-7,8-dihydroguanine

ALT alanine aminotransferase

AST aspartate aminotransferase

BER base excision repair

BSA bovine serum albumin

cDNA complementary DNA

DCFH-DA dihydrofluorescein diacetate

DDR DNA damage response

DMSO dimethyl sulfoxide

DSB double-strand break

dsDNA double-stranded DNA

FBS foetal bovine serum

Fpg formamidopyrimidine [fapy]-DNA glycosylase

FRAP ferric reducing ability of plasma

GGT gamma-glutamyl transferase

GS Gilbert's Syndrome

HPLC high-performance liquid chromatography

HR homologous recombination

NHEJ non-homologous end joining

PBMC peripheral blood mononuclear cell

PBS phosphate-buffered saline

Q-FISH quantitative fluorescence *in situ* hybridization

qPCR quantitative polymerase chain reaction

ROS reactive oxigen species

SFM serum free media

T2DM type 2 Diabetes Mellitus

TRF terminal restriction fragment

UCB unconjugated bilirubin

Part I

INTRODUCTION

1 INTRODUCTION

1.1 AGEING

Ageing is a multicomponent decline in bodily function, with decreased fertility and increased morbidity and mortality [McLean and Le Couteur, 2004]. It has been one of the most extensively studied biological phenomena, subject to a number of hypotheses throughout the years. Most of these hypotheses share common hallmarks such as oxidative stress, mitochondrial damage and apoptosis, as well as DNA damage, mutagenesis and telomere attrition [Richardson and Schadt, 2014; Monickaraj et al., 2013; López-Otín et al., 2013; Demissie et al., 2006].

The current consensus is that ageing is a result of many simultaneous changes occurring over time and an accumulation of their effects [López-Otín et al., 2013; Richardson and Schadt, 2014]. While chronological age can be measured in years since birth of an organism, it is much more difficult to estimate the "real" biological age [Belsky et al., 2015]. This corresponds to the organism's fitness, survivability and resistance to age-associated diseases. In absence of clear indicators of biological ageing, relative measures, so called biomarkers, are used. In a clinical setting it is common practice to use metabolic biomarkers to estimate the health status of an individual. As humans age, the metabolic signature also changes, leading researchers to use a clinical pattern of metabolic changes as an indicator of accelerated ageing and disease risk. A common practice is to use changes in cholesterol levels, cholesterol subfraction ratios, levels of oxidated or glycated macromolecules and many more. While all these markers can somewhat predict a disease risk, they are often unreliable, influenced by medication and lifestyle changes and do not reflect the long-term dynamics of an organism. A second group of emerging biomarkers of ageing are molecular markers, the most prominent of which is telomere length discussed in more detail in section 1.2.

While some individuals experience a plethora of age-associated diseases and disabilities already at mid-life, others survive well into their eighties and nineties with just mildly impaired abilities. Inheritable factors and environmental influences are commonly contributing to the ageing phenotype associated to an individual. Lifestyle factors, such as nutrition, exercise, smoking or psychological stress are implied to highly influence an individual's healthy ageing [Duncan et al., 2014; Haveman-Nies et al., 2003]. Nonetheless, there is still a long way to go in defining all possible external and internal influences and their exact effects on the ageing process.

As mentioned before, one of the many hallmarks of ageing is an accumulation of damage in the DNA [Franzke et al., 2014; Cooke et al., 2003]. What does this mean? To simplify the main cellular processes: genetic code is stored in DNA, which is transcribed to messenger RNA to carry the information to the ribosomes where the code dictates protein synthesis. However, in reality, there is much more going on and the entire process is supplemented by a plethora of regulatory molecules, from RNA and proteins to small molecules and ligands and even radicals that react with macromolecules to modify their structure. Each process can be considered as a separate layer of information that is added to the final product, in this case, a protein. Hence, in order to get a product which is fully functional, a cell must ensure adequate quality control at each step of the process. Here, I will only focus at the first stage of the process that conserves the genetic information encoded in DNA.

The genetic code in DNA is built up from a combination of four bases (A, C, T and G) whose sequence defines the sequence of a protein they encode for. A second layer is added by epigenetic mechanisms, which consist of modifications in individual bases of DNA (most commonly cytosines) or DNA-associated proteins, such as histones. The second layer regulates which parts of the coding genome will be transcribed at a certain time in a particular cell. As such, it is very appealing for future studies that go beyond the scope of this thesis. The basic DNA sequence is, however much more rigid, and changes are more likely to occur during cell replication than when the cell is in a nonproliferative state. If errors in replication lead to mutations in the original sequence and such errors occur stochastically, there is higher likelihood that more mutations will accumulate with more divisions a cell undergoes. On the other hand, external factors such as UV or gamma irradiation, chemicals or cigarette smoke can induce DNA damage independently of the cell's replicative state [Cooke et al., 2003].

The cell has developed protective mechanisms that do not allow too many errors to be passed on to the next generation of cells: the DNA damage response (DDR) and repair machinery. Proteins responsible for DDR are recruited at sites of injury in the DNA, caused either by an external or internal influence. Endogenously provoked lesions in the DNA can range from oxidation, deamination of cytosine or depurination, whereas external factors are usually responsible for double strand breaks in the DNA [Ciccia and Elledge, 2010]. Oxidized lesions occur frequently, especially at guanosine sites and are recognised by specific DNA glycosilases. DNA double-strand breaks (DSBs) can be repaired by three distinct mechanisms: homologous recombination (HR), non-homologous end joining (NHEJ) and alternative NHEJ. Some aspects of these repair pathways will be discussed in more detail in the following chapters, especially those implicated in telomere signalling or maintenance [Kruk et al., 1995].

1.2 TELOMERES, TELOMERASE AND SHELTERIN

Telomeres are nucleoprotein structures at the end of eukaryotic linear chromosomes. They consist of tandem DNA repeats, in humans and most mammalian species bearing the sequence TTAGGG. Since their discovery in the ciliate *Tetrahymena*, extensive research has been done to elucidate the role and dynamics of these structures [Blackburn et al., 2006; Blackburn and Gall, 1978]. Their main role is protection from chromosome deterioration or fusion with neighbouring chromosomes, hence, maintenance of chromosomal stability. Nonetheless, novel findings indicate additional telomeric roles arise from their complex structure. A telomere position effect (TPE), for instance is a mechanism for transcriptional regulation of genes located adjacent to the telomere in the so-called subtelomeric region [Robin et al., 2014]. Additionally, the transcriptional product of telomeres, a group of long non-coding RNAs called TERRAs (telomeric repeat-containing RNAs) have multiple roles in the DDR mechanism and cell integrity [Cusanelli and Chartrand, 2014].

The interest in telomere research increased drastically with the implication of telomere shortening with cell division [Levy et al., 1992]. After each mitotic event cells lose approximately 50-200 kb telomeric DNA, due to the asymmetric DNA replication called the end-replication problem. As the unique rule of unidirectional replication, telomeres cannot be fully processed by DNA polymerase on the 5′ end of the lagging strand [Levy et al., 1992]. The inability of DNA polymerase to replicate telomeres is normally compensated by an enzyme called *telomerase*. Telomerase is generally expressed at a very low level in adult cells and tissues. As a result, telomeres cannot be fully replicated leading to a loss of telomeres with each cell division. This naturally limits the number of cell divisions a cell can undergo, a phenomenon called the Hayflick limit [Shay and Wright, 2011].

TELOMERASE is a reverse transcriptase playing a central role in telomere maintenance. It was first described in the organism *Tetrahymena* [Blackburn et al., 2006]. It consists of two components, an RNA component called TERC that serves as a template for de novo synthesis and an enzymatic protein component called TERT. Telomerase is usually not expressed in adult somatic cells, with some exceptions. For instance, telomerase is upregulated in lymphocytes upon mitogen stimulation. Other highly proliferative mature cells have also retained telomerase activity [Greider, 1998]. This is also true for many different types of cancer cells that need an unlimited potential for cell division in order to maintain their invasiveness [Shay and Wright, 2011].

Apart from regenerating the chromosomal ends, telomerase has been implicated in other cell activities. Its mitochondrial localisation has been related to apoptosis

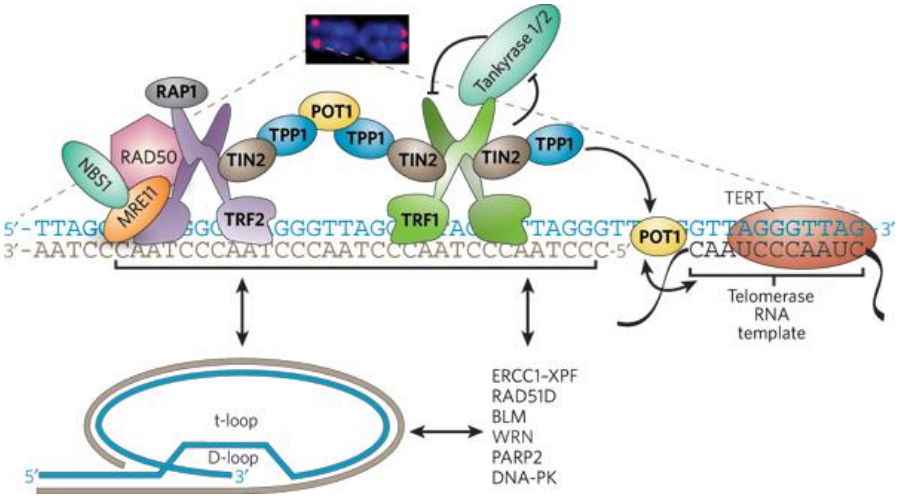


Figure 1: The mammalian telomeric complex. Adapted by permission from Macmillan Publishers Ltd: Nature [Verdun and Karlseder, 2007], copyright 2007.

and reactive oxigen species (ROS) production whereas in the nucleus TERT has been implicated in regulation of gene transcription [Chiodi and Mondello, 2012; Martínez and Blasco, 2011]. The RNA component, TERC, has been shown to inhibit apoptosis independently of its telomeric role [Gazzaniga and Blackburn, 2014].

Intact genomic DNA is crucial for species development and survival and it is of great importance to have it properly maintained by the DDR machinery. As telomeres are located at the end of chromosomes, they have to be distinguished from double strand breaks that occur within chromosomes. To accomplish this, telomeres are capped by a protein complex called *shelterin* that has been described in the late 90ties and early 2000s [De Lange, 2005]. In humans this complex comprises of 6 proteins: TRF1, TRF2, TIN2, POT1, TPP1 and RAP1 (figure 1). In the context of telomere binding and protection, TRF1 and TRF2 are both directly bound to the telomere double helix, POT1 binds to the single-stranded 3′ overhang of the telomere whereas RAP1, TIN1 and TPP1 serve as connectors between TRF1 and TRF2. Similar to telomerase, these proteins carry a number of extratelomeric roles, in addition to their specialized telomeric roles [Martínez and Blasco, 2011].

1.2.1 *Telomeres in ageing and disease*

As explained in the previous section, loss of telomeric DNA occurs progressively as the adult cells age. This is limited only by reaching a critical point, when shelterin components can no longer protect the telomeric DNA string, thus exposing a bare uncapped telomere. This exposure recruits a signalling cascade that can change the

fate of the affected cell. Several processes can be initiated by critically short telomeres, such as senescence, apoptosis or malignancy [Gobbini et al., 2014]. On the other hand, telomere uncapping does not always require critically short telomeres [Morgan et al., 2013].

Telomere length has been extensively used as an ageing biomarker, especially in human studies. However, this has proven rather difficult, especially since "telomeric age" does not always reflect actual chronological age. In addition to the normal, physiological telomere shortening, numerous studies have shown accelerated telomere shortening in non-communicable age-associated diseases. Here there is a consensus that generally shorter telomeres are associated with worse disease progression [López-Otín et al., 2013]. However, most studies are designed in a way that makes is hard to conclude a cause-effect relationship between the disease progression and telomere shortening.

Conditions caused by inherited defects in the telomere maintenance machinery, named telomeropathies, are rare and manifest with an entire spectrum of symptoms [Holohan et al., 2014]. The most widely studied telomeropathies are dyskeratosis congenita and aplastic anaemia. A common trait for these diseases are drastically shortened telomeres even though the symptoms are usually not progeria-like and differ from one case to another. In both cases, highly proliferative tissues and organs are commonly affected [Savage and Alter, 2009].

Short telomeres have been found in a range of diseases which are not primarily associated to telomere maintenance dysfunction. Haycock et al. [2014], for instance, have found an inverse association between telomere length in leucocytes and risk of coronary heart disease (CHD), independent of conventional vascular risk factors. Shorter telomere length measured by TRF associated with an increased risk of myocardial infarction and stroke [Fitzpatrick et al., 2007]. Furthermore, Strazhesko et al. [2015] have described a relationship between telomere length, insulin resistance and arterial stiffness even in individuals free of CVDs.

There has been evidence that short leucocyte telomere length is associated with twofold risk for type 2 Diabetes Mellitus (T2DM) [Zhao et al., 2014]. A recent prospective study combined with meta-analysis has concluded that there is an independent association between short leucocyte telomere lengths, without implying causality [Willeit et al., 2014]. Additionally, diabetes complications have been associated with short telomere length [Testa et al., 2011]. Kuhlow et al. [2010] have shown that telomerase deficiency in mice can impair insulin secretion, proposing this as one of the mechanisms for age-related increase in T2DM.

The role of telomeres and telomerase in cancer is perhaps, the most extensively studied one, and at the same time the most complex [Shay and Wright, 2011]. While the general consensus is that critically short telomeres associate with cancer [Ma et al., 2011; Marchesi, 2013; Swiggers et al., 2006], studies have reported that this is not always the case [Walsh et al., 2014; Zhang et al., 2015]. Furthermore, telomerase is re-expressed in a large number of cancer tissues, at a sufficient level for telomere maintenance [Greider, 1998; Lu et al., 2011]. Still a number of cancers do not exhibit telomerase activity; instead they maintain their telomeres using a so called ALT- alternative lengthening of telomeres mechanism [Dilley and Greenberg, 2015].

1.3 BILIRUBIN

1.3.1 *Haem metabolism and bilirubin*

Haem is a heterocyclic organic molecule, from the class of porphyrins or tetrapyrrols, containing a ferrous Fe^{2+} ion in the center. Porphyrins are cofactors of many important enzymes, and are present in the entire kingdom of life. The most abundant naturally occurring pigment in animals is haem, an essential component of haemoglobin and a number of physiologically important haemoproteins [Chen, 2007].

The detailed biochemistry behind haem biosynthesis has been described by Heinemann et al. [2008]. Here I will focus more attention to haem catabolism, which is ultimately the pathway for bilirubin biosynthesis. It is interesting, taken the recycling behaviour of many molecules in the human body, that haem cannot be recycled from its catabolic end products biliverdin and bilirubin. The biosynthesis of haem starts in the mitochondria of hematopoietic cells in the bone marrow.

1.3.1.1 *Haem catabolism*

Erythrocytes have a lifespan of about 100-120 days in human, after which they become senescent and are removed by the reticuloendothelial system [Franco, 2012]. Hemoglobin and other hemoproteins release two main components upon degradation: a protein component, which is further converted into amino acids that can be recycled, and haem. Haem releases the bound Iron, at which point it is named haemin. This occurs primarily in the macrophages and cells of the reticuloendothelial system. The resultant haemin is a potent oxidant, and as such, can be damaging to cells and tissues. Hence, its quick removal from the system is advantageous. This is accomplished by a series of ATP-dependent enzymatic reactions converting the haemin into, initially biliverdin, and then bilirubin [Ryter and Tyrrell, 2000].

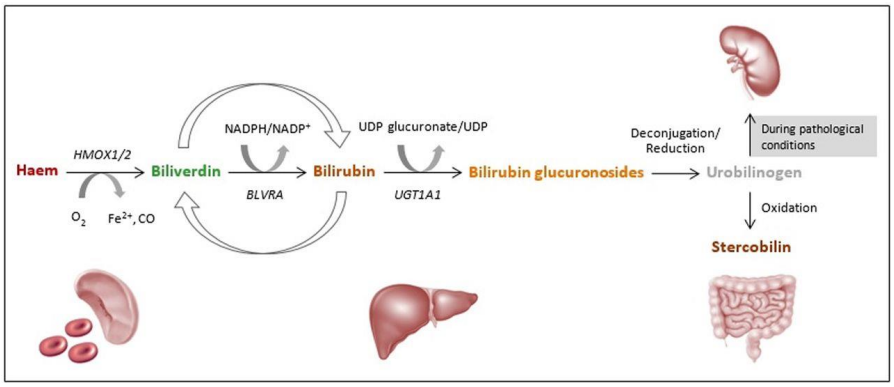


Figure 2: Haem catabolism; intermediate and final products and enzymes involved in the process. Adapted with permission from Wagner et al. [2015].

The first transition, from haem to biliverdin is catalysed by a group of isoenzymes called haem oxygenases (HO) the most prominent being HO-1 and HO-2. While HO-2 is constitutively expressed, HO-1 is the inducible form of the enzyme which is expressed following a stress stimulus. Certain conditions leading to an increase of oxidative stress can lead to upregulation of HO-1 and an increase in haem degradation. The product of this reaction is the "green pigment" biliverdin. Biliverdin is water-soluble, linear tetrapyrrol. Figure 2 shows the enzymes involved in this process, as well as where each step occurs in the body [Wagner et al., 2015]. However, the rate-limiting enzyme in bilirubin excretion is UGT1A1. The UGT1A gene locus, located on chromosome 2q37, is complex; it encodes multiple genes and pseudo genes, and alternatively spliced isoforms also exist [1].

Evolutionary, the bilirubin-producing pathway of haem metabolism has appeared later on, and it is present only in mammals. Interestingly, the lack of bilirubin production overlaps with the erythrocyte nucleation, as in birds, amphibians and reptiles. This could be an indicator that bilirubin has developed as a result of evolution. For a long time, it has been unclear why bilirubin is being produced in the first place. This question has been revisited as the antioxidative properties of bilirubin were discovered. Some hypothesized that the bilirubin pathway has developed in mammals as an efficient way to excrete haem metabolites from a foetus to his mother via the placenta [Seppen and Bosma, 2012]. Namely, while biliverdin is incapable in crossing the placenta, bilirubin can do so rather efficiently. However, bilirubin in its native, unconjugated form is highly hydrophobic. In order to be transported through the circulation, unconjugated bilirubin (UCB) binds to albumin in irreversible manner. Albumin-UCB binding is an efficient way of transporting and relocating UCB from the circulation to the intracellular space [Jacobsen and Brodersen, 1983].

1 http://www.ncbi.nlm.nih.gov/books/NBK294473/

1.3.2 *Bilirubin-related diseases*

An increase in bilirubin concentrations in newborns is a fairly common occurrence, especially in preterm infants, and if not treated correctly can lead to neurotoxicity and irreversible brain damage [Watchko and Tiribelli, 2013]. In adults, icteric symptoms and increased blood and tissue accumulation of bilirubin can indicate liver failure or bile obstruction. Routine clinical tests are performed in order to evaluate possible liver damage, measuring serum levels of liver enzymes such as aspartate aminotransferase (AST), alanine aminotransferase (ALT) or gamma-glutamyl transferase (GGT). However, in some cases, increased bilirubin levels are not accompanied by a liver disease. Inherited disorders in bilirubin metabolism can lead to an accumulation of excess in both unconjugated and conjugated forms of bilirubin.

Dubin-Jonson and Rotor Syndrome are characterized by increase in predominantly conjugated bilirubin. Both are rare and benign conditions. Some characteristics are shown in table 1.

	Dubin–Johnson Syndrome	**Rotor Syndrome**
Serum bilirubin	Predominantly conjugated, usually 50–85 M, can be as high as 340 M	Predominantly conjugated, usually 50–100 M, occasionally as high as 340 M
Routine liver function tests	Normal except for hyperbilirubinemia	Normal except for hyperbilirubinemia
Serum bile salt levels	Normal	Normal
Plasma bromsulfophthalein (BSP) retention	Normal at 45 min; secondary rise at 90 min	Elevated; but no secondary rise at 90 min
Plasma BSP clearance	T_{max} is very low; storage is normal	Both T_{max} and storage are reduced
Oral cholecystogram	Usually does not visualize the gallbladder	Usually visualizes the gallbladder
Urinary coproporphyrin excretion pattern	Total—normal; >80% as coproporphyrin I	Total—elevated; ~50–75% coproporphyrin I
Appearance of liver	Grossly black	Normal
Histology of liver	Dark pigments, predominantly in centrilobular areas; otherwise normal	Normal, no increase in pigmentation
Mode of inheritance	Autosomal recessive	Autosomal recessive
Prevalence	Rare (except in Middle Eastern Jews: 1 in 1,300 births)	Rare
Prognosis	Benign	Benign
Animal model	Mutant TR⁻ rats/mutant Corriedale sheep/golden lion Tamarin monkey	None

Table 1: Predominantly conjugated hyperbilirubinaemias. Adapted with permission from Chowdhury and Chowdhury [2001].

Crigler-Najjar and Gilbert's Syndrome, on the other hand, are characterized by mutations in the UGT1A1 enzyme and are conditions of predominantly unconjugated hyperbilirubinaemia. Crigler-Najjar is very rare and life threatening unless treated. Characteristics are given in table 2.

Gilbert's Syndrome (GS) is the most common of all conditions associated to bilirubin metabolism. Its prevalence is strongly dependent on ethnicity, as different ethnic populations have different variants in *UGT1A1* that lead to the same phenotypical outcome.

It is estimated that the phenotype is present at around 5-10% in Western Europeans [Claridge et al., 2011], even though many cases remain undetected.

	Crigler–Najjar Syndrome Type 1	Crigler–Najjar Syndrome Type 2	Gilbert Syndrome
Liver function tests other than serum bilirubin and liver histology	Normal	Normal	Normal
Serum bilirubin concentrations	20–50 mg/dL (340–850 M)	7–20 mg/dL (120–340 M)	Normal to 5 mg/dL (<85 M)
Pigments excreted in bile	Small amounts of unconjugated bilirubin and only traces of bilirubin glucuronides	Reduced proportion of bilirubin diglucuronide	Reduced proportion of bilirubin diglucuronide
Hepatic bilirubin-UGT activity	Virtually absent	Markedly reduced but detectable	Reduced to about 30% of normal
Effect of phenobarbital administration	No significant reduction of serum bilirubin levels	Reduction of serum bilirubin levels by >25%	Normalization of serum bilirubin
Inheritance	Autosomal recessive	Autosomal recessive	Autosomal recessive
Molecular basis	Genetic lesions within the coding region or at splice sites of *UGT1A1*	Point mutations within the coding region of *UGT1A1*	Insertion of a TA dinucleotide within the TATAA element of *UGT1A1*[a]
Prevalence	Rare (<1:1,000,000)	Rare (<1:1,000,000)	Phenotype in ~4% of the population; among Caucasians and Africans, ~9% are homozygous for the genotype (less common in Japan)
Prognosis	Kernicterus, unless vigorously treated; currently, liver transplantation is the only curative treatment	Kernicterus is uncommon, but has been reported	No encephalopathy; increased intensity of neonatal jaundice; toxicity of some drugs may be increased
Animal model	Gunn rat	—	Bolivian subpopulation of squirrel monkeys

[a]Some mutations of the coding region of UGT1A1 may be associated with serum bilirubin levels that overlap with the range seen in Gilbert syndrome (Table 20.3).
UGT, uridine-diphosphoglucuronate glucuronosyl-transferase.

Table 2: Predominantly unconjugated hyperbilirubinaemias. Adopted with permission from Chowdhury and Chowdhury [2001].

1.3.3 *Bilirubin: the bad vs. the good*

Bilirubin has long been considered a redundant byproduct of haem catabolism and potentially toxic if present in high concentrations in human serum. In contrast, mildly elevated bilirubin levels, characteristic of GS, are considered beneficial and have been inversely correlated with CVDs and the onset of metabolic syndrome [Schwertner and Vítek, 2008; Vitek et al., 2002]. Mechanistically, this double nature of bilirubin is attributed to its concentration-dependent pro- or anti- oxidant capacity [Boon et al., 2012; Bulmer et al., 2008]. As a potent antioxidant, bilirubin could have implications in a number of physiological and pathophysiological processes [Stocker et al., 1987]. To summarize some of the most important studies delineating cardiovascular effects of bilirubinone can refer to Wagner et al. [2015]. The interest in this topic started as Schwertner et al. [1994] have reported increased bilirubin concentrations to be inversely correlated to coronary artery disease (CAD).

Apart from its cardiovascular implications, bilirubin has been investigated in the context of metabolic diseases, especially T2DM. The risk for development of T2DM in healthy Korean men has been reduced with higher serum bilirubin [Jung et al., 2014], and there was an inverse associations of serum bilirubin with high sensitivity C-reactive protein, glycated haemoglobin, and the prevalence of T2DM in middle-aged and elderly Japanese individuals [Ohnaka et al., 2010]. Further studies support these findings [Benton et al., 2015].

Other studies have shown reduced serum bilirubin levels in cancer [Lacko et al., 2010] nonalcoholic fatty liver disease [Kwak et al., 2012], osteoporosis [Bian et al., 2013], and even schizophrenia [Vitek et al., 2010], and multiple sclerosis [Peng et al., 2011]. An involvement of higher serum bilirubin, especially the unconjugated portion present in GS, has also been linked to reduced mortality risk. Horsfall et al. [2013] have estimated the mortality in GS compared to control individuals and found a significantly decreased risk for all-cause mortality in individuals with GS. The same authors have also found a decreased risk of cardiovascular mortality in a statin-related cohort [Horsfall et al., 2012] and chronic obstructive pulmonary disease (COPD) and respiratory disease [Horsfall et al., 2011].

Even though this represents only a small fraction of all available studies, mechanistic studies are still lacking. An increased number of studies *in vitro* or in animal models are under way, in attempt to establish a more informative view on the causal role between bilirubin and human disease.

1.4 AIMS OF THE THESIS

This thesis looks at both telomere length and bilirubin, from the perspective of human ageing. Although a number of studies have been investigating at the connection of bilirubin with commonly known age-associated diseases, there have been no published data on bilirubin and telomere length. Therefore this thesis aims to:

1. establish and optimize a qPCR method for telomere length analysis in extracted DNA (Chapter 2);
2. compare telomere length in peripheral blood mononuclear cells (PBMCs) of individuals with Gilbert's Syndrome and healthy controls [Tosevska et al., 2016] (Chapter 3);
3. tackle the antioxidative properties of unconjugated bilirubin as a possible mechanism for telomere length maintenance in Gilbert's Syndrome (Chapter 4);
4. challenge the results from Chapter 3 in a cohort of elderly institutionalized individuals; explore further molecular markers related to unconjugated bilirubin and telomere length in the elderly (Chapter 5)

2

METHOD OPTIMIZATION FOR ABSOLUTE TELOMERE LENGTH MEASUREMENT BY QPCR

The ability of measuring telomere length has been invaluable for ageing research. A variety of methods exist for this purpose; the most common ones are summarized in table 3 [Montpetit et al., 2014]. Each method has its strengths and weaknesses and each of them can be specifically used for different applications. It is important to choose the method according to the question that needs to be answered, the nature and size of samples and the available instrument. Here I briefly present the most commonly used methods: terminal restriction fragment (TRF), quantitative fluorescence *in situ* hybridization (Q-FISH) and quantitative polymerase chain reaction (qPCR).

Southern blot – Terminal Restriction Fragment (TRF)

Historically, this has been the most prominent method for telomere length analyses, and it is still the method most commonly used, especially with small number of samples. It uses a southern blotting technique, and relies on the ability of restriction enzymes to cut DNA at specific points called restriction sites. As the telomeric sequence itself lacks such restriction sites, sites present in the subtelomere are being utilized instead. This results in intact DNA fragments containing and entire telomeric sequence in addition to an unknown residue of subtelomeric sequence. A probe specific for the telomeric sequence is used, and the detection can be carried out as the probe is radioactively labelled or conjugated to a tag molecule. A detailed protocol for this method has been described by Kimura et al. [2010].

This method is considered to be "the gold standard" and the most reliable among other methods. Additionally, it is highly reproducible and allows for comparison of results from different studies and different labs. However, this method has a number of disadvantages. First, it overestimates the real telomere length, as there is always a flanking subtelomeric portion attached to the measure telomeric sequence. Second, it cannot estimate single-cell or single-chromosome telomere length as it only gives an average value. Additionally, it requires a large amount of starting material, it is lengthy and labour intensive, making it rather low-throughput. It is the method of choice for cancer cell line studies with small number of samples and greater differences between samples.

Method	Advantages	Limitations
TRF	• "Gold standard"[a] • Numerous studies for comparisons • Does not require specialized equipment	• Requires large (>1µg) amount of DNA • Labor intensive • Subtelomeric polymorphisms can impact data • Provides mean length measure, but not recognition of individual short telomeres or ends lacking a telomere
qPCR MMqPCR aTLqPCR	• Can use small (ng) amounts of DNA • Less labor intensive • Referenced to standard single copy gene • Multiplex controls for DNA amount added	• Variation between and within "batches" • Reference standards lacking • Requires qPCR equipment • Does not provide absolute kilobase length estimate unless coupled with standard oligo[b] • Provides mean length measure, but does not allow recognition of individual short telomeres or ends lacking a telomere
STELA	• Allows for detection of critically short telomeres • Does not require viable cells • Does not require specialized equipment	• Only provides information for a small subset of specific chromosome ends • Does not provide mean telomere data • Does not recognize ends lacking a telomere • Limited in ability to detect long telomeres • Labor intensive
Q-FISH	• Can identify single telomere changes (higher resolution) • Can assess telomere lengths in specific cell types • When used on metaphase chromosomes, can identify individual telomeres (long or short), signal free ends, end-to-end telomeres, and a mean telomere length measure	• Labor intensive • Requires high skill level for chromosome assessment • Requires microscope (typically fluorescent) • "Length" expressed as relative fluorescence unit (often compared to standard [centromeric] value • Requires mitotically active cells for metaphase chromosomes, but not for interphase nuclei
PRINS	• Can identify single telomere changes (higher resolution) • Can assess telomere lengths in specific cell types • When used on metaphase chromosomes, can identify individual telomeres (long or short), signal free ends, end-to-end telomeres, and a mean telomere length measure	• Labor intensive • Requires high skill level for chromosome assessment • Requires microscope (typically fluorescent) • "Length" expressed as relative fluorescence unit • PCR efficiency can contribute to variability and can negatively impact accuracy • Requires mitotically active cells for metaphase chromosomes, but not for interphase nuclei
Flow-FISH	• Can determine mean "length" for specific cell populations • When coupled with antibodies can provide cell type specific information • Potential for automation	• Labor intensive • Requires high skill level • Requires flow sorting equipment • "Length" expressed as relative fluorescence unit • Provides mean length measure, but not recognition of chromosome-specific individual short telomeres or ends lacking a telomere
HT Q-FISH	• Allows recognition of short telomeres and mean telomeres • Can provide estimates for specific cell populations	• Does not recognize telomere-free ends or chromosome-specific lengths • Requires confocal microscope; length expressed as relative fluorescence unit

Note. aTL = Absolute telomere length. DNA = Deoxyribonucleic acid. HT Q-FISH = High throughput quantitative fluorescence in situ hybridization. kb = kilobase. MMqPCR = Monochrome multiplex quantitative polymerase chain reaction. qPCR = Quantitative polymerase chain reaction. STELA = Single Telomere Length Analysis, Universal STELA. TRF = Terminal restriction fragment. PRINS = Primed in situ subtype of Q-FISH. Q-FISH = Quantitative fluorescence in situ hybridization.

[a] This 'gold standard' is used as a reference when comparing advantages and disadvantages of alternative telomere length assays.

[b] O'Callaghan & Fenech, 2011.

Table 3: Methods for measurement of telomere length. Table reused with permission from Montpetit et al. [2014].

Quantitative Fluorescence in Situ Hybridization Q-FISH

Quantitative *in situ* hybridization is an improvement of the classical *in situ* hybridization method, where cells are labelled with fluorescent probes in order to detect DNA (or RNA) sequences of interest [O'Sullivan et al., 2005]. If performed on chromosomes in metaphase, this technique can provide information about the length of individual telomeres as well as atelomeric chromosomes. However, this technique requires living cells and is very labour intensive.

Quantitative Polymerase Chain Reaction qPCR

The first efficient qPCR method for telomere length analysis has been developed by Cawthon [2002]. Since then a number of modifications have been published, most notably the monochrome multiplex qPCR method [Cawthon, 2009] and the absolute qPCR method for telomere length measurement [O'Callaghan and Fenech, 2011]. The disadvantages of this method are similar to the TRF, that is, only the average telomere length in a population of cells can be estimated. In addition, qPCR is a highly sensitive method which is both an advantage and a disadvantage. On one hand, it can detect even minor differences in telomere length, but on the other, it can be easily affected by technical errors and inconsistencies.

2.1 CHOOSING A METHOD FOR TELOMERE LENGTH MEASUREMENT

The previous chapter gave a summary on the most relevant methodology used for telomere length analysis. In order to choose an appropriate method one must set up a step by step assessment of the research goals and answer the following points:

1. What is being measured?
2. What is the starting material?
3. How much starting material is available?
4. What kind of infrastructure is available in the laboratory?
5. What is the long-term goal of the project?

The first thing to determine is whether one is interested in capturing single-cell single-telomere length or only a mean measure from a population of cells. Often studies are limited in the type or amount of material that can be used. Human studies are usually more restricted, especially observational studies. The most commonly used material is blood or buccal mucosa, both materials consisting of a large number of

cell varieties. Additionally, the amount of available sample can be restricted due to ethical or other reasons. Taking all these limitations into consideration, we have chosen a qPCR method for absolute telomere length measurement as a method of choice. The main goal was to establish this method as a long term solution aiming to satisfy the requirements of the projects presented in this work and other similar side-projects. The advantage of this method, compared to the other methods, is that it is easily transferable, requires a very small amount of test material and due to the use of external standards the comparability between experiments is possible. Moreover, this method is very sensitive and can detect very small differences in telomere content between samples.

When performing a human study over a long time-period it is essential to keep a high level of reproducibility and use appropriate controls. Two possibilities exist when measuring these samples over a prolonged time period: a) freezing the starting material before DNA extraction, then extracting DNA from all samples simultaneously or over the course of a few hours/day followed by simultaneous measurement; b) extracting DNA from fresh material, then storing the extracted DNA for simultaneous measurement of the samples; c) extracting DNA from fresh material and performing the measurement on freshly extracted DNA samples. In order to find an optimal and flexible approach to sample preparation, without losing quality, these approaches were tested and the results compared.

The next step was choosing materials and reagents, such as commercially available kits or in-house established protocols. Again, the key factor here is the consistency in the used materials, and often, commercially available kits are superior in this regard.

The design of the qPCR assay was the last important point of consideration. Older real time qPCR cyclers, typically contained a heating block in a 96-well format. This is enough for a low-scale experiment without putting too much consideration into inter-assay variability. In any case, it is helpful to consider the intra-assay variability since, as mentioned earlier, qPCR is a very sensitive method. Technical errors, especially pipetting errors can occur, hence, using technical replicates to account for intra-assay variability is highly recommended. For large-scale experiments where samples are run on more than one plate and over a long time period, a control sample must be included in each assay, to provide information on the comparability of the assays.

This chapter describes the entire procedure starting with sample preparation, DNA extraction, quality assessment and concentration measurement and qPCR measurement. The findings are reported in the results section, and a general guideline is presented in the discussion section.

2.2 DNA EXTRACTION

High-quality unsheared genomic DNA is the most essential prerequisite for reliable downstream analysis [Fernandez-Jimenez et al., 2011]. High throughput sampling requires reproducibility and robustness in the method used. Hence, for our studies, the use of a commercial kit-based assay was advantageous over the classical phenol-chloroform extraction method. Initially three commercial kits were compared and DNA was extracted from human whole blood as a starting material. The kits were evaluated after spectrophotometric analysis and according to the final yield of purified DNA as well as the absorbance ratio at 260nm:280nm as an indicator of sample purity. The procedures for each kit separately are described in detail in the following sections.

2.2.1 *Qiagen DNeasy blood and tissue kit*

100 µl fresh whole blood in a 1.5 ml microcentrifuge tube was used for DNA extraction, as recommended in the manufacturer's handbook[1]. The volume was adjusted to 200 µl using sterile PBS and 20 µl Proteinase K was added to each sample in order to disrupt cellular proteins. Cell lysis buffer (AL buffer) at 200 µl was added, and the samples were mixed vigorously using a vortex, in order to get a homogeneous mixture. Samples were incubated at 56°C in a water bath for 10 minutes in order to lyse cells and protein and release intact DNA. Following incubation, DNA was precipitated from solution by addition of 200 µl 96-100% ethanol. The mixture was quickly transferred to a DNeasy Mini spin column and centrifuged at 8000 rpm for 1 minute at room temperature. The columns contain silica-based membrane that adsorbs DNA in a presence of chaotropic salts, removing residual water from the molecule. This should provide that DNA is retained on the membrane, while the flow-through contains all potential contaminants. After discarding the flow-through, the column was reinserted in the collection tube, and 500 µl wash buffers AW1 and AW2 were added subsequently in order to wash away residual protein or reagents. An important consideration for the washing step is addition of ethanol to wash buffers AW1 and AW2. Ethanol keeps the DNA in an insoluble form, hence preventing its elution in the washing step. AW1 is a high ionic strength buffer, forcing clearance of residual proteins whereas buffer AW2 is a milder wash buffer. It has to be considered that before the final elution step the column should be dry with no residual ethanol droplets. Failure to completely remove ethanol can lead to interference with downstream reactions, such as PCR. In the final step, DNA was eluted from the column using 200 µl AE buffer. Extracting DNA from blood cells with and without the use of RNase A did not yield great differences. However, I

1 https://www.qiagen.com/us/resources/resourcedetail?id=6b09dfb8-6319-464d-996c-79e8c7045a50&lang=en

did include this as an additional step in the further optimization of the protocol. This step is essential when working with cancer cells or liver tissue for instance.

2.2.2 *PeqGOLD Blood DNA Mini Kit Plus*

The protocol for this kit is available at the distributor website[2]. The protocol was tested in its original form, as provided by the manufacturer, without modification. Briefly, after starting with 100 µl fresh blood, adjusted to 200 µl with PBS, the sample was incubated with 25 µl Proteinase K solution and 200 µl of DNA Lysis Buffer BL at 60°C for 10min. At this stage Rnase A was added, at a concentration of 100 mg/ml. The next steps involved addition of 50 µl Binding Solution BL, transferring the sample to a membrane column and centrifugation. Two washing steps were performed, first using 400 µl of DNA Wash Buffer BL I, followed by 600 µl of DNA Wash Buffer BL II twice. After drying the sample was eluted from the column with 200 µl Elution Buffer preheated to 60°C.

2.2.3 *Bio&Sell*

The last kit used in this test was a generic kit [3]. The extraction was carried out using protocol 4 from the manual, with minor modifications, as follows: 100 µl whole blood was diluted to 400 µl with Lysis Buffer and 25 µl Proteinase K was added. The mixture was incubated at 50°C for 10 min after which 4 µl RNase A (100 mg/ml) was added and incubated briefly at room temperature. The sample was mixed with 400 µl binding buffer and transferred to a column. The column was washed twice; first using 500 µl Wash Buffer HS, followed by 750 µl Wash Buffer MS. The sample was eluted using 200 µl Elution Buffer.

2.3 DNA YIELD AND QUALITY ASSESSMENT

In order to make sure an equal amount of high-quality double stranded genomic DNA is present in each sample, DNA quantification and quality control are of great importance. The most commonly used method for DNA quantification is a spectrophotometric measurement using Nanodrop 2000c (Thermo Scientific), whereas an accurate measure of double stranded DNA concentration can be achieved using Quanti-Fluor®dsDNA System (Promega).

2 https://at.vwr.com/assetsvc/asset/de_AT/id/17035092/contents
3 http://www.bio-sell.com/images/stories/pdf/Molekularbiologie/dna-mini-kit.pdf

2.3.1 *Nanodrop 2000c*

Each sample was measured at a volume of 2µl, using the sample solvent as a blank. Double-stranded DNA as well as other types of nucleic acids typically absorb at 260 nm, showing a clear peak. Absorbance at other wavelengths, typically 230 nm and 280 nm are assessed in order to establish the purity of nucleic acid. For genomic DNA a ratio of 1.7-1.9 between the absorption maxima at 260 and 280 nm (called A260/280 ratio) indicates pure DNA. Lower ratios could point to protein contamination, as proteins typically show an absorption maximum at 280 nm. Ratios higher than two are characteristic for RNA samples. The ratio at 260/230 nm can indicate other types of contamination such as phenol or salts contamination. Even though Nanodrop can be used as a good indicator of DNA quality and quantity, this method often tends to overestimate the real DNA concentration, especially in samples with high abundance of RNA. Hence, in order to accurately estimate the concentration of DNA for downstream analyses, a method specific for double-stranded DNA was used in addition.

2.3.2 *QuantiFluor®dsDNA System*

The QuantiFluor®dsDNA System (Promega) has been utilized based on its properties to discriminate double-stranded DNA (dsDNA) from other types of nucleic acid in solution. The intercalating fluorescent dye binds specifically to double-stranded DNA and to a very small extend to single-stranded nucleic acids, allowing for accurate quantification of high quality genomic DNA. The assay was performed according to the protocol given by the manufacturer[4]. Briefly, samples were diluted 100x with 1x TE buffer supplied with the kit. Additionally, λ DNA standard (100 µg/mL as supplied by the manufacturer) has been diluted in 1x TE buffer according to the scheme in table 4. The DNA binding dye provided in the kit at 200x was diluted to 1x with TE buffer. The dye is photosensitive, so the work should be carried out by dim light. The diluted samples/standards were mixed with the 1x DNA dye in a 1:1 ratio and incubated for 5 minutes in the dark before measurement. The samples were measured in triplicates, in a 96-well format, using non-transparent black well plates, in order to minimize loss of signal. The measurement was carried on a FLUOstar Optima (BMG Labtech) plate reader, using a fluorescent measurement head. Before measurement, the gain was adjusted relative to the most concentrated standard. The analyses were performed using a linear regression method. A standard curve was calculated for each measured plate separately. When more samples from the same batch were to be assessed, a control sample with known concentration was included on each plate. This method was very robust with high comparability between plates. The inter-plate

4 https://at.promega.com/~/media/files/resources/protocols/technical%20manuals/101/quantifluor%20dsdna%20system%20protocol.pdf

	Blank	St1	St2	St3	St4	St5	St6	St7
dsDNA	0 µl	20 µl of λ	250 µl of St1	250 µl of St2	250 µl of St3	250 µl of St4	250 µl of St5	250 µl of St6
1xTE Buffer	1000 µl	980 µl	750 µl	750 µl	750 µl	750 µl	750 µl	750 µl
Conc.		2000 ng/ml	500 ng/ml	125 ng/ml	31 ng/ml	7.8 ng/ml	2.0 ng/ml	0.5 ng/ml
Conc. after adding Dye		1000 ng/ml	250 ng/ml	62.5 ng/ml	16 ng/ml	3.9 ng/ml	1.0 ng/ml	0.2 ng/ml

Table 4: Dilution scheme for λ standard preparation.

coefficient of variation (CV) was between 1 and 5% for very dilute samples (< 10 ng/µl) to less than 1% for more concentrated samples.

2.3.3 *Gel electrophoresis for quality assessment*

In order to assess the sample quality, a random subset of DNA samples were run on a standard agarose gel electrophoresis. For genomic DNA assessment gels were prepared at 1% in 1x TAE buffer, and stained with EZ-VIZION DNA dye (Amresco Int.) which acts simultaneously as a tracking and DNA visualization dye. The gels were visualized using a ChemiDoc™XRS+ System (BioRad) after exposure to UV light and analysed using an Image Lab™software (BioRad). A representative gel image of genomic DNA is shown in figure 3.

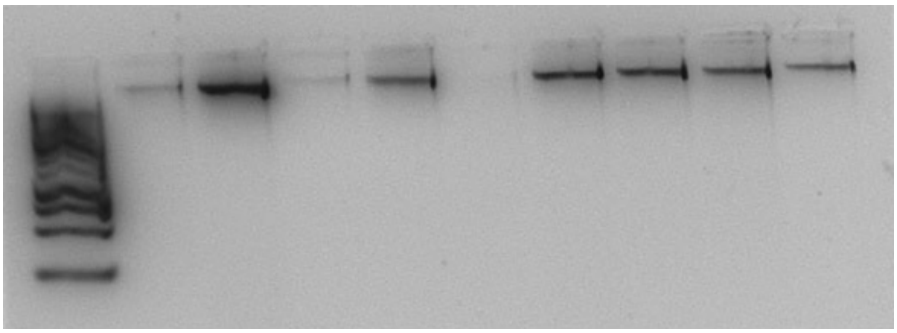


Figure 3: A representative gel image of genomic DNA extracted from blood samples (VAAS study). Lane 1 represents a 1kb DNA ladder.

2.4 RESULTS – DNA EXTRACTION

As described in the methods section, three DNA extraction kits have been tested on the same biological sample in order to find the optimal conditions. The criteria for comparison were DNA yield in µg, and A260/A280 ratio, measured by Nano drop. The kits were compared on a freshly taken whole blood sample. The results are depicted in table 5. DNA extracted using the Qiagen kit had a clearly higher yield and purity compared to the other two kits. In addition, both bio&sell and peqGOLD kits showed an unusually high A260:280 ratio. This ratio indicates the purity of DNA, as DNA absorbs at 260 nm and proteins at 280 nm. A ratio between 1.7-1.9 is typical for pure DNA; RNA has a somewhat higher ratio, around 2-2.1. Hence, we can interpret the higher ratios as either carryover RNA or protein interference. As the Qiagen kit performed better in both test criteria, all subsequent experiments are carried out using this kit.

	Yield		**A260/280**	
	Average	StDev	Average	StDev
Qiagen	3.127	0.098	1.933	0.017
bio&sell	1.46	0.071	2.157	0.034
peqGOLD	2.033	0.1	2.227	0.142

Table 5: Comparison of yield and quality of DNA extracted with three different DNA extraction kits. N (technical replicates) = 3.

The next step was to evaluate the influence of sample storage condition on DNA yield and quality. Using frozen starting sample instead of fresh can substantially simplify the workflow and logistics, especially in large or multi-laboratory studies. Moreover, collecting all samples and extracting them at a single time-point has the advantage of lower variability due to: different researches extracting different batches of samples, seasonal influences, potential changes in the constitution of used chemical by the supplier. As evident from table 6, there was no difference in the yield between fresh and frozen blood sample, whereas the quality estimated by the A260/230 was better in the frozen sample compared to the fresh one. Thus, we could conclude that storing the samples at -80°C does not reduce the yield and quality of the DNA. It should be noted that we have not tested the quality of DNA after prolonged storage. We have tested samples stored for a year at most and we did not test samples stored for a longer time period.

	Yield (µg)	A260/280	A260/230
Fresh blood	4.6	1.91	2.68
Frozen blood	4.58	1.76	2.01

Table 6: Yield and quality of DNA extracted from fresh and frozen blood sample. Final volume is 200 µl.

2.5 QPCR ANALYSES OF TELOMERE LENGTH

The following method for telomere length measurement utilizes the concept of PCR amplification of a specific fragment of DNA in order to estimate the copy number of the fragment in a given sample. This concept is already widely used in estimating gene expression with real-time PCR, where the template is mRNA previously transcribed to complementary DNA (cDNA). An important part of this assay is designing a primer pair which will specifically and unambiguously recognize only one site in the genome or transcriptome. As we already know, telomeres consist of long stretches of repetitive sequence, making the design of such specific primers difficult. This problem was solved by Cawthon [2002], when he designed primers that would specifically amplify the telomeric DNA without annealing to each other and forming large amounts of primer-dimers. This method can quantify the total telomeric content in a sample, assuming that the primers will cover the entire stretch of telomeric sequence present in the sample. In order to normalize for sampling errors and calculate the telomeric content per genome, the copy number of a so-called single-copy gene is evaluated. A single copy gene or region is a unique sequence that only occurs once per genome and is not subject to duplications.

The qPCR assay, as much as all others, assumes perfect hybridization of primers (or probes, respectively) to telomeric sequence, covering its entire length. Realistically, however, it is much more likely that the probe hybridization follows a probabilistic manner of filling the available binding sites [Göhring et al., 2013]. In addition, the theory of linear hybridization does not take in account the tertiary structure of the nucleic acids taking part. It is possible that longer sequences exhibit features (such as G-quadruplexes) that do not allow for proportional binding.

In order to control for primer binding biases, we have decided to use an approach utilizing telomere and single copy gene standards. The standards have to show an exponential dependency in a broad dilution range that covers the amplification profile of genomic DNA samples. This approach additionally allows for absolute quantification

of average telomere content in a sample expressed in kilobases. An extensive protocol has been published by O'Callaghan and Fenech [2011], giving a step-by-step explanation of the procedures. Here, I will discuss the modifications to this protocol as well as the optimization procedure.

2.5.1 *qPCR reagents, master mix and primers*

The original article from citeocallaghan:2011a uses a commercially available master mix Power SYBR (Applied Biosystems), whereas the article from Cawthon [2002] suggests an in-house made master mix. In order to maintain continuous quality and reproducibility, using a commercial kit might be a better choice, as the composition is constant throughout a production batch. The downside of using a commercial master mix, apart from the higher price, is the unavailability of information about the master mix composition. Most master mixes available state that they have an "optimized buffer composition" without specifying its constituents. Some buffer components, such as Mg^{2+} for instance, plays a very important role in the amplification efficiency, and even a minor inconsistency in its concentration can lead to significantly distinct results.

To verify the reaction efficiency and linearity and test the master mix we used genomic DNA sample we used DNA extracted from a T-cell leukemia cell line, called 1301, known to have very long telomeres. Figure 4 shows standard amplification plots of 10-fold dilutions of the 1301 control DNA using the POWER SYBR Master Mix[5]. Only three out of five tested dilutions, starting at 25 ng/µl, have been amplified and the overall qPCR efficiency was 36.22% (slope of -7.45). In addition, the amplification plots do not have a clear exponential phase and amplification plateau which are characteristic for qPCR amplification curves.

As an alternative master mix, we tested a different commercial master mix, SYBR Select (Life Technologies). Similarly to the Power SYBR, the exact buffer composition for this master mix is not specified. It contains a thermo labile uridine glycosilase that should degrade any reaction contaminants already before the Hot-start polymerase activation[6]. We tested this master mix using the 1301 control DNA. The results were linear in a range from 25 ng/µl to 2.5 x 10-4 ng/µl. Figure 1301 shows the amplification plot for 1301 cell line (figure 5).

The primers were used according to the original protocol. The dry oligos from the supplier were reconstructed to 100 µmol/l, and diluted to a working solution of 2 µmol/l. The stock solution was stored at -20°C for up to one year whereas the working

5 https://tools.thermofisher.com/content/sfs/manuals/cms_042179.pdf
6 https://www3.appliedbiosystems.com/cms/groups/mcb_support/documents/generaldocuments/cms_103304.pdf

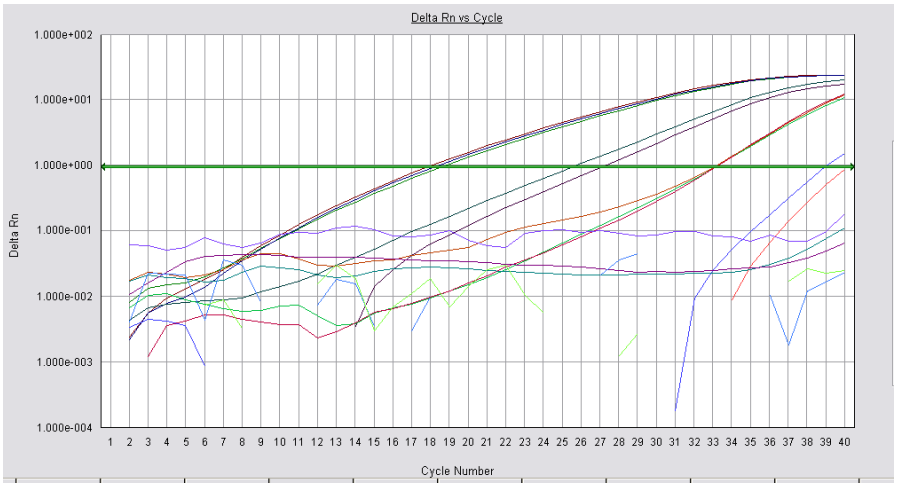


Figure 4: Representative amplification plot of 1301 cell line-derived DNA, using the Power SYBR master mix. Concentrations of 1301 DNA range from 25 ng/µl to 0.25 ng/µl.

solutions were stable at +4°C for several weeks. The final concentration of each primer was 100 nmol/l. Details on the primer sequence and properties are shown in chapter 3.

2.5.2 *Standards design and preparation*

The idea of using standard oligonucleotides telomere length measurement by qPCR was introduced by Thomas et al. [2008]. The idea was simple: a pre-designed oligo of a certain length containing TTAGGG repeats will be used in serial dilutions to construct a standard range where the logarithmic value of the input amount will be proportional to the Ct observed in a linear manner. In order to normalize the amount of telomeric sequence obtained, a similar approach was used for a single copy gene (SCG). A SCG is a gene that is present only once per haploid genome. Hence, the normalisation procedure gives the telomeric content in bases per genome i.e. the average length per telomere as an output.

The telomere sequence standard was designed as 84-bases long oligonucleotide containing 14 TTAGGG repeats. The standard oligos are relatively long and their single-strandedness makes them prone to instability. In order to keep the oligos stable over longer time periods in solution, they should be stored in TE buffer instead of water. Water solutions are prone to reduction of pH over time, which can lead to hydrolysis of nucleic acids. The TE buffer has a pH-value of 8 which keeps DNA stable over prolonged periods, even when stored at +4°C or at room temperature. However, TE

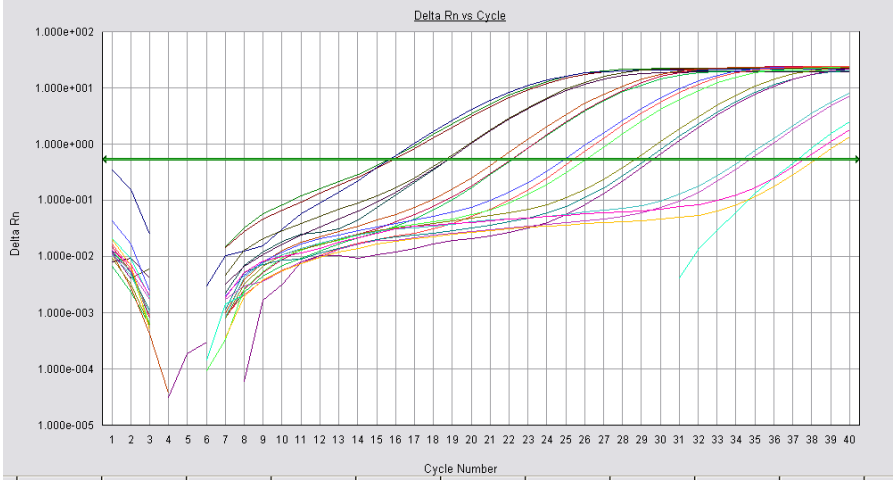


Figure 5: Representative amplification plot of 1301 cell line-derived DNA, using the SYBR Select master mix. Concentrations of 1301 DNA range from 25 ng/µl to 2.5 x 10^{-4} ng/µl.

buffer is a 1 mmol/l solution of EDTA. EDTA is a chelator that can bind metal ions and as such it is known to interfere with a number of downstream reactions, especially PCR. This is due to the use of Mg2+ ions as cofactors in PCR and other enzymatic reactions. Therefore, we used the AE buffer[7] instead, which is a modified version of the TE buffer with lower EDTA concentration. In addition, all DNA test samples prepared in our laboratory were stored in AE buffer which enabled similar conditions for both standard oligos and samples used in subsequent qPCR reactions.

The standard oligos were supplied as a dry powder which was initially resuspended in AE buffer to a concentration of 1 µg/µl of stock solution. This stock solution was further diluted to a working solution of 10 ng/µl which was used for subsequent dilutions. The working solution was stored at -20°C for a maximum of one year.

Standards were prepared as 10-fold dilutions starting with 50 pg/µl as the highest concentration. At concentrations higher than 50 pg/µl the reaction was saturated and linearity could not be established as shown in figure 6. Moreover, concentrations lower than 0.005 pg/µl appeared later than cycle 35 on the amplification plot. For that reason we used 5 dilutions only. The PCR efficiency was consistently between 90 and 110%, whereas regression coefficient of at least 0.989 was considered acceptable.

Standards for the single copy gene 36b4, were prepared similarly. The sequence is given by O'Callaghan and Fenech [2011] and in supplementary table S4 of chapter 3

7 https://www.qiagen.com/at/resources/faq?id=c484a4ad-6f46-4cb5-96f3-875b72f41512&lang=en

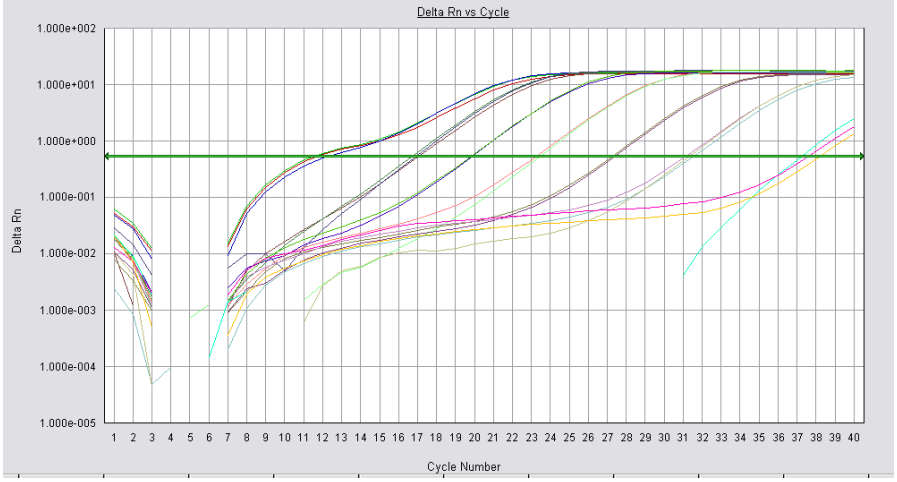


Figure 6: Representative amplification plot of synthetic telomere standards A1-A6 and a negative control, using the SYBR Select master mix. Concentrations of standards range from 500 pg/µl to 5 x 10^{-3} ng/µl.

in this thesis. The 36b4 standards amplified much earlier compared to the telomere standard at a same concentration, which contradicts the observations of O'Callaghan and Fenech [2011]. The amplification curves are shown in figure 7 The linear range of the standard curve covered all 8 concentrations tested (from 50 pg/µl to 5 x 10^{-6} pg/µl. For further analyses we used standards 3 through 7 (also named B3-B7), as test DNA samples amplified within that range. The efficiencies of the 36b4 reactions were usually between 90-100%, with some exceptions when it was not lower that 85%.

2.5.3 *Calculation of telomere length*

The calculation of telomere length is explained in detail by O'Callaghan and Fenech [2011]. Here, a brief description adopting the modifications.

- Telomere Standard Curve

1. The oligomer standard is 84 bp in length (14 x TTAGGG), with a molecular weight (MW) of 26673.
2. The weight of one molecule is MW/Avogadro's number. The weight of telomere standard is: 2.6673 x 10^4/6.02 10^{23} = 0.44 x 10^{-19}g.
3. The highest concentration standard (St A2) has 200 pg (50 pg/µl x 4 µl per reaction) of telo oligomer (200 x 10^{-12}g) per reaction.
4. Therefore there are 200 x 10^{-12}/0.44 x 10^{-19} = 4.54 x 10^9 molecules of oligomer in Telo A2.

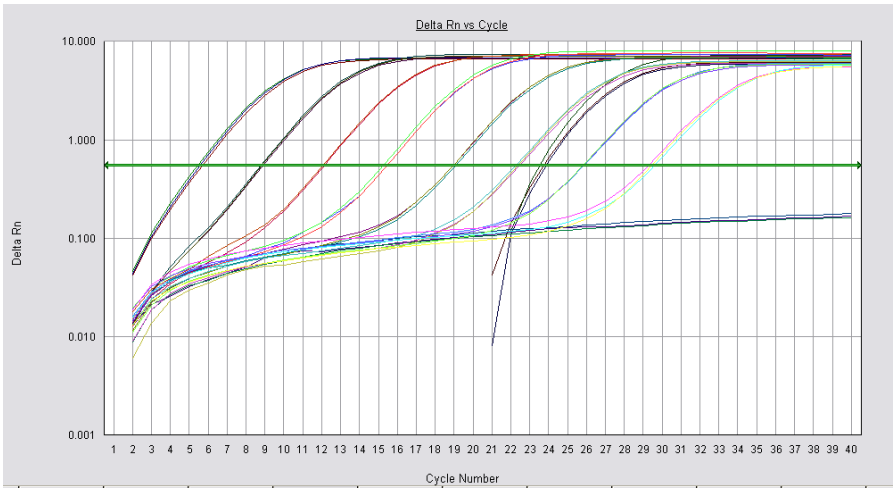


Figure 7: Representative amplification plot of synthetic 36b4 standards B1-B7 and a negative control, using the SYBR Select master mix. Concentrations of standards range from 500 pg/µl to 5 x 10^{-4} ng/µl.

5. The amount of telo sequence in Telo A2 is 4.54 x 10^{9} x 84 (oligomer length) = 3.81 x 10^{8} kb.

- 36b4 Standard Curve

1. The 36b4 oligomer standard is 75 bp long with a MW of 23275.
2. The weight of one molecule is MW/Avogadro's number. Therefore, weight of the synthesized 36b4 oligomer standard is: 2.3275 x 10^{4}/6.02 x 10^{23} = 0.38 x 10^{-19} g.
3. The highest concentration standard (B3) had 2 pg of 36b4 oligomer (2 x 10^{-12}g) per reaction.
4. Therefore there are 2 x 10^{-12}/0.38 x 10^{-19} = 5.26 x 10^{7} copies of 36b4 amplicon in St B3.
5. Therefore St B3 is equivalent to 2.63 x 10^{7} diploid genome copies, because there are two copies of 36b4 per diploid genome (Adapted from O'Callaghan and Fenech [2011]).

To construct a standard curve the logarithmic values of each standard dilution are plotted against the Ct value obtained by qPCR. The linear regression formula obtained can then be used to calculate the telomere content in the unknown sample. If we look at an example where the sample has a Ct value of 26.71 for the telo assay and 27.504 for the 36b4 assay. The regression formula for telo is y = -3.347x + 60.07; for 36b4 y = -3.522x + 42.146. Therefore the logarithmic values for telo and 36b4 respectively are

9.965 and 4.156. If we calculate the power of the exponent with base 10 ($n = 10^{telo}$ or $n = 10^{36b4}$) it would amount to 9.236×10^9 and 1.433×10^4 respectively. In order to get the telomeric content per genome, we divide the telo by the 36b4 content which amounts to 6.445×10^5 bases or 644.5 kb of telomeric sequence per sample. As there are 46 chromosomes in the diploid genome and each has two telomeres, we can divide the result by 92 to get a value of 7 kb per telomere as an average length.

Part II

PRELIMINARY, SUBMITTED AND PUBLISHED RESULTS

3

LONGER TELOMERES IN CHRONIC, MODERATE, UNCONJUGATED HYPERBILIRUBINAEMIA: INSIGHTS FROM A HUMAN STUDY ON GILBERT'S SYNDROME

ARTICLE

Anela Tosevska, Christine Moelzer, Marlies Wallner, Milan Janosec, Ursula Schwarz, Carina Kern, Rodrig Marculescu, Daniel Doberer, Wolfram Weckwerth, Karl-Heinz Wagner.
Longer telomeres in chronic, moderate, unconjugated hyperbilirubinaemia: insights from a human study on Gilbert's Syndrome.
in *Scientific reports* (2016), **Volume** 6, **Article number** 22300
doi: doi:10.1038/srep22300

AUTHOR CONTRIBUTIONS

Anela Tosevska, C.M. and M.W. designed and established the majority of the experiments and methods; M.J. prepared the DNA samples and performed the qPCR assays; U.S. performed the FRAP assay and prepared DNA extracts from rat liver; C.K. performed the HPLC measurements; Anela Tosevska, C.M., M.W., M.J. and C.K. processed the blood samples; M.W. prepared the rat liver samples and measured UCB in rat tissues; Anela Tosevska and W.W. did the statistical analyses; C.M., M.W., R.M., D.D. and K.H.W. designed and conceived the human study; R.M. and D.D. oversaw the routine clinical measurements; K.H.W. provided financial support; Anela Tosevska made the figures; Anela Tosevska wrote the manuscript; all authors critically revised the manuscript.

LICENCE

This is an Open Access article distributed under the terms of the Creative Commons Attribution License (http://creativecommons.org/licenses/by/4.0), which permits unrestricted use, distribution, and reproduction in any medium, provided the original work is properly cited.

www.nature.com/scientificreports

SCIENTIFIC REPORTS

OPEN

Received: 05 November 2015
Accepted: 11 February 2016
Published: 01 March 2016

Longer telomeres in chronic, moderate, unconjugated hyperbilirubinaemia: insights from a human study on Gilbert's Syndrome

Anela Tosevska[1,2], Christine Moelzer[2], Marlies Wallner[2,3], Milan Janosec[2], Ursula Schwarz[2], Carina Kern[2,4], Rodrig Marculescu[5], Daniel Doberer[6], Wolfram Weckwerth[7,8] & Karl-Heinz Wagner[1,2]

Bilirubin (BR) is a natural endogenous compound with a potent bioactivity. Gilbert's Syndrome (GS) is a benign hereditary condition of increased unconjugated bilirubin (UCB) in serum and serves as a convenient model for studying the effects of BR in humans. In absence of liver disease, increased UCB levels are inversely associated to all-cause mortality risk, especially from cardiovascular diseases (CVDs). On the other hand, telomere malfunction is linked to a higher risk of CVDs. To our knowledge, there is no data on whether UCB is linked to telomere length in healthy or diseased individuals In the present study we have observed a relationship between mildly increased serum UCB and telomere length. We used an *in vivo* approach, assessing telomere length in PBMCs from individuals with GS (n = 60) and matched healthy controls (n = 60). An occurrence of longer telomeres was observed in male individuals chronically exposed to increased UCB, as well as in Gunn rats, an animal model of unconjugated hyperbilirubinaemia. Previously identified differences in immunomodulation and redox parameters in individuals with GS, such as IL-6, IL-1β and ferric reducing ability of plasma, were confirmed and proposed as possible contributors to the occurrence of longer telomeres in GS.

Gilbert's Syndrome is a condition where mild unconjugated hyperbilirubinaemia is the main phenotypical characteristic[1]. Bilirubin is a natural and ubiquitous bile pigment that has caused a lot of contradictions throughout the years because of its double-faced nature[2,3]. It is the end-product of haem catabolism in mammals, formed in subsequent enzymatic reactions in which haem is transformed into biliverdin (BV) and then to bilirubin[4,5]. A graphical representation of the processes has been given by Wagner *et al.*[6].

From an evolutionary perspective, it is puzzling why the BV-BR system has developed, since BR is a potent neurotoxin if present at very high concentrations in the circulatory system[7]. Biliverdin is hydrophilic and can be easily excreted[5]. In fact, BV is the end product of heme catabolism in most birds, reptiles and amphibians[8]. Unconjugated BR, on the other hand, is highly hydrophobic, making its excretion impossible without prior conjugation, a process that yields hydrophilic conjugated BR. This process in mammals is mediated by the UGT1A1 isoenzyme.

[1]Research Platform Active Ageing, University of Vienna, Althanstrasse 14, 1090, Vienna, Austria. [2]Department of Nutritional Sciences, University of Vienna, Althanstrasse 14, 1090 Vienna, Austria. [3]Institute of Dietetics and Nutrition, University of Applied Sciences, FH JOANNEUM, Alte Poststraße 149, 8020 Graz, Austria. [4]Institute of Pharmacology, Medical University of Vienna, Waehringer Str. 13a, 1090 Vienna, Austria. [5]Clinical Institute of Laboratory Medicine, Medical University of Vienna, Waehringer Guertel 18–20, 1090 Vienna, Austria. [6]Department of Clinical Pharmacology, Medical University of Vienna, Waehringer Guertel 18–20, 1090 Vienna, Austria. [7]Department of Ecogenomics and Systems Biology, University of Vienna, Althanstrasse 14, 1090 Vienna, Austria. [8]Vienna Metabolomics Center (VIME), University of Vienna, Althanstrasse 14, 1090, Vienna, Austria. Correspondence and requests for materials should be addressed to A.T. (email: anela.tosevska@univie.ac.at)

	Gilbert's Syndrome (n = 49–60)	Controls (n = 49–60)
Age (years)	37 ± 14	37 ± 14
Female gender	33%	33%
Unconjugated BR (μmol/l)	33.12 ± 9.86	9.22 ± 3.41**
Haem (μmol/l)	0.75 ± 0.14	0.76 ± 0.11
AST (U/l)	26.02 ± 8.31	25.43 ± 8.31
ALT (U/l)	23.56 ± 8.15	24.78 ± 9.07
GGT (U/l)	21.10 ± 15.04	23.78 ± 17.47
LDH (U/l)	160 ± 22	163 ± 29
CO-hemoglobin (%)	1.21 ± 0.35	1.32 ± 0.72
Haemoglobin (g/dl)	14.53 ± 1.30	14.27 ± 1.21
Haematocrit (%)	42 ± 3.37	41 ± 3.50
Iron (μmol/l)	30.26 ± 10.05	23.11 ± 9.48**
Transferrin (mg/dl)	266 ± 45	268 ± 40
Transferrin saturation (%)	45 ± 15.60	35 ± 14.14**
Ferritin (μg/l)	120 ± 111	120 ± 87
Haptoglobin (mg/dl)	78 ± 33	103 ± 51**
Hemopexin (mg/dl)	84 ± 10	87 ± 14*
Albumin (g/l)	47 ± 3	47 ± 3
Free BR (nmol/l)	2.20 ± 0.79	0.25 ± 0.23**
BMI (kg/m^2)	22.81 ± 3.03	25.38 ± 4.91**
Lean body mass (%)	78 ± 6.51	75 ± 8.59*
Body fat (%)	22 ± 6.51	25 ± 8.59*
BP systolic (mmHg)	129 ± 13	133 ± 16
BP diastolic (mmHg)	67 ± 12	69 ± 12
Framingham risk score (%)[¥]	1.5 ± 2.9	2.3 ± 4.2*

Table 1. Characteristics of the study population (demographics, variables defining haem and iron metabolism, anthropometrical measurements and CVD risk parameters). Values are presented as mean ± standard deviation or percentage. The indices represent different levels of significance obtained using paired t-test or [¥]Wilcoxon signed ranks test for non-parametric variables: *$P < 0.05$; **$P < 0.01$ cases vs. controls. The variable sample sizes presented are due to missing values in some of the parameters.

Gilbert's Syndrome is associated with genetic variations in the UGT1A1 gene promoter region, of which the so-called UGT1A1*28 is the most common among Caucasians. This polymorphism is characterized by insertion of an additional TA repeat in the TATA box of the promoter, yielding 7 TA repeats instead of the common 6, and leading to a decreased expression and activity of the UGT enzyme[9]. Since the isoenzyme A1 exhibits the highest affinity towards endogenous BR[10], its conjugation becomes hindered resulting in increased concentrations of the hydrophobic unconjugated BR (UCB) in the serum of affected individuals, leading to increased measurable UCB and total BR concentrations.

Epidemiological studies indicate a strong association between increased serum BR and decreased incidence of age-related metabolic and cardiovascular diseases[11,12]. In addition, individuals with GS have been found to exhibit delayed all-cause mortality, especially that from CVDs[11,13] (summarized in[6,14]). In an earlier study, we have shown that GS individuals exhibit a serum lipid profile indicative of lower CVD risk as compared to age-matched controls[15]. These studies investigate mainly the unconjugated portion of serum bilirubin and total serum bilirubin. However, the underlying mechanism of cardiovascular protection remains unclear.

Bilirubin has been described as a potent antioxidant with immune-modulatory activity[16]. This could in turn explain the previous epidemiological findings, as aging and chronic disease are associated with increased baseline inflammation and redox-imbalance[17,18]. Another common hallmark of aging is increased telomere attrition[19]. Telomeres are nucleo-protein structures capping the ends of eukaryotic chromosomes. Due to the end-replication problem occurring during mitosis, telomeres cannot be replicated entirely and shorten after each cell division, which is exacerbated by increased oxidative stress[20–22]. A link between accelerated telomere shortening and a number of age-associated diseases and conditions has already been established[23,24]. Bilirubin might play a role in maintaining a balanced redox environment delaying telomere attrition and disease onset.

Here we present a case-control study of healthy age- and gender-matched GS individuals and controls within a broadly defined age range. The aim was to provide a link between moderately increased unconjugated bilirubin and telomere length *in vivo* and to propose an involvement of telomeres as mediators of bilirubin signalling in healthy aging.

Results

Characteristics of the study population. A total of 120 participants were allocated to two groups: case and control, according to the levels of UCB as determined by high-performance liquid chromatography (HPLC),

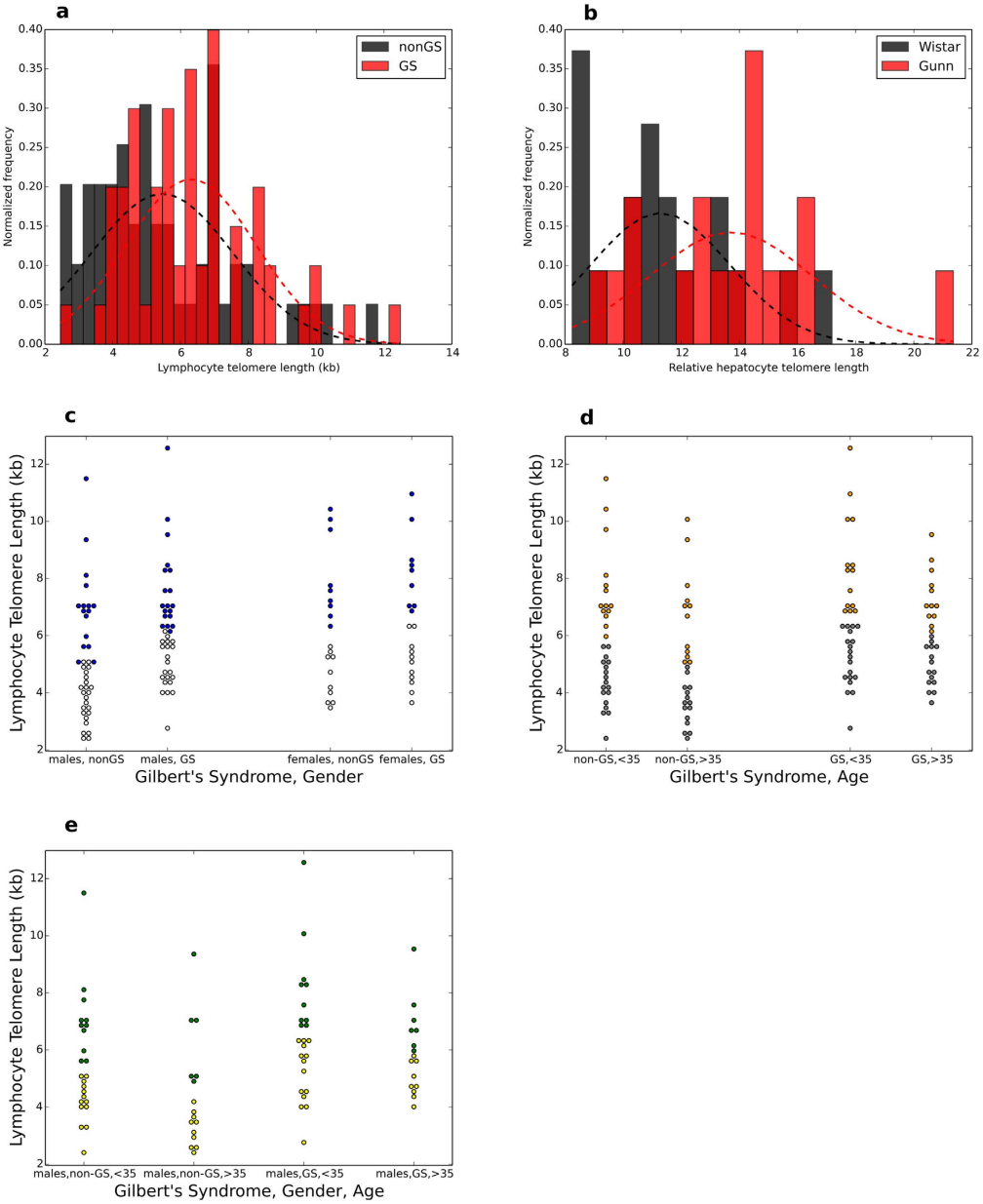


Figure 1. Telomere length distribution in human and animal samples. (**a,b**) Dark red bars represent frequency overlap between the groups. (**c,d,e**) Different colours represent values below and above the group mean (**a**) Distribution of absolute lymphocyte telomere length in Gilbert's individuals; P = 0.01, Mann Whitney U test; P = 0.031, independent samples t-test, two-sided. (**b**) Distribution of relative liver telomere length in homozygous Gunn rats vs. heterozygous Wistar rats, P = 0.013, Mann Whitney U test; P = 0.01, independent samples t-test, two-sided. (**c**) Lymphocyte telomere length in GS and non-GS, age groups; P = 0.024, Kruskall-Wallis 1-way ANOVA; P = 0.053 for ≥35 years old GS vs. non-GS, independent samples t-test, two-sided. (**d**) Lymphocyte telomere length in GS and non-GS, gender; P = 0.013, Kruskall-Wallis 1-way ANOVA; P = 0.013 for GS males vs. non-GS males. (**e**) Lymphocyte telomere length in GS and non-GS, age groups, males only; P = 0.01, Kruskall-Wallis 1-way ANOVA; P = 0.02 for ≥35 years old GS vs. non-GS males, independent samples t-test, two-sided.

with a cut-off point at 17.1 µmol/L. Each case was matched with an age- and gender-appropriate control. The study characteristics are depicted in Table 1.

Telomere length analysis. Mean telomere length (TL) was greater in GS subjects (6.25 kb ± 1.97, mean ± s.d.) compared to controls (5.47 kb ± 2.09, P = 0.033; paired t-test), which became more pronounced after correcting for age and gender (P = 0.002 for the whole model, P = 0.02 for GS phenotype). The differences

in TL distribution are shown in Fig. 1a. We further examined liver tissue of Gunn rats, an animal model of hyperbilirubinemia[25], vs. healthy Wistar rats. Gunn rats exhibited significantly longer telomeres (13.71 ± 2.88 vs. 11.28 ± 2.46; $P = 0.01$; relative units; Fig. 1b).

We then set to assess which variables most markedly affect TL, independent of the GS condition. Age and gender cumulatively contributed to an almost negligible variance in telomere length data (6.7%, $P < 0.05$). As expected, and consistent with previous findings[26], TL decreased with age at a rate of around 30 bases per year, after correction for gender. On the other hand, females tended to have longer telomeres than males, with a difference of around 1 kb after age correction ($P = 0.025$). When dividing the cohort according to gender, a significant difference between GS and controls was only evident in males ($P = 0.01$, Fig. 1c,e, supplementary Table S1). No gender-specific difference concerning TL was observed in rats (Supplementary Fig. S1b,c, supplementary Table S2).

Unconjugated bilirubin and telomere length. As expected, UCB was significantly different between the groups (Table 1). There was no effect of gender on UCB in the entire population, however, males had slightly higher levels in the GS group (supplementary Table S1). UCB levels had a tendency to decrease with age in the control group ($r = -0.274$, $P = 0.034$, supplementary Table S3).

Serum UCB levels strongly correlated with the ferric reducing ability of plasma (FRAP) in both males and females ($r = 0.729$, $P < 0.001$ Fig. 2d), but not with other markers of oxidative stress such as GSH/GSSG or malondialdehyde. Baseline inflammation markers in serum such as CRP and SAA were only weakly inversely associated with UCB ($r = -0.2$, $P = 0.02$ and $r = -0.19$, $P = 0.04$, respectively), whereas IL-6 and IL-1β in monocytes showed a stronger inverse correlation ($r = -0.301$, $P = 0.001$ and $r = -0.211$, $P = 0.023$ respectively) which remained significant after age correction. After gender stratification, a strong inverse relationship with IL-1β was evident in males, but not in females (Fig. 2c).

Intracellular IL-1β was by far the best single predictor of telomere length (Fig. 2a,d,e). When combined with the variables age, gender and FRAP in total a contribution of 22% to TL variability in the entire study population became evident in the model ($P < 0.001$). UCB and TL were only weakly correlated after correcting for age and gender, though a U-shaped model could fit the data more precisely (Fig. 2a). Other parameters affected by the GS condition such as plasma iron, BMI or blood pressure showed no correlation with telomere length.

UGT1A1 genotype and telomere length. To better characterize the nature of the hyperbilirubinaemia, we performed UGT1A1 genotyping of the human subjects. While the GS group almost entirely consisted of individuals with the 7/7 genotype (homozygous for the allele with 7 TA-repeats, sup. Table S4) more than 50% of the control subjects turned out to be heterozygous carriers of the UGT1A1 7 allele, which often presents with intermediately high UCB levels (Fig. 3b). UCB concentrations differed significantly when comparing the 7/7 genotype to the 6/6 and 6/7 UGT1A1 genotype ($P < 0.001$, sup. Table S5). No significant difference was present between the 6/6 and 6/7 genotype before or after adjustment for multiple comparison. The groups did not differ significantly in age and gender distribution (sup. Table S5).

Telomere length across genotypes showed a similar pattern as UCB, with heterozygous carriers showing an intermediate mean telomere length. The difference remained significant only between 6/6 and 7/7 homozygous subjects ($P = 0.044$, after adjustment for multiple comparison, Fig. 3c, supplementary Table S5).

PCA, multivariate correlations and clustering. We further performed a more in-depth multivariate principal component analysis (PCA) and bi-clustering using COVAIN[27]. Bi-clustering of the data revealed a clear discrimination between GS and non-GS individuals (Fig. 4a,b). The main separation is seen as two clusters of female and male subjects. Young individuals ($\leq$35 years of age, GS and non-GS) and older GS subjects ($\geq$35 years) always grouped closely together, whereas the older controls deviated more in their characteristics (Fig. 4a,b). This was as well evident for telomere length and observed previously for lipid metabolism[15]. Additionally, analysis revealed a strong negative correlation between TL and blood pressure, BMI and HOMA-IR as outcome variables, when considering the mean group values (Fig. 4c–e). This was not evident when employing a simple bivariate correlation.

Discussion

Our findings reveal a novel characteristic of Gilbert's Syndrome, potentially related to a chronic exposure to moderately increased unconjugated serum bilirubin. We show that individuals with a GS phenotype have on average longer telomeres compared to age- and gender-matched controls. This difference appears to be more pronounced with age, suggesting a reduced or slower telomere attrition in GS.

The liver is the key organ involved in heme catabolism that is affected by differences in UGT1A1 expression and UCB accumulation. However, due to ethical guidelines and based on the invasiveness of liver biopsies, human hepatocytes were inaccessible in this study. Using rat liver tissue instead, we could observe that telomere length distribution in GS individuals was clearly reflected by the animal model. Interestingly, in rats the differences were evident, despite the very young age at sacrifice (7–8 weeks). However, at this age, telomerase is still active in rat hepatocytes[28], indicating there could be a different telomere maintenance mechanism compared to humans.

Due to a lack of human liver samples and rodent PBMCs, respectively, we can only presume that TL is retained across different tissues, as is supported by the findings of Daniali *et al.*[26].

The difference in telomere length between GS and non-GS individuals was only evident in males. This goes in line with previous findings on the dimorphic effect of increased serum BR as a protective agent against CVDs[6]. Steroid hormones, such as 17β-estradiol are also glucuronidated by the UGT1A1 isoenzyme[10], but with a lower affinity compared to BR. Hence, we expected to observe an increase in serum concentrations of 17β-estradiol in

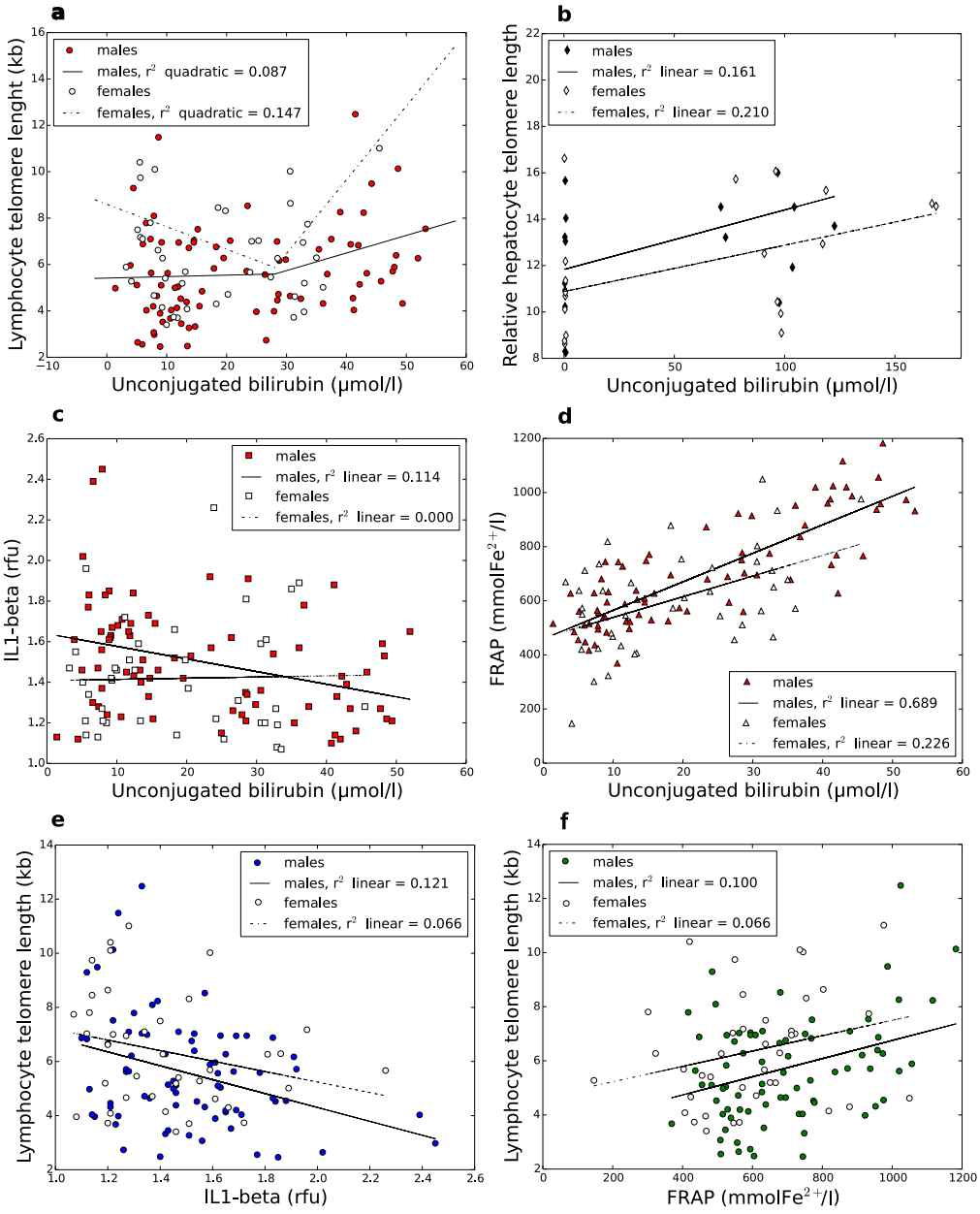


Figure 2. Correlation of serum UCB with telomere length, serum antioxidant capacity and intracellular interleukins in humans; plasma UCB and hepatocyte telomere length in rats. (**a**) Association between UCB and telomere length in males and females; quadratic model: P(males) = 0.03, P(females) = 0.053; linear model: P(males) = 0.012, P(females) = 0.713. (**b**) Plasma UCB and relative hepatocyte telomere length in rats; P(males) = 0.110, P(females) = 0.048. (**c**) UCB and IL1β; P(males) = 0.003, P(females) = 0.879. (**d**) UCB and FRAP; P(males) < 0.001, P(females) = 0.002. (**e**) IL1β and lymphocyte telomere length; P(males) = 0.002, P(females) = 0.110. (**f**) FRAP and lymphocyte telomere length; P(males) = 0.005, P(females) = 0.111.

GS. In addition, oestrogen is a known inducer of telomerase, the main enzyme involved in telomere maintenance. However, serum 17β-estradiol concentrations could not explain the occurrence of longer telomeres in GS males (sup. Table S1). Thus, the reasons for the observed gender differences remain unclear. In the rodent models, increased telomere length accompanied hyperbilirubinaemia in both male and female animals. As mentioned above, comparison to the human GS condition is difficult, as telomerase is highly active in rat liver.

The most plausible hypothesis explaining slower telomere shortening in GS, is that UCB via its immune-modulatory activity leads to slower cell turnover and hence, a slower exhaustion of hematopoietic stem cells[29]. This, combined with the antioxidant potential of BR could explain most of the differences observed in TL. A strong direct relationship between serum UCB and TL could not be established, likely due to the transient

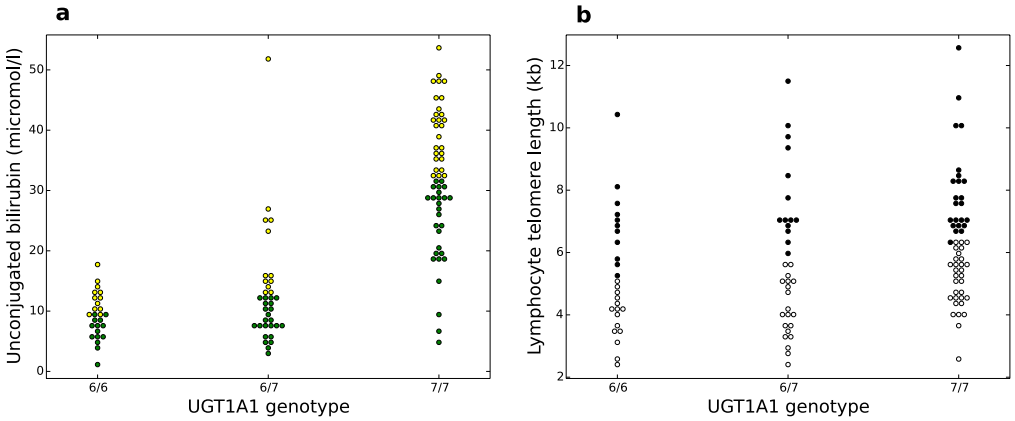


Figure 3. UGT1A1 genotypes and their influence on telomere length. (**a**) UCB concentration distribution according to genotype, $P < 0.001$, Kruskall-Wallis 1-way ANOVA. (**b**) Telomere length according to genotype $P = 0.034$, Kruskall-Wallis 1-way ANOVA.

nature of measurable UCB concentrations, which are subject to day-to-day fluctuations. On the other hand, changes in TL are steady and can be only observed on a long-term basis. UCB might affect the immune response by downregulating intracellular production of cytokines, as evident from the lower levels of IL6 and IL-1β in monocytes from GS individuals, in particularly males (sup. Table S1). A telomere shortening effect of IL-1β has already been observed as a result of faster cell turnover influenced by increased baseline inflammation[30].

Although it is tempting to propose a strong intracellular immune-modulatory effect of UCB, there is no data on uptake of bilirubin by immune cells *in vivo*. Although UCB can be readily taken up by PBMCs in Gunn rats (Fig. 3, supp. Fig. S2), we could not detect it in PBMCs from GS individuals. This might be in turn due to the low levels of free BR (Table 1), which are able to enter the cells and are much lower than the limit of detection (18 nmol/l) of the HPLC method used[31]. In addition, even in Gunn rats, lymphocytes showed significantly lower affinity to UCB uptake compared to hepatocytes and colonocytes (supplementary Fig. S2b).

While increased UCB levels are so far the only identified outcome in Gilbert's Syndrome, we cannot exclude that UGT1A1 mutations might exhibit other effects on human health. UGT1A1 genotyping confirmed previous findings of high occurrence of the UGT1A1*28 allele even in the control population not exhibiting GS phenotype, as more than 50% of the controls have proven to be heterozygous carriers of the allele[32,33]. Additionally, a small number of heterozygous individuals showed a GS phenotype (sup. Table S4). However, taken in account the general characteristics such as UCB, BMI and Iron (sup. Table S5), the heterozygous carriers appeared to be phenotypically closer to the 6/6 than to the 7/7 individuals, indicating that both copies of the aberrant UGT1A1 promoter are necessary for beneficial health outcomes related to GS.

The present study aimed to investigate differences between healthy individuals with no history or present indication of a CVD. Even though we could identify a mildly increased risk for cardiovascular events (Framingham 10-year risk score, Table 1) in the control population compared to the GS population, we could not attribute the observed difference to either UCB or telomere length differences.

An interesting parallel between the importance of telomere and bilirubin biology in CVD protection can be made looking at previous reports[34–36]. These studies employ a method of exogenously introduced telomerase/bilirubin treatment on myocardial ischemia/infarction injury, resulting in a reduced cardiac muscle damage, possibly by modulating cell death. Bilirubin might offer cardiac protection via telomere targeting and more studies in this direction should be performed to test this possibility.

Being the first study reporting this results and dealing with a relatively small sample size, additional similar studies are needed in order to confirm our findings. Besides, the current study design is characterized by a heterogeneous age range, and a larger sample size would compensate for its effects. In order to properly assess telomere dynamics in GS, a longitudinal approach following the same individuals over a prolonged time period, could be employed. It is of major importance to take a more in-depth look at the mechanisms behind the telomere length differences, and while our proposed model of reduced inflammation and cell turnover is very plausible, specific pathways remain to be uncovered. In addition, in order to properly assess the implications of the UCB-telomere length axis in CV health, a study investigating telomere length and Gilbert's Syndrome in CVD patients should be conducted.

In conclusion, we could observe a further link between Gilbert's Syndrome, and possibly unconjugated bilirubin, and longevity, with emphasis on healthy aging. This work is important when considering bilirubin as a natural therapeutic in fighting cardio-metabolic diseases[14], as it emphasizes a long-term benefit on a cellular and molecular level.

Materials and Methods

Subject recruitment and sample preparation. This study was a case-control study (60 patients in each group) at a single centre in Austria. The study was performed at the Department of Clinical Pharmacology of the

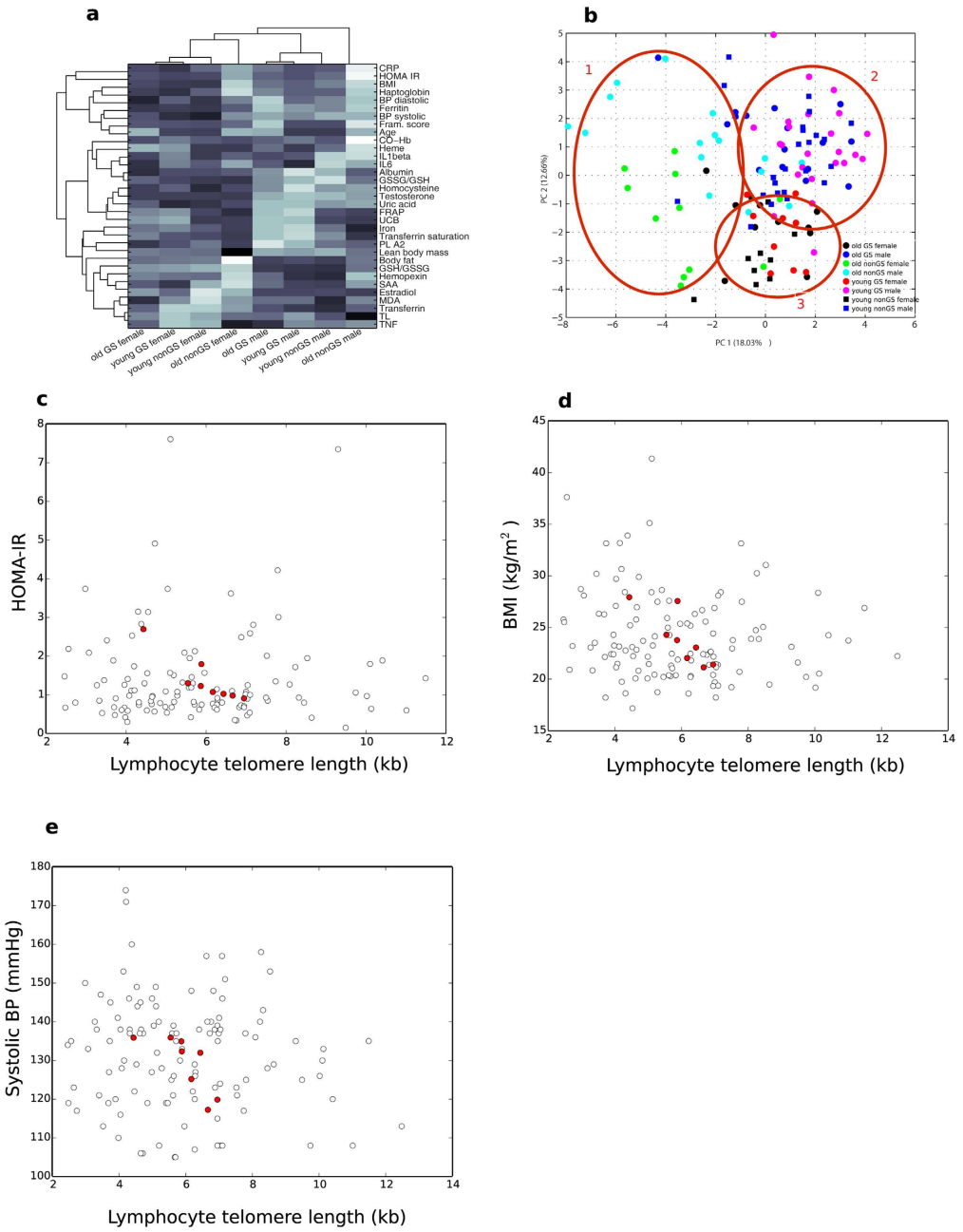


Figure 4. COVAIN analyses revealed distinct clustering among the eight study groups, divided according to age, gender and GS phenotype. Males and females form two distinct clusters with a small distance between "young" (<35 years old) individuals and "old" (≥35 years old) GS individuals, whereas there is a clearly greater distance of "old" control subjects. (**a**) Heat map shows clustering of groups and contributing variables. For individual differences in variables between groups refer to supplementary Tables S1 and S2. (**b**) Principal components analysis contribute to formation of three distinct clusters (marked with red circles). Circle 1: old, non-GS males and females; circle 2: males, young GS and non-GS and old GS; circle 3: females, young GS and non-GS and old GS. (**c**) Pearson correlation between TL and HOMA-IR, white circles represent all data, $P > 0.1$; red circles represent group mean, $r = -0.906$, $P = 0.002$. (**d**) Pearson correlation between TL and systolic blood pressure, white circles represent all data, $P > 0.1$; red circles represent group mean, $r = -0.762$, $P = 0.028$. (**e**) Pearson correlation between TL and BMI, white circles represent all data, $P > 0.1$; red circles represent group mean, $r = -0.827$, $P = 0.011$.

Medical University of Vienna and subjects (both control and GS) were recruited between 06/2014 and 01/2015 by direct advertising (bulletin boards, posters and flyers) and from the department's subject database.

A total of 128 subjects (men and women) from the general population were recruited after a screening examination including liver enzyme values for γ-glutamyl transferase (γ-GT), alanine transferase (ALT), aspartate aminotransferase (AST), lactate dehydrogenase (LDH), alkaline phosphatase, and blood count including reticulocytes, haemoglobin, and haematocrit. Inclusion criteria were normal liver function, absence of acute and chronic disease, and age between 20 and 80 years. Subjects with liver, heart or kidney conditions, haemolysis, diabetes, cholelithiasis, organ transplants, history of cardiovascular disease (CVD), cancer, smoking, excessive physical activity, and any medication that might alter liver metabolism as well as vitamin supplementation (4–5 weeks prior the blood sampling) were excluded. As an important diagnostic procedure, subjects were required to complete 400 kcal restricted fasting-protocol on the day preceding blood sampling, leading to increased serum UCB levels in absence of liver disease[37]. The criterion for group allocation (Gilbert's Syndrome or control group), was based on a fasting serum unconjugated bilirubin (UCB) concentration of $\geq$ or $<$17.1 µmol/L respectively, measured by high-performance liquid chromatography (HPLC). Finally, subjects were stratified for the GS and control group and matched by age and gender to result in 40 men and 20 women in both groups, respectively, which reflects the occurrence of GS phenotype in the population[15].

The study was approved by the Ethical Committee of the Medical University of Vienna and the General Hospital of Vienna (#1164/2014) and conducted in accordance with the approved guidelines by the Declaration of Helsinki. All subjects provided written informed consent.

For each subject, fasting blood samples were collected on a single occasion, a maximum of two week following the screening test. Samples were drawn by venepuncture and a peripheral venous catheter, into EDTA, Li-Heparin and serum vacutainers (Vacuette K_2EDTA and Z Serum Sep respectively, Greiner Bio-one GmbH). Samples were stored in cool and dark and subsequently processed, to yield aliquoted fractions thereof (whole blood, plasma, serum). The aliquots were stored at −80 °C until further analysis.

Peripheral blood mononuclear cells (PBMCs) were isolated from EDTA blood using Leucosep separation tubes (Greiner bio one), by centrifugation according to the manufacturer's instructions and washed twice with ice-cold PBS. Cell count and viability was estimated using the Trypan blue exclusion test on a Countess Automated cell counter (Life Technologies). Cells were aliquoted in freezing medium (FBS + 10% DMSO) and cooled gradually to −80 °C using CoolCell (Biozym).

Anthropometric measurements. Standing height was measured without shoes to the nearest 0.5 cm with a commercial stadiometer (Seca, Hamburg, Germany), and body mass was evaluated with a digital scale (BWB 700, Tanita, Amsterdam, Netherlands) to the nearest 0.1 kg with subjects lightly dressed and barefoot. BMI was calculated as the ratio between the weight measured in kilograms and the square of the height measured in meters. To determine body composition (muscle and fat mass) Bioelectric Impedance Analysis (BIA) was used, which has been shown to provide reliable data of body composition in comparison to Dual-Energy X-ray Absorptiometry (DXA)[38]. BIA was performed in the morning after an overnight fast using a BIA Analyzer 2000-S (Data-Input GmbH, Darmstadt, Germany).

Blood biochemistry. Liver enzymes (AST, ALT, γ-GT, LDH), iron, ferritin, transferrin, hemopexin, haptoglobin, homocysteine, hormones (estradiol, testosterone, TSH, triiodthyronine, thyroxin) were analysed in the routine core laboratory of the hospital (Olympus 5400 clinical chemistry analysers from Beckman Coulter) and measured on the day of blood sampling. Carboxy haemoglobin (CO-Hb) was measured directly from heparinized syringes, using a blood gas analyser ABL 700 (Radiometer, Brønshøj, Denmark).

Unconjugated bilirubin measurement by HPLC. Serum samples for UCB measurement were stored in dark tubes, immediately after separation, as described previously[37]. Unconjugated bilirubin and heme were measured in serum samples, using a high-performance liquid chromatograph (Merck, Hitachi, LaChrom, Vienna, Austria) equipped with a photodiode array detector (PDA, Shimadzu,) and a Fortis C18 HPLC column (4·6 × 150 mm, 3 µm) with a phenomenex C18 HPLC guard column (4·0 × 3·0 mm). Sample preparation and analysis were performed as previously published[37]. Unconjugated bilirubin and haemin (both Frontier Scientific Europe, Carnforth, Lancashire, UK) served as external standards.

Free bilirubin was calculated from serum UCB and albumin levels, using a formula kindly provided by Dr. Silvia Gazzin and Dr. Claudio Tiribelli.

Gunn rat liver sample preparation. Hyperbilirubinaemic Gunn rats (20 in total, 9 males and 11 females), homozygous for a mutation in *UGT1A1*, and the same number of normobilirubinaemic Wistar rats, heterozygous for a mutation in *UGT1A1*, were obtained from Charles University in Prague (Prague, Czech Republic) and acclimatized in the breeding facility of the Medical University of Vienna (Himberg, Austria). The animals were housed in plastic cages (Macrolon type IV; Techniplast), under standard conditions (24 ± 1 °C, humidity 50 ± 5 °C, 12 h light/dark cycle) and fed with a standard diet (ssniff R/M-H Extrudat; ssniff Spezialdiäten) and *ad libitum* access to fresh water. The animals were sacrificed at the 7–8-week of age. The study was approved by the committee of animal experiments of the Austrian Federal Ministry of Science and Research (BMF-66.006/0008-II/3b/2011), and was carried out in accordance with the approved guidelines. Frozen liver samples, were used for DNA extraction. After thawing, not more than 20 mg rat liver was harvested and homogenized in ALT buffer (DNeasy Blood and Tissue Kit, QIAGEN) and Proteinase K. The samples were incubated at 37 °C overnight, until complete lysis. DNA extraction was completed the next day, using the kit manufacturer's standard protocol. Purity of the samples was determined by Nanodrop 2000c spectrophotometer (Thermo Scientific), and double stranded DNA concentration was measured by QuantiFluor® dsDNA System (Promega).

For UCB measurement, cells and tissue samples were homogenized in HPLC mobile phase and prepared as described in the previous paragraph. Protein concentrations were measured using the Bradford reagent (Sigma Aldrich), as instructed by the manufacturer.

DNA extraction from PBMCs and concentration measurement. DNA from human PBMCs was extracted from two million cells, using DNeasy Blood and Tissue Kit (QIAGEN), according to manufacturer's instructions. DNA concentration was measured using the QuantiFluor® dsDNA System (Promega), as a plate-based assay. A random subset of samples were measured using NanoDrop 2000c spectrophotometer (Thermo Scientific) and DNA integrity was estimated by agarose gel electrophoresis. Samples were stored at −20 °C, for no longer than 6 months prior to analysis.

Absolute telomere length measurement in PBMCs by qPCR. Telomere length measurement was performed as described[39], with modifications. Shortly, SYBR Select Master Mix (Life Technologies) was used to amplify telomeric sequences and SCG (36b4). Primers were used at a final concentration of 100 nM. Primer sequences are shown in supplementary Table S6. Genomic DNA samples were diluted to a concentration of 2.5 ng/μl, and 4 μl were used in each reaction (10 ng/reaction). 84-base oligonucleotide standards were diluted to a stock solution of 50 pg/μl. To generate a telomere standard curve, 10-fold serial dilutions of the stock solution were prepared. For the SCG standard curve, the stock solution was diluted to 0.5 ng/μl, and serial dilutions were prepared thereof. All samples and standards were run in triplicate. Assays were run on an ABI 7300 Real-Time PCR System (Life Technologies), using a transparent 96-well plate and optical seals (4titude®).

Analyses were performed at a manual threshold of 2.461 for both targets, with a qPCR efficiency ranging between 90–110%. Samples with a standard deviation exceeding 0.5 Ct were excluded from the analysis. Absolute telomere length was calculated as kb/telomere as previously described[39].

Relative telomere length measurement in liver by qPCR. For measuring rat liver TL, we used a similar method to the one described above, on a QuantStudio™ 6 Flex Real-Time PCR System (Thermo Fisher), using a 384-well block, in a single run. Relative telomere length was calculated as 2^dCt (dCt = Ct(Telomere) – Ct(36b4)).

Intracellular cytokines. IL-6, IL-1b and TNF were measured in monocytes following the standard intracellular protein staining protocol (BD) using a FACSCalibur (BD) flow cytometer. Briefly, heparinized whole blood was treated with brefeldin A solution for 4 h, to block cytokine excretion. Red blood cells were lysed (Cell Lysis Solution 1:10, BD) and cells were stained with CD14 surface antibody (Biolegend). In the next step, cells were permeabilised (Permeabilizing Solution 2, 1:10, BD), and treated with intracellular antibodies against IL-6, IL-1b and TNF (BD). Cells were measured immediately following fixation and relative fluorescence intensity was estimated against isotype control.

Ferric Reduction Ability of Plasma (FRAP) assay. The reducing capacity in serum was measured using the FRAP assay[40]. The method is based on the reduction of ferric (Fe^{3+}-) tripyridyl triazine resulting in the blue-coloured ferrous (Fe^{2+}-) tripyridyl triazine complex. All samples were analysed at wavelength of 593 nm, on a BMG FLUOstar OPTIMA Microplate Reader (BMG LABTECH GmbH) in triplicate in a 96-well format. Ascorbic acid served as standard, and results were expressed as Trolox equivalents in μmol/l.

GSH/GSSG. Oxidized and reduced glutathione were measured using N-Ethylmaleimide and O-phthalaldehyde, as described previously[41]. All samples were analysed in triplicates using external GSSG and GSH standards, in a 96-well plate fluorometer (BMG FLUOstar OPTIMA Microplate Reader, BMG LABTECH GmbH).

MDA. MDA levels were determined in plasma as described earlier[42]. The samples were neutralized after heating (60 min, 100 °C) with methanol/NaOH, centrifuged (3 min, 3000 rpm) and MDA was measured with high-performance liquid chromatography (HPLC) (excitation: λ 532 nm, emission: λ 563 nm, LaChrom Merck Hitachi Chromatography System, Vienna, Austria; HPLC column (125 × 4 mm, 5 μm; Merck, Vienna, Austria). Each sample was analysed in duplicate.

UGT1A1 Genotyping. DNA for UGT1A1 genotyping was extracted from whole blood, using the QIAsymphony SP automated system with QIAsymphony DSP DNA Midi Kit (QIAGEN), according to manufacturer's instructions.

Analyses were performed as described previously[43]. Primers and probes were used as 10 μM working solutions. LightCycler FastStart DNA Master HybProbe Mix (Roche) was used on a LightCycler 480 Instrument II (Roche). Alleles were determined according to the melting curves obtained.

Statistical analysis. The current study is of explorative nature without a specified primary outcome parameter. The sample size calculation was done taking in account data from a previous study in hyperbillirubinemic humans[44] where based on the assumption of a difference in DNA damage of 12 ± 2.5% vs 10 ± 2.5% (non-GS vs GS) with a type I error of 0.05 and type 2 error of 0.1 a sample size of 33 persons per group was calculated. For the current study we doubled the sample size.

Statistical analyses were done using SPSS (version 21, IBM). Paired Student's t-test or Mann Whitney U test were performed to evaluate the differences between cases and controls. Bivariate correlations were evaluated using either Pearson or Spearman coefficients, depending on data distribution. PCA and bi-clustering analysis were performed using COVAIN toolbox for MATLAB[27]. The bi-clustering uses average linkage of

Euclidean distance between groups as the metric. Plots were created using the Matplotlib library for Python 2.7 and 3.3.

References

1. Radu, P. & Atsmon, J. Gilbert's syndrome - Clinical and pharmacological implications. *Israel Medical Association Journal*. **3(8),** 593–598 (2001).
2. Kapitulnik, J. Bilirubin: An endogenous product of heme degradation with both cytotoxic and cytoprotective properties. *Molecular Pharmacology*. **66(4),** 773–779 (2004).
3. Lightner, D. A. Bilirubin: Jekyll and Hyde pigment of life; pursuit of its structure through two world wars to the new millenium. *Prog Chem Org Nat Prod*. **98,** 1–776 (2013).
4. Klatskin, G. Bile pigment metabolism. *Annu Rev Med*. **12,** 211–50 (1961).
5. Schmid, R. & McDonagh, A. F. The enzymatic formation of bilirubin. *Ann N Y Acad Sci*. **244,** 533–52 (1975).
6. Wagner, K. H. *et al.* Looking to the horizon: the role of bilirubin in the development and prevention of age-related chronic diseases. *Clin Sci (Lond)*. **129(1),** 1–25 (2015).
7. Ostrow, J. D. *et al.* Molecular basis of bilirubin-induced neurotoxicity. *Trends Mol Med*. **10(2),** 65–70 (2004).
8. Sedlak, T. W. & Snyder, S. H. Bilirubin benefits: Cellular protection by a biliverdin reductase antioxidant cycle. *Pediatrics*. **113(6),** 1776–1782 (2004).
9. Bosma, P. J. *et al.* The Genetic Basis of the Reduced Expression of Bilirubin UDP-Glucuronosyltransferase 1 in Gilbert's Syndrome. *New England Journal of Medicine*. **333(18),** 1171–1175 (1995).
10. Zhou, J., Tracy, T. S. & Remmel, R. P. Correlation between Bilirubin Glucuronidation and Estradiol-3-Gluronidation in the Presence of Model UDP-Glucuronosyltransferase 1A1 Substrates/Inhibitors. *Drug Metabolism and Disposition*. **39(2),** 322–329 (2011).
11. Horsfall, L. J., Nazareth, I. & Petersen, I. Cardiovascular Events as a Function of Serum Bilirubin Levels in a Large, Statin-Treated Cohort. *Circulation*. **126(22),** 2556–2564 (2012).
12. Lin, J. P. *et al.* Association between the UGT1A1*28 allele, bilirubin levels, and coronary heart disease in the Framingham heart study. *Circulation*. **114(14),** 1476–1481 (2006).
13. Horsfall, L. J. *et al.* Gilbert's syndrome and the risk of death: a population-based cohort study. *J Gastroenterol Hepatol*. **28(10),** 1643–7 (2013).
14. Schwertner, H. A. & Vitek, L. Gilbert syndrome, UGT1A1*28 allele, and cardiovascular disease risk: possible protective effects and therapeutic applications of bilirubin. *Atherosclerosis*. **198(1),** 1–11 (2008).
15. Wallner, M. *et al.* Protection from age-related increase in lipid biomarkers and inflammation contributes to cardiovascular protection in Gilbert's syndrome. *Clin Sci (Lond)*. **125(5),** 257–64 (2013).
16. Brito, M. A. *et al.* Bilirubin injury to neurons: contribution of oxidative stress and rescue by glycoursodeoxycholic acid. *Neurotoxicology*. **29(2),** 259–69 (2008).
17. Franceschi, C. & Campisi, J. Chronic Inflammation (Inflammaging) and Its Potential Contribution to Age-Associated Diseases. *Journals of Gerontology Series a-Biological Sciences and Medical Sciences*. **69,** S4–S9 (2014).
18. Finkel, T. & Holbrook, N. J. Oxidants, oxidative stress and the biology of ageing. *Nature*. **408(6809),** 239–247 (2000).
19. Lepez-Otin, C. *et al.* The Hallmarks of Aging. *Cell*. **153(6),** 1194–1217 (2013).
20. Blackburn, E. H., Greider, C. W. & Szostak, J. W. Telomeres and telomerase: the path from maize, Tetrahymena and yeast to human cancer and aging. *Nat Med*. **12(10),** 1133–8 (2006).
21. Blasco, M. A. Telomeres and human disease: ageing, cancer and beyond. *Nat Rev Genet*. **6(8),** 611–22 (2005).
22. Richter, T. & von Zglinicki, T. A continuous correlation between oxidative stress and telomere shortening in fibroblasts. *Experimental Gerontology*. **42(11),** 1039–1042 (2007).
23. Haycock, P. C. *et al.* Leucocyte telomere length and risk of cardiovascular disease: systematic review and meta-analysis. *BMJ*. **349,** g4227 (2014).
24. Nilsson, P. M. *et al.* Telomeres and cardiovascular disease risk: an update 2013. *Translational Research*. **162(6),** 371–380 (2013).
25. Gunn, C. H. Hereditary acholuric jaundice - In a new mutant strain of rats. *Journal of Heredity*. **29(4),** 137–139 (1938).
26. Daniali, L. *et al.* Telomeres shorten at equivalent rates in somatic tissues of adults. *Nature Communications*. **4,** 1597, doi: 10.1038/ncomms2602 (2013).
27. Sun, X. L. & Weckwerth, W. COVAIN: a toolbox for uni- and multivariate statistics, time-series and correlation network analysis and inverse estimation of the differential Jacobian from metabolomics covariance data. *Metabolomics*. **8(1),** S81–S93 (2012).
28. Golubovskaya, V. M. *et al.* Expression of telomerase in normal and malignant rat hepatic epithelia. *Oncogene*. **15(10),** 1233–40 (1997).
29. Wong, J. Y. Y. *et al.* The Relationship between Inflammatory Biomarkers and Telomere Length in an Occupational Prospective Cohort Study. *Plos One*. **9(1),** e87348, doi: 10.1371/journal.pone.0087348 (2014).
30. Baylis, D. *et al.* Inflammation, telomere length, and grip strength: a 10-year longitudinal study. *Calcif Tissue Int*. **95(1),** 54–63 (2014).
31. Molzer, C. *et al.* Extracellular and intracellular anti-mutagenic effects of bile pigments in the Salmonella typhimurium reverse mutation assay. *Toxicol In Vitro*. **27(1),** 433–7 (2013).
32. Raijmakers, M. T. M. *et al.* Association of human liver bilirubin UDP-glucuronyltransferase activity with a polymorphism in the promoter region of the UGT1A1 gene. *Journal of Hepatology*. **33(3),** 348–351 (2000).
33. Monaghan, G. *et al.* Genetic variation in bilirubin UDP-glucuronosyltransferase gene promoter and Gilbert's syndrome. *Lancet*. **347(9001),** 578–581 (1996).
34. Bar, C. *et al.* Telomerase expression confers cardioprotection in the adult mouse heart after acute myocardial infarction. *Nat Commun*. **5,** 5863 (2014).
35. Bakrania, B. *et al.* Pre- or post-ischemic bilirubin ditaurate treatment reduces oxidative tissue damage and improves cardiac function. *Int J Cardiol*. **202,** 27–33 (2015).
36. Ben-Amotz, R. *et al.* Intraperitoneal bilirubin administration decreases infarct area in a rat coronary ischemia/reperfusion model. *Front Physiol*. **5,** 53 (2014).
37. Wallner, M. *et al.* Haem catabolism: a novel modulator of inflammation in Gilbert's syndrome. *Eur J Clin Invest*. **43(9),** 912–9 (2013).
38. Roubenoff, R. *et al.* Application of bioelectrical impedance analysis to elderly populations. *J Gerontol A Biol Sci Med Sci*. **52(3),** M129–36 (1997).
39. O'Callaghan, N. J. & Fenech, M. A quantitative PCR method for measuring absolute telomere length. *Biol Proced Online*. **13,** 3 (2011).
40. Benzie, I. F. & Strain, J. J. The ferric reducing ability of plasma (FRAP) as a measure of "antioxidant power": the FRAP assay. *Anal Biochem*. **239(1),** 70–6 (1996).
41. Boon, A. C. *et al.* Reduced circulating oxidized LDL is associated with hypocholesterolemia and enhanced thiol status in Gilbert syndrome. *Free Radical Biology and Medicine*. **52(10),** 2120–2127 (2012).
42. Ramel, A., Wagner, K. H. & Elmadfa, I. Plasma antioxidants and lipid oxidation after submaximal resistance exercise in men. *Eur J Nutr*. **43(1),** 2–6 (2004).

43. von Ahsen, N., Oellerich, M. & Schutz, E. DNA base bulge vs unmatched end formation in probe-based diagnostic insertion/deletion genotyping: genotyping the UGT1A1 (TA)(n) polymorphism by real-time fluorescence PCR. *Clin Chem.* **46(12),** 1939–45 (2000).
44. Wallner, M. *et al.* Anti-genotoxic potential of bilirubin *in vivo*: damage to DNA in hyperbilirubinemic human and animal models. *Cancer Prev Res (Phila).* **6(10),** 1056–63 (2013).

Acknowledgements

The authors want to thank Annemarie Grindel and Daniel Simon for performing the GSH/GSSG measurements and Daniel Simon for data input; Nazli Khoei for performing a rat TL measurement; Petra Hinterleitner and George Mare for assisting sample preparation; George Mare for performing MDA measurements; Dr. Xiaoliang Sun for assisting with the statistical analyses; Dr. Silvia Gazzin and Dr. Claudio Tiribelli for assistance with free BR calculations; Stefan Badelt and Dr. Nick Fulcher for critically reading and revising the manuscript. The research was funded by the research platform Active ageing at the University of Vienna, and the Grant of the Austrian National Bank, Project No. 14541. This article was supported by the Open Access Publishing Fund of the University of Vienna.

Author Contributions

A.T., C.M. and M.W. designed and established the majority of the experiments and methods; M.J. prepared the DNA samples and performed the qPCR assays; U.S. performed the FRAP assay and prepared DNA extracts from rat liver; C.K. performed the HPLC measurements; A.T., C.M., M.W., M.J. and C.K. processed the blood samples; M.W. prepared the rat liver samples and measured UCB in rat tissues; A.T. and W.W. did the statistical analyses; C.M., M.W., R.M., D.D. and K.H.W. designed and conceived the human study; R.M. and D.D. oversaw the routine clinical measurements; K.H.W. provided financial support; A.T. made the figures; A.T. wrote the manuscript; all authors critically revised the manuscript.

Additional Information

Supplementary information accompanies this paper at http://www.nature.com/srep

Competing financial interests: The authors declare no competing financial interests.

How to cite this article: Tosevska, A. *et al.* Longer telomeres in chronic, moderate, unconjugated hyperbilirubinaemia: insights from a human study on Gilbert's Syndrome. *Sci. Rep.* **6**, 22300; doi: 10.1038/srep22300 (2016).

This work is licensed under a Creative Commons Attribution 4.0 International License. The images or other third party material in this article are included in the article's Creative Commons license, unless indicated otherwise in the credit line; if the material is not included under the Creative Commons license, users will need to obtain permission from the license holder to reproduce the material. To view a copy of this license, visit http://creativecommons.org/licenses/by/4.0/

3.1 SUPPLEMENTARY MATERIAL

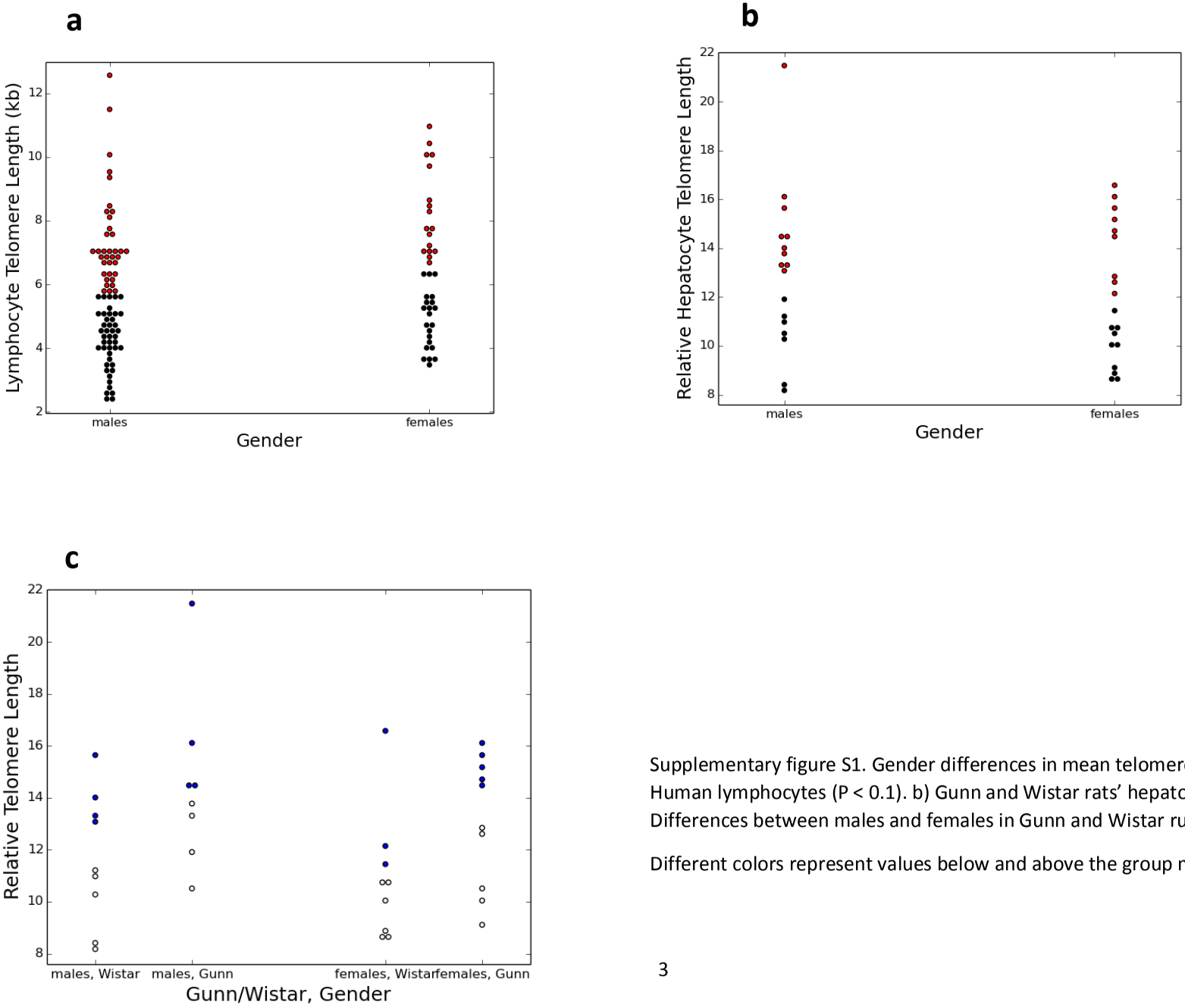
Supplementary data for *"Longer telomeres in chronic, moderate, unconjugated hyperbilirubinaemia: insights from a human study on Gilbert's Syndrome"*

Tosevska A.[1]*, Moelzer C.[2], Wallner M.[2,3], Janosec M.[2], Schwarz U.[2], Kern C.[2,4], Marculescu R.[5], Doberer D.[6], Weckwerth W.[7,8], Wagner K. H.[1, 2]*

1 Research Platform Active Ageing, University of Vienna, Austria
2 Department of Nutritional Sciences, University of Vienna, Althanstrasse 14, 1090 Vienna, Austria
3 Institute of Dietetics and Nutrition, University of Applied Sciences, FH JOANNEUM, Alte Poststraße 149, 8020 Graz, Austria
4 Institute of Pharmacology, Medical University of Vienna, Waehringer Str. 13a, 1090 Vienna, Austria
5 Clinical Institute of Laboratory Medicine, Medical University of Vienna, Waehringer Guertel 18-20, 1090 Vienna, Austria,
6 Department of Clinical Pharmacology, Medical University of Vienna, Waehringer Guertel 18-20, 1090 Vienna, Austria
7 Department of Ecogenomics and Systems Biology, University of Vienna, Althanstrasse 14, 1090 Vienna, Austria
8 Vienna Metabolomics Center (VIME), University of Vienna, Austria

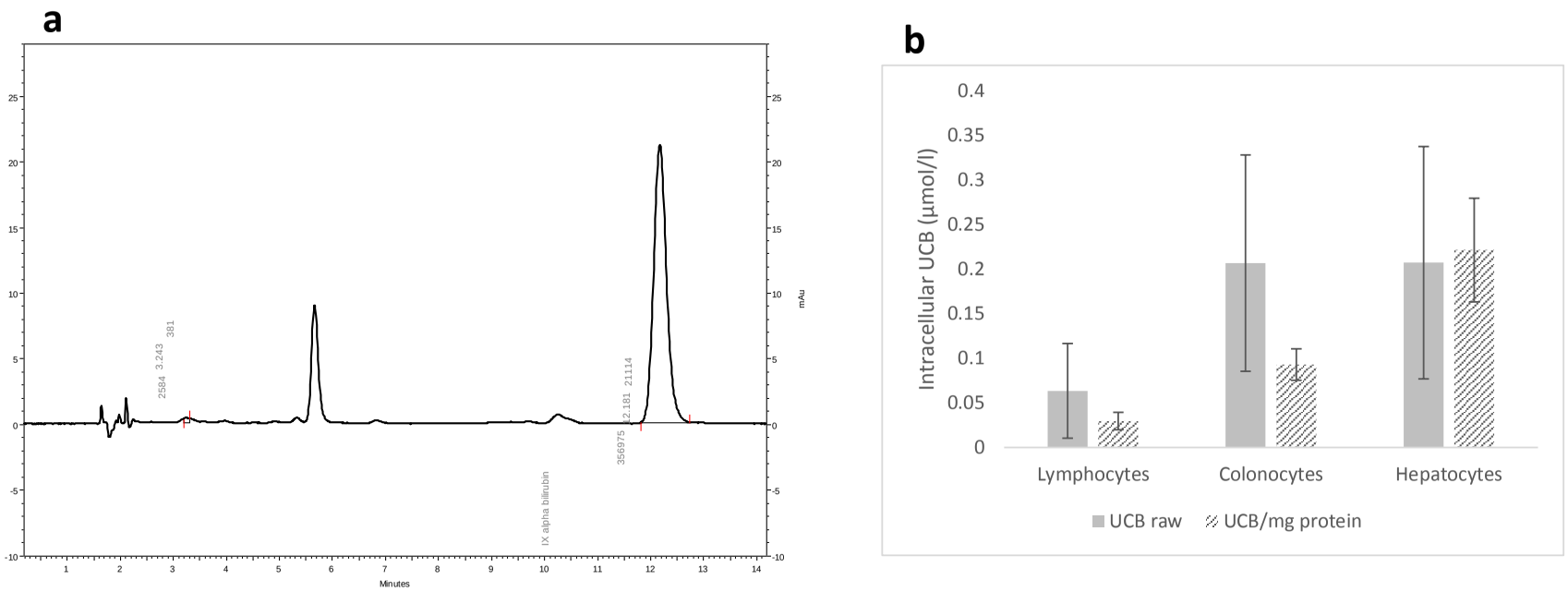
List of abbreviations:

BMI = Body mass index
BP = Blood pressure
CO-Hb = Carboxyhaemoglobin
CRP = C-reactive protein
FRAP = Ferric reducing ability of plasma
GSH/GSSG = Reduced/oxidized glutathione
HCY = Homocysteine
HOMA-IR = Homeostatic model assessment – insulin resistance
IL = Interleukin
MAP = Mean arterial pressure
MDA = Malondialdehyde
PLA2 = Phospholipase A2
SAA = Serum amyloid alpha
TL = Telomere Length
TNF = Tumor necrosis factor



Supplementary figure S1. Gender differences in mean telomere length in a) Human lymphocytes ($P < 0.1$). b) Gunn and Wistar rats' hepatocytes (n.s.) c) Differences between males and females in Gunn and Wistar ruts separately.

Different colors represent values below and above the group mean.



Supplementary figure S2. UCB measurements in human serum and rat lymphocytes, hepatocytes and colonocytes. a) A representative chromatogram of unconjugated bilirubin measurement in serum. Only IX-α Bilirubin isomer is detectable in serum samples and tissue samples derived from rats. No peak present in human lymphocytes. b) Intracellular content of UCB in Gunn rat lymphocytes, colonocytes and hepatocytes. Error bars represent standard deviation.

Supplementary Table S1. Gender differences in mean values between GS and non-GS individuals. Values are presented as mean ± standard deviation. The indices represent different levels of significance obtained using two-tailed independent samples T-test:

[a] $P < 0.05$, [aa] $P < 0.01$ when comparing females to males within the same condition (GS or control), *$P < 0.05$, **$P < 0.01$ when comparing GS to controls of the same gender, [b] $P < 0.1$ females compared to males within the same condition (GS or control), [#] $P < 0.1$ GS compared to controls of the same gender.

The variable sample sizes presented are due to missing values in some of the parameters.

	Control		*GS*	
	Males (n = 36-40)	Females (n = 19-20)	Males (n = 37-40)	Females (n = 18-20)
Age (years)	36 ± 14	41 ± 14	36 ± 14	41 ± 14
UCB (µmol/l)	9.65 ± 3.53	8.35 ± 3.05	35.21 ± 10.53**	28.94 ± 6.85[a]**
Lymph. TL (kb)	5.10 ± 2.00	6.19 ± 2.12[b]	6.20 ± 1.87*	6.52 ± 2.03
BMI (kg/m^2)	25.74 ± 5.15	24.66 ± 4.42	23.34 ± 3.07*	21.75 ± 2.71[a]*
Body fat (%)	21.82 ± 7.37	30.76 ± 7.77[aa]	20.90 ± 6.05	24.42 ± 6.96[b]*
CO-Hb (%)	1.42 ± 0.85	1.13 ± 0.30[b]	1.23 ± 0.30	1.18 ± 0.44
Heme (µmol/l)	0.77 ± 0.12	0.73 ± 0.09	0.74 ± 0.13	0.78 ± 0.18
Iron (µmol/l)	23.27 ± 8.98	22.79 ± 10.71	32.14 ± 10.73**	26.43 ± 7.32[a]
Albumin (g/l)	47.00 ± 3.18	45.75 ± 1.77[b]	48.06 ± 3.42	45.17 ± 2.15[aa]
Estradiol (pg/ml)	31.75 ± 9.91	117 ± 104.38[aa]	31.87 ± 11.71	70.20 ± 74.47[aa]
Testosterone (ng/ml)	5.60 ± 1.54	0.31 ± 0.14[aa]	6.12 ± 1.90	0.34 ± 0.13[aa]
HCY (µmol/l)	11.28 ± 3.87	8.77 ± 2.02[aa]	12.24 ± 5.20	9.28 ± 1.88[aa]
FRAP (mmol Fe^{2+}/l)	561 ± 91	518 ± 167	827 ± 170**	691 ± 169[aa]**
GSH/GSSG	1.15 ± 0.46	1.47 ± 0.32[aa]	1.11 ± 0.36	1.37 ± 0.42[a]
MDA (nmol/ml)	1.65 ± 0.55	1.95 ± 0.52[b]	1.75 ± 0.50	1.68 ± 0.47
IL6 (rfu)	2.58 ± 0.26	2.48 ± 0.31	2.35 ± 0.25**	2.40 ± 0.32
IL1β (rfu)	1.59 ± 0.28	1.41 ± 0.21[aa]	1.41 ± 0.23**	1.43 ± 0.33
TNF (rfu)	26.17 ± 5.24	25.13 ± 4.85	25.38 ± 5.92	26.37 ± 4.74

CRP (mg/dl)	0.17 ± 0.29	0.15 ± 0.18	0.10 ± 0.12	0.05 ± 0.05*
SAA (mg/dl)	4.62 ± 1.88	5.73 ± 2.78[b]	4.42 ± 1.34	4.31 ± 1.18*
Uric acid (mg/dl)	52.30 ± 18.36	38.85 ± 14.39[aa]	56.55 ± 14.52	40.15 ± 15.32[aa]
PLA2 (mg/dl)	32.60 ± 47.10	30.15 ± 42.34	43.65 ± 51.48	27.75 ± 34.20
BP systolic (mmHg)	136 ± 15	126 ± 15[a]	133 ± 11	123 ± 13[aa]
BP diastolic (mmHg)	71 ± 11	64.79 ± 11[b]	70.25 ± 10	60.94 ± 12[aa]
MAP (mmHg)	114 ± 12	105 ± 13[a]	111 ± 10	101 ± 11[aa]
HOMA_IR	1.84 ± 1.62	1.43 ± 0.90	1.11 ± 0.87*	1.00 ± 0.66[#]

Supplementary table S2. Gender differences in mean values between Gunn and Wistar rats. Values are presented as mean ± standard deviation. The indices represent different levels of significance obtained using two-tailed independent samples T-test:

[a] P < 0.05, [aa] P < 0.01comparing females to males within the same rodent model (Gunn/ Wistar), *P < 0.05, **P < 0.01 comparing Gunn to Wistar rats of the same gender, [b] P < 0.1 females to males within the same rodent model (Gunn/Wistar), [#] P < 0.1 comparing Gunn to Wistar rats of the same gender.

The variable sample sizes presented are due to missing values in some of the parameters.

	Wistar		*Gunn*	
	Males (n = 9)	Females (n = 9-11)	Males (n = 8-9)	Females (n = 10-11)
UCB (µmol/l)	0.58 ± 0.18	0.55 ± 0.20	97.88 ± 19.77**	112.38 ± 29.64**
Relative TL	11.66 ± 2.54	10.91 ± 2.47	14.46 ± 3.27[#]	13.12 ± 2.55[#]

Supplementary Table S3. Age differences in mean values in GS and non-GS individuals. Values are presented as mean ± standard deviation. The indices represent different levels of significance obtained using two-tailed independent samples T-test:

[a] $P < 0.05$, [aa] $P < 0.01$ when comparing individuals ≥ 35 years old to < 35 y.o. within the same condition (GS/control), *$P < 0.05$ comparing GS and control of the same age group, [b] $P < 0.1$ comparing individuals ≥ 35 years old to < 35 y.o. within the same condition (GS/control), [#] $P < 0.1$ comparing GS and control of the same age group.

The variable sample sizes presented are due to missing values in some of the parameters.

	Control		*GS*	
	< 35 y.o. (n = 30-33)	≥ 35 y.o. (n = 25-27)	< 35 y.o. (n = 30-33)	≥ 35 y.o. (n = 23-27)
Age (years)	27 ± 4	50 ± 11[aa]	27 ± 4	50 ± 11[aa]
UCB (µmol/l)	10.03 ± 3.63	8.22 ± 2.87[a]	33.57 ± 10.12**	32.57 ± 9.69**
Lymph. TL (kb)	5.83 ± 2.10	5.02 ± 2.01	6.57 ± 2.17	5.99 ± 1.52[#]
BMI (kg/m^2)	23.43 ± 3.74	27.77 ± 5.15[aa]	22.61 ± 3.01	23.06 ± 3.09**
Body fat (%)	21.30 ± 5.58	29.33 ± 9.61[aa]	22.23 ± 6.06	21.79 ± 7.12**
CO Hb (%)	1.15 ± 0.37	1.53 ± 0.97[a]	1.26 ± 0.43	1.14 ± 0.18*
Heme (µmol/l)	0.75 ± 0.11	0.77 ± 0.11	0.74 ± 0.13	0.77 ± 0.16
Iron (µmol/l)	25.47 ± 9.53	20.20 ± 8.75[a]	31.31 ± 10.45*	29.06 ± 9.63*
Albumin (g/l)	47.15 ± 3.07	45.88 ± 2.39[b]	47.91 ± 3.68	46.11 ± 2.59 [a]
Estradiol (pg/ml)	62.00 ± 71.49	57.78 ± 74.29	38.58 ± 25.87[#]	52.85 ± 65.00
Testosterone (ng/ml)	4.51 ± 2.80	2.91 ± 2.62	4.86 ± 3.14	3.27 ± 3.00
HCY (µmol/l)	10.38 ± 3.95	10.56 ± 3.04	12.22 ± 5.68	10.11 ± 2.41 [a]
FRAP (mmol Fe^{2+}/l)	568 ± 106	521 ± 139	806 ± 190**	748 ± 166**
GSH/GSSG	1.17 ± 0.45	1.37 ± 0.41[b]	1.17 ± 0.41	1.22 ± 0.40
MDA (nmol/ml)	1.68 ± 0.58	1.83 ± 0.52	1.77 ± 0.50	1.68 ± 0.46
IL-6 (rfu)	2.56 ± 0.30	2.54 ± 0.26	2.35 ± 0.26**	2.38 ± 0.29*
IL1-β (rfu)	1.53 ± 0.24	1.53 ± 0.31	1.43 ± 0.23	1.40 ± 0.30

TNF (rfu)	26.34 ± 4.97	25.19 ± 5.27	26.73 ± 5.34	24.56 ± 5.59
CRP (mg/dl)	0.10 ± 0.10	0.25 ± 0.35[a]	0.07 ± 0.07	0.10 ± 0.14*
SAA (mg/dl)	4.54 ± 1.55	5.54 ± 2.84[b]	4.18 ± 0.86	4.64 ± 1.65
Uric acid (mg/dl)	47.36 ± 17.31	48.37 ± 19.50	50.76 ± 20.38	51.48 ± 10.69
PLA2 (mg/dl)	33.61 ± 44.39	29.56 ± 46.97	38.12 ± 49.48	38.63 ± 44.11
BP systolic (mmHg)	131.10 ± 16.71	134.44 ± 14.58	128.97 ± 12.73	131.19 ± 13.56
BP diastolic (mmHg)	66.61 ± 13.10	72.07 ± 9.75[b]	66.06 ± 9.55	68.96 ± 14.38
MAP (mmHg)	109.17 ± 14.00	113.24 ± 11.32	107.58 ± 10.57	110.03 ± 12.19
HOMA_IR	1.22 ± 0.77	2.32 ± 1.79[aa]	1.00 ± 0.49	1.17 ± 1.05**

Supplementary table S4. Percentage of individuals carrying the GS-related (7/7) genotype among the 2 phenotypes: 6/6 - homozygotes with alleles containing 6 TA – repeats (short allele), 6/7 - heterozygotes with one short and one long allele, 7/7- homozygotes with two 7-TA long alleles.

		GS Phenotype		Total %
		no	yes	
UGT1A1 Genotype	6/6	43 %	2 %	26
	6/7	52 %	9 %	35
	7/7	5 %	89 %	54
Total N		58	57	115

Supplementary table S5. Descriptive values of UGT1A1 genotypes (6/6 wildtype homozygous, 6/7 heterozygous, 7/7 homozygous with reduced UGT1A1 activity). Values are expressed as mean ± standard deviation. *P < 0.05, **P < 0.01, #P < 0.1; Kruskal-Wallis ANOVA for nonparametric data.

	Genotype		
	6/6 (n = 25)	6/7 (n = 34)	7/7 (n = 52)
Age (years)	37 ± 14	36 ± 15	39 ± 14
Female gender (%)	31	31	35
UCB (µmol/l)**	9.27 ± 3.67	12.74 ± 9.07	31.93 ± 10.90
Lymphocyte telomere length (kb)*	5.22 ± 1.88	5.70 ± 2.27	6.33 ± 1.91
BMI (kg/m^2)#	25.32 ± 4.91	25.08 ± 4.87	23.12 ± 3.30
Iron (µmol/l)	23.94 ± 8.49	26.96 ± 12.44	27.84 ± 9.72

Supplementary table S6. Oligos used for qPCR-based telomere length measurement. Oligos a-e were designed according to (O'Callaghan and Fenech 2011).

Target/name	Species	Sequence (5'-3')	Amplicon size
Telomere standard[a]	Human/rodent	$(TTAGGG)_{14}$	84bp
36B4 standard[b]	Human	CAGCAAGTGGGAAGGTGTAATCCGTCTCCACAGACAAGGCCAGGAC TCGTTTGTACCCGTTGATGATAGAATGGG	75bp
Telomere F primer[c]	Human/rodent	CGGTTTGTTTGGGTTTGGGTTTGGGTTTGGG TTTGGGTT	>76 bp
Telomere R primer	Human/rodent	GGCTTGCCTTACCCTTACCCTTACCC TTACCCTTACCCT	
36B4 F primer[d]	Human	CAGCAAGTGGGAAGGTGTAATCC	75bp
36B4 R primer[e]	Human	CCCATTCTATCATCAACGGGTACAA	
36B4 F primer	Rodent	AGGTCGAAGCAAAGGAAGAGTCG	84bp
36B4 R primer	Rodent	CTGACTTGGTGTGAGGGGCTT	

References

O'Callaghan, N. J. and M. Fenech (2011). "A quantitative PCR method for measuring absolute telomere length." Biol Proced Online **13**: 3.

4

IN VITRO ANTIOXIDATIVE CAPACITY OF UNCONJUGATED BILIRUBIN AGAINST OXIDATIVE LESIONS IN TELOMERES

4.1 IN VITRO EXPERIMENTS USING PRIMARY PBMCS AND BILIRUBIN

The antioxidant potential of UCB has already been discussed previously (chapters 1 and 3). In the light of previous findings we hypothesized that UCB exerts a protective effect on telomeres at least partly via reducing the extent of oxidative damage that can occur in telomeres. For that purpose, we decided to establish a short-term primary cell culture model consisting of human PBMCs. These cells would be extracted from whole blood of healthy volunteers and cultured without propagation until further treatment and analysis. This experiments were primarily carried out to assess the antioxidant capacity of UCB in culture against formation of oxidative lesions in the telomeric sequence. Cells treated with H_2O_2 were used as positive control for oxidative damage in telomeres.

The results presented in this chapter are only preliminary and have not been published.

4.2 OXIDATIVE DAMAGE IN TELOMERES

Oxidative damage of DNA occurs rather frequently, and results in a chemical change of the bases in DNA. The most common oxidative products are 8-oxo-7,8-dihydroguanine (8-oxo-dG) and 2,6-diamino-4-hydroxy-5-formamidopyrimidine (FapyG), both derived from oxidative modification of guanine [Wang et al., 2010]. As telomeric repeats are G-rich due to their stretch of guanine triplets, they are very susceptible to 8-oxo-dG formation. The accumulation of unrepaired oxidized guanine lesions can induce single or double strand breaks (SSBs or DSBs) and GC to TA transition in the telomere [Coluzzi et al., 2014]. Additionally, telomeres with a high frequency of oxidative lesions cannot bind to the protective shelterin components efficiently, which might lead to telomere uncapping, telomere fusion and genomic instability [Opresko et al., 2005].

A human glycosilase hOGG1, part of the base excision repair (BER) pathway [Muftuoglu et al., 2006], is responsible for recognition and excision of these sites in humans. This enzyme recognizes the erroneous base and removes it from the DNA stretch leaving an apurinic site. Another enzyme, called lyase is responsible for cutting the DNA backbone at an apurinic site, which can then be repaired appropriately. A bacterial enzyme isolated from E. coli called formamidopyrimidine [fapy]-DNA glycosylase (Fpg) has the same function as the human OGG1 and additional lyase activity. This enzyme is commonly used in experimental evaluation of the BER pathway, due to its higher stability and reproducibility compared to the hOGG1 enzyme.

In comparison to established cell lines PBMCs differ greatly with regards to their mitotic potential since they are quiescent, meaning they do not readily divide unless stimulated. Upon introduction to a mitogen, however, they start propagating, which is a useful feature for long-term maintenance of these cells in culture [Hofmann et al., 2010]. It is of note that, whereas most somatic cells do not express telomerase once they reach maturity, blood peripheral lymphocytes express fully active telomerase in order to maintain their telomeres during clonal expansion [Weng, 2002]. This is important to have in mind when using human PBMCs as a cell model for telomere length studies. Hence, for the following experiments we have only used non-stimulated PBMCs, in order to avoid any confounding effects from telomerase.

4.3 METHODS

4.3.1 *Solubilisation of Unconjugated Bilirubin*

Unconjugated bilirubin ($C_{33}H_{36}N_4O_6$) is an organic heterocyclic component, with a molar mass of 584.67 g/mol. It is classified as a member of the tetrapyrrol family. According to HMDB[1] it has a water solubility of 0.0096 mg/ml at room temperature, making it a very hydrophobic molecule. Interestingly, the solubility of UCB in apolar solvents has also been reported to be very poor [Brodersen, 1979].

Solubilisation of UCB in water is practically impossible at a concentration that allows for accurate weighing. To this end, the UCB isomer IXα (> 90% purity) was prepared as a stock solution in DMSO at a concentration no greater than 20 µmol/l. In order to assist solubilisation, the mixture was incubated in an ultrasonic bath for no longer than 10 min, on ice. As UCB is photosensitive [McDonagh, 2008], the entire procedure had to be conducted in a dark room and, ideally, using brown or amber glass- or plastic ware. The solution has a bright orange colour with no visible particles. A change of colour from deep orange to dark indicates oxidative changes in the molecule. The prepared stock solution can be stored at -80°C for several months or at +4°C for several days. Repetitive freeze-thaw cycles are not recommended, as they lead to oxidation and degradation of the bilirubin IXα.

4.3.2 *HPLC method for bilirubin concentration measurement*

In order to determine the concentration of unconjugated bilirubin in different biological or chemical samples, a previously developed high performance liquid chromatography (HPLC) method was used [Wallner et al., 2013]. The method is based on reverse-phase chromatography, using a Fortis C18 HPLC column (dimensions 4.6 x 150

1 http://www.hmdb.ca/metabolites/HMDB00054

mm, 3 µm). The mobile phase was an isocratic mixture of 0.1 mol/l n-dioctylamine in methanol/water (95:5 v/v) and glacial acetic acid (6.01 g/l). Samples were prepared by adding 160 µl mobile phase to 40 µl test sample and centrifugation. After centrifugation 50 µl of the clear supernatant containing free bilirubin was injected to the system at a flow of 1 ml/min. The retention time of the IXα peak was between 8 and 13 min. A standard curve was constructed using unconjugated bilirubin IXα (Frontier Scientific; purity of > 99%; 3.3% IIIα, 92.8% IXα and 3.9% XIIIα isomers).

4.3.3 *PBMCs isolation and cultivation*

Isolation of primary PBMCs from blood for culturing purpose has to be performed in a sterile laminar flow hood. Additionally, all used materials and reagents had to be sterilized prior to being used. PBMCs were isolated from whole blood using a gradient centrifugation method. Ficoll solution packed as commercially available LeucoSep™tubes was used for separation. Non-chilled whole blood was collected in either EDTA or heparinized vacuum-collection tubes (Vacuette®) and slowly added to the LeucoSep tube. After 15 minutes of centrifugation at room temperature and without a break, a clear separation of erythrocytes, Ficoll and plasma was visible. The PBMC fraction was found on the interphase of the Ficoll and the lighter plasma, as mononuclear non-granulated cells are lighter than the Ficoll. In contrast, heavier red blood cells and granulocytes precipitated on the bottom of the tube. The collected interphase fraction was transferred in a new tube, and washed twice with cold sterile phosphate-buffered saline (PBS), then centrifuged at +4°C for 10 minutes at 3000rpm. The supernatant was discarded and the pellet containing PBMCs was used in subsequent experiments.

4.3.4 *Storage of viable PBMC*

Separated PBMCs can be cultured immediately after isolation, or cryopreserved in a freezing medium that allows them to stay viable for a prolonged storage. Best results are achieved with freshly isolated cells, however, if this approach is not suitable, cells can be frozen in a freezing media containing 90% foetal bovine serum (FBS) and 10% dimethyl sulfoxide (DMSO) at a maximum of 20 million cells per ml. It is recommended however that the cell density does not exceed 10 million cells/ml. In order to keep maximum cell viability and minimum cell damage, cells should be frozen at a rate of 1-3°C per minute, first in a -80°C freezer, and then they should be transferred to liquid nitrogen or nitrogen vapours for a long-term storage. We used Cool Cell (Biozym) to gradually cool down the cells to -80°C. Due to unavailability of a liquid nitrogen storage solution, we kept the cells at -80°C for maximum of 3 months, after which the cells were still viable. Thawing the cells was quick, 1-2 minutes at 37°C, followed by centrifugation and quick removal of the freezing media. Cells were washed once or

twice with sterile PBS, in order to remove any residual DMSO that could be potentially toxic for the cells.

4.3.5 *Cell count and viability*

Cell count and viability was determined right after separation of fresh PBMCs of after thawing of cryopreserved PBMCs. We used an automated cell counted (Countess II FL Automated Cell Counter, Thermo Fisher Scientific), based on a Trypan blue exclusion assay. Trypan blue is a lipophilic dye that easily penetrates the membranes of dead cells, whereas live cells are not stained. The stain was added to cell suspension in 1:1 ratio, and the mixture was added to pre-designed slides that can be imaged and analysed directly. It is important to have the machine properly calibrated before measurement. However, even following calibration, it is often impossible to avoid counting red blood cells, especially if the cells are counted immediately post-isolation. Furthermore, it is important to dilute the samples so that the cells can be accurately measured. The ideal density should be between 1x 10^5 to 1x10^6 /ml. Everything below 1x 10^4 and 3 x10^7 is above the accurate range of the machine and should be centrifuged and resuspended in a smaller volume or further diluted, respectively.

4.3.6 *Cultivation of human primary PBMCs*

PBMCs form suspension cultures in vitro, and can be cultivated in well plates, petri dishes, cell culture flasks or falcon tubes. For our experimental procedure we used 24-well plates and utilized only wells that had one outer border. The original cell culture medium was RPMI-1640 enriched with L-glutamate, supplemented with 10% heat inactivated fetal bovine serum (FBS) and 1% pyruvate. The culture conditions were 37°C and 5% CO2. Cells were maintained in culture for up to 21 days partial media exchange every 2-3 days (data not shown). The composition of serum free media (SFM), prepared according to Jeon et al. [2010], is shown in the table below:

Components of the SFM	Concentration (/l RPMI1640)
Bovine serum albumin	2.5 g
Insulin	5 mg
Ferric citrate	2 mg
Ethanolamine	1.22 mg
Fatty acids supp.	0.4 ml
L-glutamine	584 mg
Sodium pyruvate	110 mg
2-mercaptoethanol	0.78 mg
1-thioglycerol	5.41 mg
RPMI1640 nonessential amino acids	20 ml

4.3.7 *Cellular uptake of UCB in PBMCs*

Cells were treated with 17.1 µmol/l of UCB for 24h, and a 100 µl cell suspension aliquot was collected at 6h and 24h of incubation. Additionally, an aliquot of the cell media was collected at 3h, 6h and 24h of incubation. In order to estimate whether cells take up UCB from media, collected cells at each timepoint were lysed and the concentration of UCB in the lysate was measured by high-performance liquid chromatography (HPLC).

4.3.8 *Cellular and nuclear uptake of UCB measured by* flow cytometry

Cells were seeded at 1 million per ml in a 24 well plate. Control cells were resuspended in SFM with 0.1% DMSO, whereas treated cells were resuspended in SFM supplemented with 0.1% 17.1mmol/l stock solution of UCB in DMSO. The plates were incubated at 37°C and 5% CO2 and aliquots were taken after 6 and 24h. Moreover, cells treated with 17.1 µmol/l UCB were fractionated using the REAP protocol [Suzuki et al., 2010] up to the point when intact nuclei were produced. The nuclei were washed and measured with the flow cytometer without using any staining. Free bilirubin has a very weak fluorescent emission at around 500-550nm [Amin and Lamola, 2011]. Albumin-bound UCB has a much stronger fluorescent emission at the same wavelength [Lamola and Russo, 2014] so, we have utilized this property to measure any shift in the fluorescence observed in nuclei at FL1 that roughly corresponds to 530 nm, assuming that interactions of UCB with other proteins or lipids in the nucleus will yield measurable shift in fluorescence.

4.3.9 *Oxidative stress and cell cycle analysis by flow cytometry*

In order to evaluate oxidative stress or cell cycle changes induced by UCB, cells treated with 0.5, 1, 5, 10 and 17.1 µmol/l UCB and aliquots were taken after 3 and 6h post incubation. Cell cycle measurements were performed after 6h of incubation only. The oxidative stress levels were estimated after staining cells with DCFH-DA according to the protocol by citemolzer:2013. Briefly, 25 µmol/l dihydrofluorescein diacetate (DCFH-DA), both in DMSO, were added individually to incubated cells. DCFH-DA is cell permeable, and in the cell is cleaved by intracellular esterases to form DCFH, which is then non-specifically oxidized by hydroperoxides to the fluorescent 7'-dichlorodihydrofluorescein (DCF) (excitation wavelength: 498, emission: 522 nm; FL-1). After washing in PBS and prior to measurement, $1x10^6$ cells/ml were stained with DCFH (in falcon tubes) and were left to incubate for 20 min in the dark. Cell cycle analysis was performed using a FxCycle™PI/RNAse Solution (Thermo Scientific), carried out according to the supplied protocol by the manufacturer.

4.3.10 *An extended qPCR telomere assay for measuring oxidized guanine lesions in the telomere*

Cells were treated with 17.1 µmol/l UCB for 4h, after which H2O2 was added in selected wells (one without UCB as a positive control for oxidative stress and one with UCB as a test sample). Plates were incubated for additional 2h, after which cells were harvested and viability was estimated via Trypan blue exclusion test. All treatment resulted with at least 80% cell viability. Cells were washed and DNA was extracted immediately. This was followed by concentration measurement using Quanti Fluor ds DNA system and appropriate dilution of samples. We further used a method published by O'Callaghan et al. [2011], which follows similar principles to the method described in chapter 2 for absolute telomere length measurement with the difference that samples were pre-treated with Fpg, a bacterial DNA glycosylase that removes oxidized guanines from DNA and leaves a nick at the site. The idea is based on the fact that the Taq polymerase is less efficient in amplifying nicked sites; the more such sites are present in the template, the less efficient the amplification and the lower the Ct value obtained. The night before running qPCR samples were diluted to a concentration double than the concentration needed for the PCR reaction (for qPCR reactions using 2.5 ng/µl it was prepared at a concentration of 5 ng/µl). The sample was divided between 2 tubes labeled as FPG+ and FPG-. Both were supplied with 10X Neb Reaction buffer (New England Biolabs) to a final concentration of 1x Fpg (New England Biolabs) was added at 1 µl per reaction in the FPG+ tubes, which was replaced with nuclease-free water in the FPG- tube. Finally, nuclease-free water was added to both tubes, to a final volume twice the volume of the added sample. For example if 40 µl of 5 ng/µl sample was used, the volume of 10X Reaction buffer would be 8 µl

and the final reaction volume 80 µl. Both samples were incubated at 37°C for exactly 16h, and then cooled down quickly before running a qPCR (according to the method described in section 2.5). The results of this method can only be expressed relatively, as Fpg-treated vs. non-treated sample. Hence, the qPCR standards described in section 2.5.2 are not essential here. However, running a standard curve with each qPCR assay is recommended, in order to assess the qPCR efficiency for the specific run. The calculation was carried out using the obtained Ct values for both telo and 36b4 assays and enzyme treated and non-treated samples. The formula is ΔΔCt:

$$\Delta\Delta Ct = ({}^{FPG+}Ct_{telo} - {}^{FPG-}Ct_{telo}) - ({}^{FPG+}Ct_{36b4} - {}^{FPG-}Ct_{36b4})$$

where ${}^{FPG+}Ct_{telo}$ for instance, represents the Ct value obtained from qPCR, using primers for the telomere sequence in an sample treated with Fpg; whereas ${}^{FPG-}Ct_{36b4}$ is the Ct value obtained from qPCR, using primers for the single copy gene 36b4 in an sample without Fpg treatment. The final result can be further normalized to the non-treatment control or reference sample.

4.4 RESULTS

4.4.1 *UCB solubility in different cell culture media*

For the in vitro UCB treatment we choose the concentration of 17.1 µmol/l, which represents the cut-off point for Gilbert's Syndrome (GS) diagnosis in humans. Figure 8 shows the cellular uptake of UCB, measured by HPLC in cell lysates. Cell viability in 17.1 µmol/l of UCB was high after 6h, but decreased slightly after 24h (data not shown).

Furthermore, the measured concentration of UCB in the culture media was much lower than expected. Under the assumptions that bilirubin solubility will increase with higher levels of albumin, we increased the percentage of FBS in the media, a main source of bovine serum albumin (BSA) and measured the UCB concentrations after 1h incubation at 37°C. These results are presented in figure 9. The increase of bovine serum decreased the availability of measurable UCB. To test the concentrations of UCB in absence of serum we made series of experiments with RPMI only, RPMI enriched with albumin, and a newly composed SFM.

In order to measure the availability of UCB in SFM, we dissolved different starting concentrations of UCB and measured their concentrations. In parallel, we tested UCB availability in RPMI medium supplemented with BSA only, at a concentration of 2.5 g/l (same as in the SFM). The results are shown in figure 10.

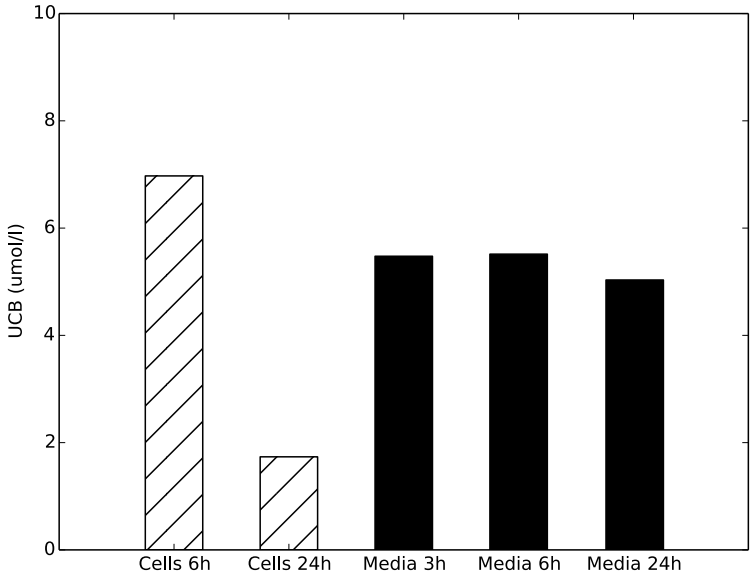


Figure 8: Concentration of UCB measured in cells or culture media after treatment with 17.1 µmol/l unconjugated bilirubin. Results in cells are only semi-quantitative, as no quantification of cells was possible.

Cell viability was tested in SFM, in order to make sure that the newly composed media had no adverse effects on the cells. After extended cultivation of PBMCs in SFM and RPMI supplemented with BSA only cells showed a viability over 75initial count of live cells is given in figure 11.

4.4.2 *UCB uptake, oxidative stress and cell cycle changes measured by flow cytometry*

We further estimated the cellular uptake of UCB by measuring fluorescent shift at 530nm from cells previously treated with UCB, compared to non-treated controls (figure 12, upper panel) Additionally we observed a small shift in fluorescence (figure 12, lower panel) in nuclei from cells previously treated with UCB compared to control cells.

We next estimated the induction of oxidative stress in cells treated with 0.5, 1, 5, 10 and 17.1 µmol/l UCB for 3 and 6h, using DCFH-DA, as described in the methods section. No change was observed in cells treated with UCB compared to non-treated control at a concentration up to 5 µmol/l after 3 or 6h, although a minor increase in

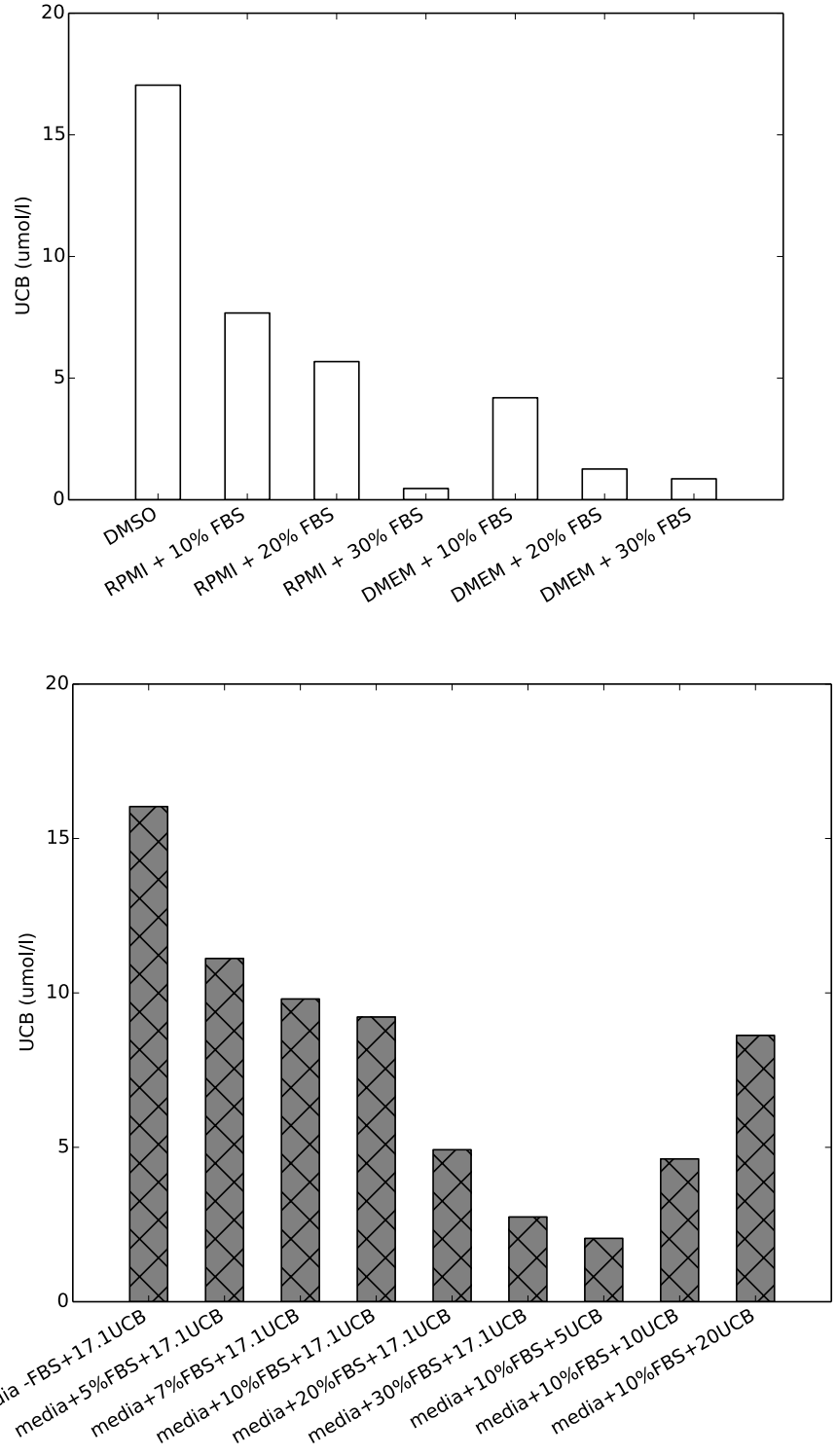


Figure 9: Measured concentration of UCB in two different media (RPMI and DMEM) supplemented with FBS; the initial concentration of UCB added in the media was 17.1 µmol/l (upper panel). Measured concentration of UCB in two different media (RPMI and DMEM) supplemented with FBS; the initial concentration of UCB added in the media was 17.1 µmol/l (lower panel). Measurements were done by HPLC.

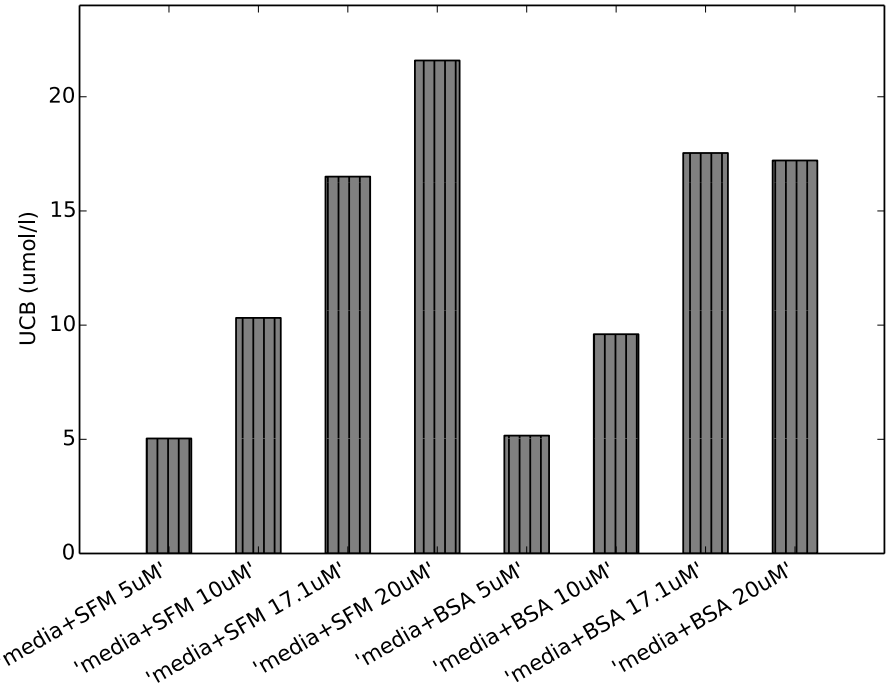


Figure 10: Availability of measurable UCB in serum free media (SFM) or RPMI supplemented with BSA only (BSA). Concentrations of added UCB vary between 5 and 17.1 µmol/l. Measurements were done by HPLC.

fluorescence was observed in the 10 µmol/l UCB sample after 3h and 17 µmol/l after 6h.

Additionally, no considerable change was observed in the cell cycle progression of PBMCs treated with UCB (figure 13, upper panel). In contrast, when treated with the putative positive control, 100 µmol/l of H_2O_2, not only the percentage of cells undergoing apoptosis increased, but also a substantial number of cells shifted to S and G2 phase in the overnight treatment (figure 13, lower panel).

4.4.3 *Oxidized guanine lesions in the telomeric sequence*

H_2O_2 at 100 µmol/l exhibited an increase in Fpg-sensitive lesions in telomeres after 2h of incubation (figure 14). Hence, this treatment was chosen as a positive control in the assessment of the protective effects of UCB against H_2O_2-induced oxidative lesions in telomeres. Interestingly, in some of the initial experiments, PBMCs treated with H_2O_2 for 2h showed an increase in telomere length. However, this effect could not be observed in any later experiments. At the same time, the 30% H_2O_2 with stabilizer, from Sigma Aldrich has been replaced with a similar product containing a different stabilizer, which might explain the discrepancy in the observation.

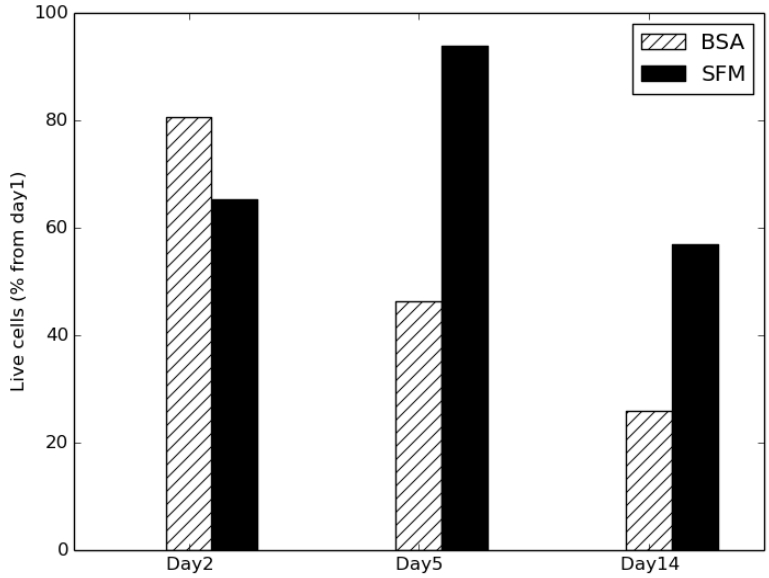


Figure 11: Viability of PBMCs in cell culture as a percentage of live cells compared to day 1 in culture. BSA = RPMI media supplemented with 2.5g/l bovine serum albumin; SFM = serum free media.

UCB had an inverse U-shaped dose-dependent effect on the extent of Fpg-sensitive lesions in telomeres, with the highest damage occurring at 5 µmol/l UCB (figure 14). This concentration corresponds to a higher risk of age-associated diseases and mortality in humans. UCB had no effects on telomere length after 6h in culture (data not shown).

Figure 15 shows the relative abundance of Fpg-sensitive lesions in the telomere in cells treated with UCB only (6h), H_2O_2 only (2h), or UCB and H_2O_2 co-treatment (4h only UCB, 2h co-treatment). As shown, co-treatment with UCB can reverse the damaging effects of H_2O_2 to a level which is not significantly higher than non-treatment control.

4.5 DISCUSSION AND CONCLUSIONS

In order to test the effects of UCB on telomeres in vitro we utilized primary cultures of human PBMCs, treated with UCB and hydrogen peroxide as a stress inducer. We used HPLC and flow cytometry to assess cellular uptake of UCB, and a qPCR-based method for measuring oxidized guanine lesions in the telomere. Measured UCB concentrations in FBS-supplemented media were much lower than anticipated. We hypothesized that

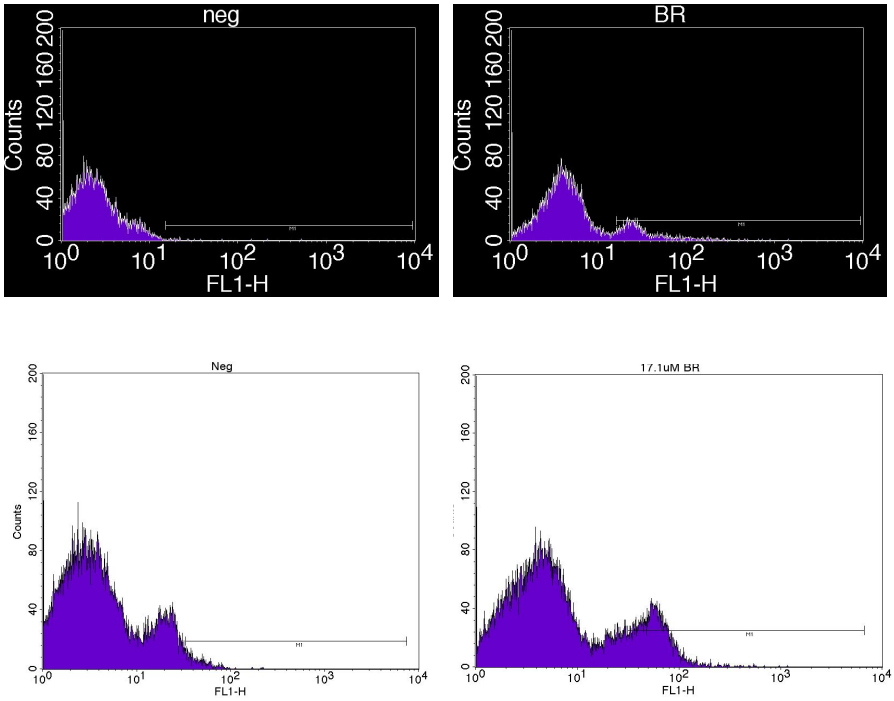


Figure 12: Cellular uptake (upper panel) and nuclear uptake (lower panel) of UCB, expressed as a shift in fluorescent signal in flow cytometry. Left: non-treated cells; right: cells treated with 17.1 µmol/l UCB for 6h.

this might be due to bilirubin insolubility in media, which causes it to form crystals. Hence, we increased the amount of FBS in the media, which should presumably increase the solubility of UCB due to the increased content of albumin available to bind the insoluble free UCB. Surprisingly, the concentrations of UCB decreased upon increase of FBS. As UCB is normally bound to albumin and the mobile phase treatment disrupts this bond and precipitates proteins, we could not attribute this to increased albumin content in FBS. However, it is possible that different constituent of FBS, protein or other, binds unconjugated bilirubin irreversibly, thus lowering the measurable concentration. While this experiment does not confer a definite evidence that UCB localizes in the cell nucleus, it shows that this is a very real possibility. Using a much more robust experimental design, it was recently shown that UCB is indeed localized in the nucleus after being taken up by cells, [Park et al., 2016]. Taken together, these results reveal potential mechanisms for telomere protection by UCB. The reduction of Fpg lesions in telomere by UCB was only observed when cells were simultaneously treated with both UCB and H_2O_2 suggesting that UCB scavenges reactive oxygen species before an oxidative transformation of guanine can take place. However, these results require validation as this method for estimating oxidative lesions in the telomere has the following weaknesses:

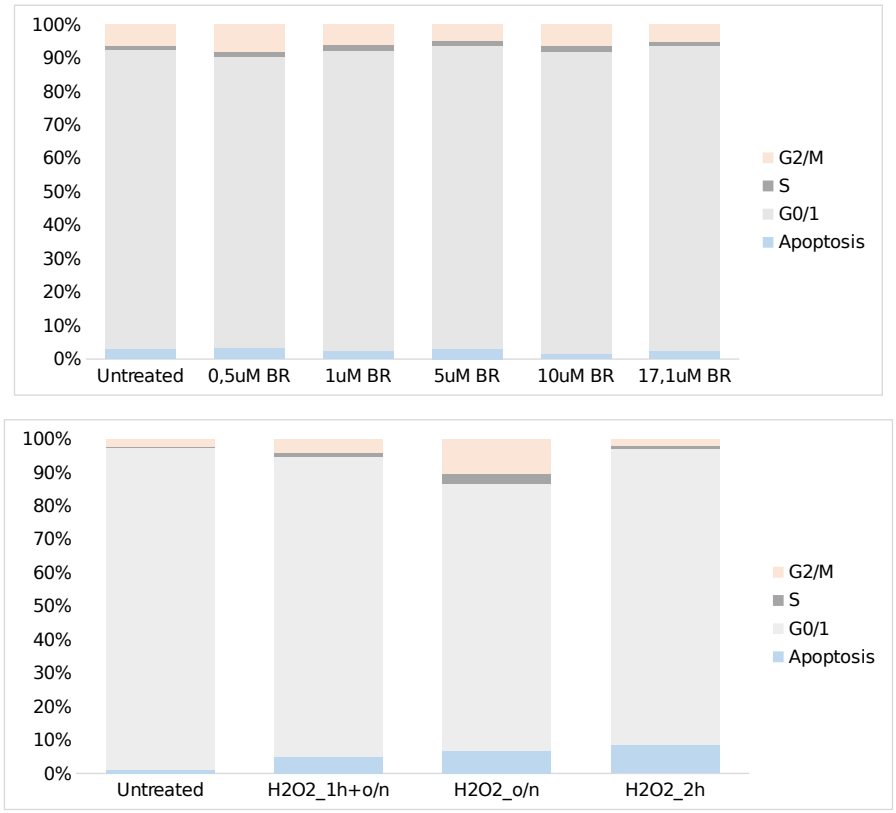


Figure 13: Cell cycle analysis of PBMCs without treatment or treated with increasing concentrations of unconjugated bilirubin (BR) (upper panel); without treatment or treated with 100 µmol/l of H_2O_2 after 1h with overnight recovery; overnight treatment or 2h without recovery (lower panel).

1. The buffer used for optimal Fpg activity contains Mg^{2+} ions that can interfere with and enhance the polymerase activity in downstream qPCR reactions;

2. While the tests show that practically no damage occurred in the 36b4 gene upon treatment [O'Callaghan et al., 2011] and there was no oxidized lesions detected with this method, still it cannot be excluded that there is a variable level of damage occurring in this sequence, which might influence normalization.

4.6 ACKNOWLEDGEMENTS

The cell culture experiments and flow cytometry measurements in this chapter were performed with kind assistence of Dr. Christine Mölzer. Bar plots in this chapter were made using matplotlib [Hunter, 2007] and numpy [Van Der Walt et al., 2011] for Python 2.7.3.

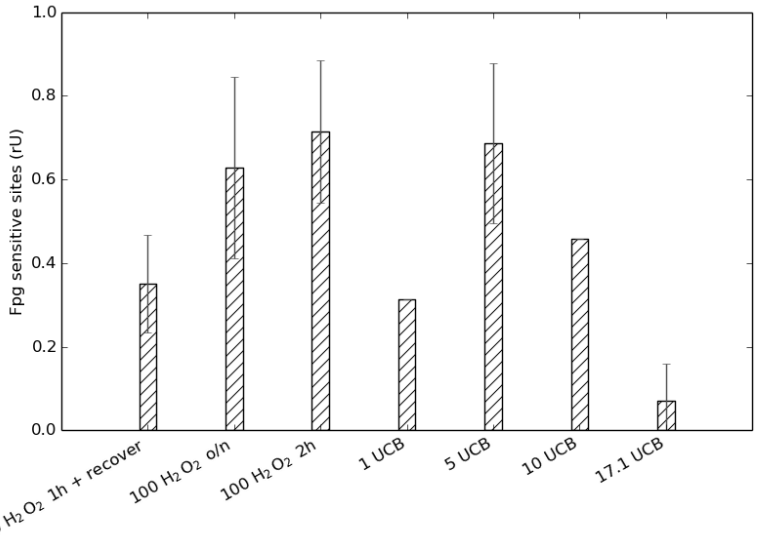


Figure 14: Fpg-sensitive lesions in telomere caused by either positive control (H2O2) or UCB. All concentrations are in µmol/l. Error bars, where applicable represent standard deviation (n = 3). All values are normalized to a non-treatment control (value = 0). Bars 2, 3 and 5 represent damage significantly different from non-treatment control ($p < 0.05$).

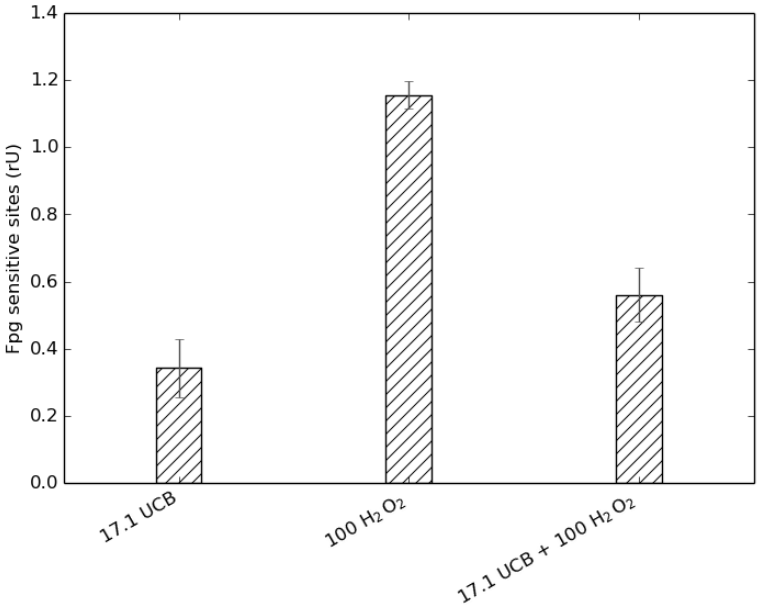


Figure 15: Fpg-sensitive lesions in telomere caused by either positive control (H2O2), UCB or co-treatment. All concentrations are in µmol/l. Error bars, represent standard deviation (n = 3). All values are normalized to a non-treatment control (value = 0). Bar 2 represent damage significantly different from non-treatment control ($p < 0.05$), and to both bar 1 and 3. Bar 1 and 3 are not significantly different from non-treatment control or each other.

5

CIRCULATING CELL-FREE DNA, TELOMERE LENGTH AND UNCONJUGATED BILIRUBIN IN THE VIENNA ACTIVE AGEING STUDY: AN EXPLORATORY ANALYSIS

ARTICLE

Anela Tosevska, Bernhard Franzke, Marlene Hofmann, Immina Vierheilig, Barbara Schober-Halper, Stefan Oesen, Oliver Neubauer, Barbara Wessner, Karl-Heinz Wagner, Vienna Active Ageing Study Group (VAAS).
Circulating cell-free DNA, telomere length and unconjugated bilirubin in the Vienna Active Ageing Study: an exploratory analysis.
submitted to *Scientific reports* (July, 2016)

AUTHOR CONTRIBUTIONS

B.F., B.H-S., S.O., B.W., and K.-H.W. designed and concieved the primary study; B.F., B.H-S., S.O., and M.H. performed the Anela Tosevska, B.F. designed, established, and analysed the majority of the experiments and methods; Anela Tosevska and K.H.W. prepared the DNA samples and Anela Tosevska performed the qPCR assays; Anela Tosevska performed the HPLC measurements; I.V. performed and analysed the cfDNA measurements; Anela Tosevska did the statistical analyses; K.H.W. and B.W. provided financial support; Anela Tosevska made the figures; Anela Tosevska wrote the manuscript; O.N. and M.H. assisted in writing the manuscript.

"Circulating cell-free DNA, telomere length and unconjugated bilirubin in the Vienna Active Ageing Study: an exploratory analysis"

Anela Tosevska [1]*, Bernhard Franzke [1], Marlene Hofmann [3], Immina Vierheilig [2], Barbara Schober-Halper [1], Stefan Oesen [1], Oliver Neubauer [1,4], Barbara Wessner [1,3], Karl-Heinz Wagner [1, 2]*, Vienna Active Ageing Study Group (VAAS)

[1] Research Platform Active Ageing, University of Vienna, Althanstrasse 14, 1090, Vienna, Austria

[2] Department of Nutritional Sciences, University of Vienna, Althanstrasse 14, 1090, Vienna, Austria

[3] Centre for Sport Science and University Sports, Department of Sport and Exercise, University of Vienna, Auf der Schmelz 6, 1150 Vienna, Austria.

[4] Queensland University of Technology, Faculty of Health, School of Biomedical Sciences, Institute of Health and Biomedical Innovation (IHBI), Tissue Repair and Regeneration Group, 60 Musk Avenue, Kelvin Grove Campus, Brisbane, QLD 4059, Australia

Telomere length (TL) in blood cells is widely used in human studies as a molecular marker of ageing. Circulating cell-free DNA (cfDNA) as well as unconjugated bilirubin (UCB) are dynamic blood constituents whose involvement in age-associated diseases is largely unexplored. To our knowledge, there are no published studies integrating all three parameters, especially in individuals of advanced age.

Here we present a secondary analysis from the Vienna Active Aging Study (VAAS), a randomized controlled intervention trial in institutionalized elderly individuals (n = 101). Using an exploratory approach we combine three blood-based molecular markers (TL, UCB and cfDNA) with a range of primary and secondary outcomes from the intervention. We further look at the changes occurring in these parameters after 6-month resistance exercise training with or without supplementation.

A correlation between UCB and TL was evident at baseline ($p < 0.05$), and both were associated with increased chromosomal anomalies such as nucleoplasmatic bridges and buds ($p < 0.05$). Of the three main markers explored in this paper, only cfDNA decreased significantly ($p < 0.05$) after 6-month training and dietary intervention. No clear relationship could be established between cfDNA and either UCB or TL.

The trial was registered at ClinicalTrials.gov (NCT01775111).

Introduction

Ageing is accompanied by an accumulation of macromolecular damage, leading to cellular dysfunction and ultimately tissue and organ malfunction [1]. In humans, the ageing process appears to be a mixture of stochastic events leading to a high variability of phenotypical outcomes between individuals of the same age.

Telomere length is one of the most commonly used markers of ageing [2]. Telomere shortening is a result of the mitotic activity of a cell, and in humans it roughly corresponds to the age of the organism [3]. On the other hand, telomere length has a limited power as an age biomarker due to a very high inter-individual variation [4,5]. While

a clear decline is visible when comparing healthy individuals throughout a broad age range, this difference is often negligible over a more narrow range. This is especially the case when comparing individuals at a more advanced age, when telomeres appear to shorten at a reduced rate [6]. Moreover, studies in humans often use blood cells as a test material for measuring telomere length [7,8]. As blood cells comprise a mixture of different individual cell types with different mitotic history, telomere length measured in these samples can additionally show a large intra-individual variability [7,9]. Therefore, there is an increased need for identifying reliable and clinically accessible molecular markers of ageing, which would complement telomere length as a marker [10].

It has been previously [11–13] shown that chromosomal abnormalities arise more frequently in the elderly population. The increased chromosomal instability, in absence of malignancy, will ultimately lead to increase in cell death. Dying and dead cells release their content extracellularly, and a portion of the genomic DNA can be found circulating in the bloodstream before final excretion as a waste product [14]. A recent review [15] suggests the possibility of cell-free genomic-derived DNA (cfDNA) integration into the genome of living cells, leading further to increased genome instability.

Breitbach et al. [16] proposed that this circulating cfDNA can be additionally excreted in an active manner from living cells and could play a role in cell signalling. Circulating concentrations of cfDNA have been shown to increase rapidly after strenuous exercise, and return to normal within hours or days [16]. However, much of the physiological and pathophysiological relevance of cfDNA remains unknown, so far.

Jylhava et al. [17–19] have investigated cfDNA as a possible ageing biomarker in healthy individuals. In a genome-wide association study (GWAS) a potential involvement of the UDP-glucuronosyltransferase UGT1A1 in the excretion of cfDNA was revealed [20]. This enzyme is highly specific for metabolising unconjugated bilirubin (UCB) into water-soluble products that can be easily excreted of the organism [21]. However, there is no published data looking at a potential relationship or interaction between UCB and cfDNA in humans.

Unconjugated Bilirubin has been suggested to play an important role in human disease prevention, especially in relation to age-associated diseases [22]. A number of

epidemiological studies have found an inverse relationship between increased serum bilirubin and age-associated disease incidence [23–25]. We have recently identified a relationship between mildly increased UCB, characteristic for a condition called Gilbert's Syndrome, and telomere length [26]. These individuals present with serum bilirubin levels above 17.1 umol/L whereas non-affected individuals range between 3 and 17.1 umol/L. There are indications that even in non-Gilbert's Syndrome individuals concentrations higher than 10 umol/L can be indicative for a reduced disease risk [23]. However, it is not clear whether this intermediately increased UCB concentration is linked with longer telomeres in non-affected individuals.

The Vienna Active Ageing Study (VAAS) has been investigating different aspects of the ageing process in institutionalized elderly individuals, and the effects of resistance training and nutritional supplementation intervention on overall fitness and health-related parameters. Published data on this study has shown an improvement in physical performance in individuals undergoing a training intervention, compared to sedentary controls [27], as well as a trend for a decreased chromosomal and DNA damage in the entire study population [28]. The main aim of this paper was to investigate a potential relationship between blood telomere length, cfDNA and unconjugated bilirubin at baseline and after a 6-month training intervention. We further conducted an exploratory analysis in order to identify relationships between cfDNA, UCB and TL on one side and chromosomal damage endpoints, physical performance measures, CVD markers and oxidative damage end products on the other. Based on previous knowledge we hypothesized that there is an inverse relationship between TL and UCB on one side, and cfDNA and markers of chromosomal instability on the other.

Results

Baseline characteristics of the entire cohort

The baseline study characteristics have been described elsewhere [11]. From the 105 individuals that complied to the initially established inclusion criteria [15,27], we additionally excluded 4 individuals with increased reference values of liver enzymes (ALT, AST or GGT). Increased liver enzymes were an important indicator for liver abnormality which might influence bilirubin levels, a key variable in this analysis. As the percentage of

males in this study population was too low to achieve statistical relevance, we carried out all further analyses on a pooled population of both genders. Supplementary figure S1 shows that no clear distinction and clustering by gender can be seen between males and females using a Principal Component Analysis (PCA).

Five individuals fitted the criterion for Gilbert's Syndrome (UCB concentration ≥ 17.1 M, figure 1b), corresponding to an incidence of about 5% in our study population. This goes in line with the estimated incidence of this condition in the general population [29]. PCA analyses showed that these individuals cluster close together, but are not distinct from the rest of the participants in this study cohort (supplementary figure S2).

Correlations at baseline

We used Pearson and Spearman correlation matrices (figure 1) to explore collinearity between variables and baseline. As most variables were non-parametric (Supplementary Figure S3.) we only considered Spearman statistics (Supplementary table S1). Pearson correlation matrix is shown only as a descriptive. We summarize only the most important observations.

Age had no effect on cfDNA levels in the study population at baseline. Additionally, we could not detect any relationship between age and telomere length. UCB, on the other hand, showed a monotonic increase with age in our study sample ($\rho = 0.23$, $p = 0.025$).

Although baseline UCB showed a moderate positive Pearson correlation with cfDNA ($r = 0.257$), Spearman statistics showed no significance. In contrast, telomere length and UCB showed a significant correlation at baseline ($\rho = 0.238$, $p = 0.047$). In addition, a relationship of UCB with blood haemoglobin was observed ($\rho = 0.26$, $p = 0.012$).

Both UCB and telomere length at baseline correlated positively with the number of nucleoplasmatic bridges ($\rho = 0.21$, $p = 0.043$ and $\rho = 0.41$, $p = 0.001$, respectively) and nuclear buds ($\rho = 0.24$, $p = 0.019$ and $\rho = 0.51$, $p = 0.004$). On the contrary, MDA showed an inverse correlation with both bridges and buds ($\rho = -0.32$, $p = 0.001$ and $\rho = -0.34$, $p < 0.001$), but not with TL or UCB. Whole blood telomere length and urinary levels of oxidized guanine showed a negative Pearson correlation ($r = -0.34$) which was not significant using Spearman statistics. There were no significant correlations

between TL and cfDNA and any physical performance parameters such as chair rise test or 6-minutes walking test.

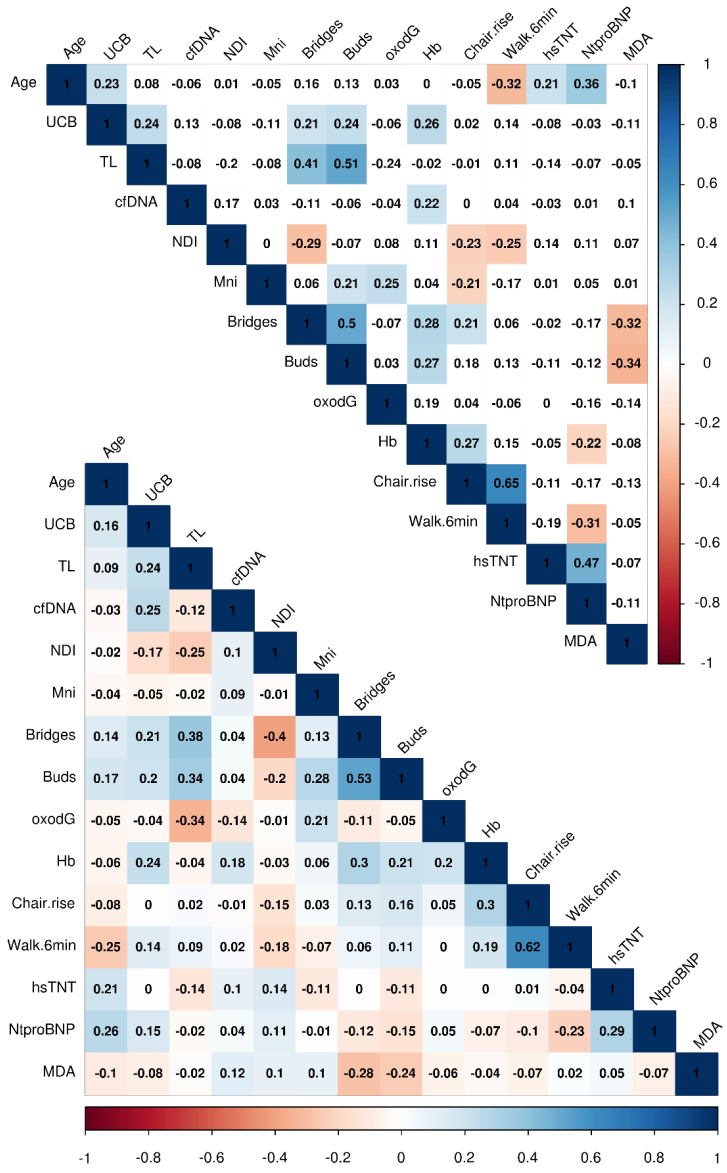


Figure 1. Pearson and Spearman correlation matrices at baseline. Values of Pearson r or Spearman ρ coefficients are given in the correspondent glyph. Pearson correlation matrix (lower panel); Spearman correlation matrix (upper panel). The glyphs are marked with colour only if they show a correlation at $P < 0.05$ level. Numerical p-values are shown in supplementary table S1.

Six-months-finishers at baseline

The study participants were randomly assigned to three intervention groups: resistance exercise training (RT), resistance training and supplementation (RTS), and a control group (CT) undergoing a cognitive intervention only. Table 1 shows the baseline characteristics of the 6-months finishers, divided by intervention groups.

Table 1. Characteristics of 6-months finishers divided by intervention group. Values are represented as mean ± standard deviation. Differences between intervention groups are marked with * for P-value < 0.05, ** for P-value < 0.01 and # for trend (P < 0.1). One way ANOVA.

	RT (n = 23-30)	*RTS (n = 21-23)*	*CT(n = 20-26)*	*Total (n = 64-79)*
Age (years)	82 ± 6	81 ± 8	84 ± 5	83 ± 6
BMI (kg/m^2)	28.97 ± 3.86	29.41 ± 5.31	27.94 ± 5.12	28.76 ± 4.72
NDI	1.95 ± 0.08	1.98 ± 0.06	1.98 ± 0.07	1.97 ± 0.07
MNi frequency/1000 BN cells	28.60 ± 15.60	28.17 ± 18.43	23.70 ± 9.53	26.90 ± 14.90
NPBs/1000 BN cells	1.17 ± 1.21	0.93 ± 0.88	1.36 ± 1.03	1.16 ± 1.06
Buds/1000 BN cells	3.47 ± 2.67	3.35 ± 2.46	4.42 ± 4.85	3.74 ± 3.46
Stand-up Test (repetitions)	12.31 ± 3.07	13.77 ± 4.28	12.13 ± 4.44	12.68 ± 3.92
6 min Walking Test (m)	384 ± 79	373 ± 99	382 ± 97	380 ± 90
Hand grip AV	20.19 ± 6.82	19.51 ± 6.58	16.40 ± 5.78	18.76 ± 6.56
Waist-to-hip Ratio	0.85 ± 0.06	0.85 ± 0.08	0.86 ± 0.08	0.86 ± 0.07
Body Fat (%)	33.87 ± 7.36	33.89 ± 9.14	32.59 ± 9.69	33.48 ± 8.55
Glucose (mg/dl)	108 ± 25	99 ± 11	107 ± 22	105 ± 21
hs-Insulin (IU/ml)	9.77 ± 6.91	10.43 ± 6.33	8.60 ± 7.74	9.58 ± 6.98

Cholesterol (mg/dl)	205 ± 41	209 ± 37	205 ± 38	206 ± 38
HDL (mg/dl)	62.57 ± 14.03	66.74 ± 17.88	63.69 ± 20.09	64.15 ± 17.20
LDL (mg/dl)	120 ± 37	119 ± 39	118 ± 32	119 ± 35
Chol/HDL Ratio (%)	3.40 ± 0.86	3.33 ± 1.01	3.45 ± 0.95	3.40 ± 0.92
Triglycerides (mg/dl)	113 ± 38	118 ± 45	114 ± 47	115 ± 43
Lipoprotein A1 (mg/dl)	16.22 ± 19.66	36.85 ± 50.70	26.42 ± 37.69	25.58 ± 37.35
hs-CRP (mg/l)	6.50 ± 13.27	5.66 ± 9.08	3.96 ± 4.02	5.42 ± 9.75
UCB (mol/l)	8.75 ± 5.68*	6.15 ± 3.33	6.35 ± 2.13	7.16 ± 4.20
hsTroponin-T (ng/ml)	0.01 ± 0.01	0.01 ± 0.01	0.02 ± 0.02	0.01 ± 0.02
NT-pro BNP (pg/ml)	393 ± 779	280 ± 370	467 ± 672	385 ± 644
mir21 (copies/pg)	2508 ± 1181	2582 ± 1209	2795 ± 1004	2621 ± 1128
HOMA-IR	2.87 ± 3.17	2.54 ± 1.47	2.37 ± 2.44	2.61 ± 2.51
cfDNA ng/ml	185 ± 47	197 ± 55	185 ± 62	188 ± 54
MDA mol/l	1.97 ± 0.42	1.89 ± 0.44	1.89 ± 0.36	1.92 ± 0.41
Telomere Length (kb)	2.92 ± 1.16	2.76 ± 1.63	3.05 ± 0.94	2.91 ± 1.27

Changes after six months exercise training

Cell-free DNA concentrations were reduced significantly after 6 months RTS intervention (t-statistics = 2.92, p-value = 0.008), but not in the CT or RT-only groups. There was no significant difference in telomere length or UCB concentrations in any of the intervention groups after 6 months, as shown is figure 2.

We consecutively determined whether the baseline concentrations of our key variables correlated with the change in the same parameter after 6 months intervention. The 6-month change in telomere length correlated inversely with telomere length at baseline in the entire cohort and all intervention groups separately ($p < 0.001$, figure 3a). The same was observed for cfDNA concentrations in the entire cohort ($p < 0.001$, figure 3b), even though the correlation did not reach significance in the RT group. UCB concentrations at baseline had no influence on the observed 6-month change in any of the intervention groups (figure 3c).

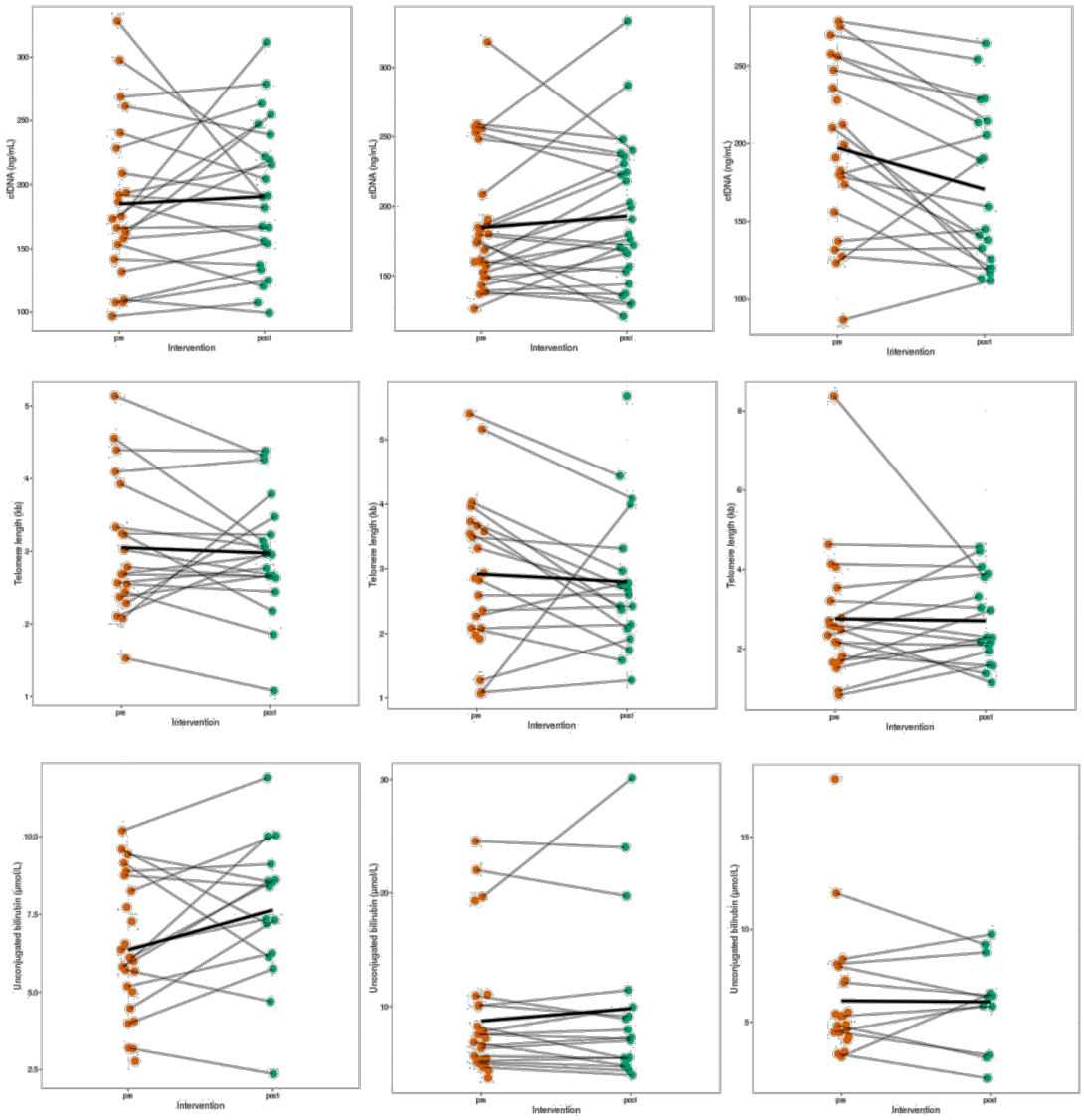
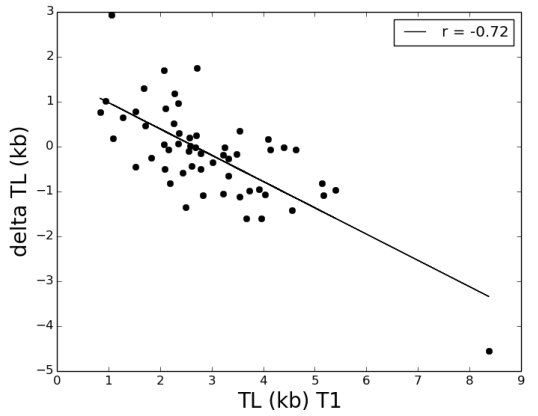
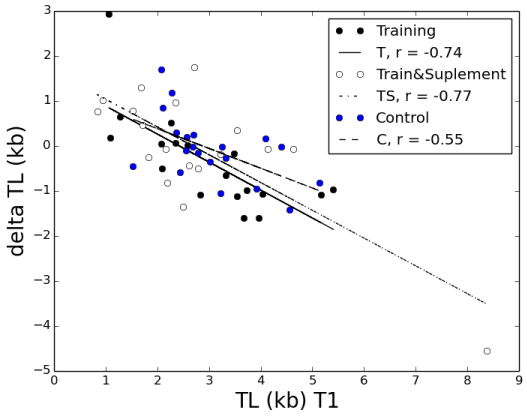
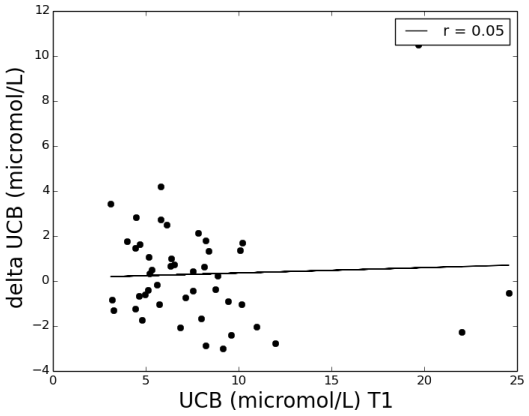
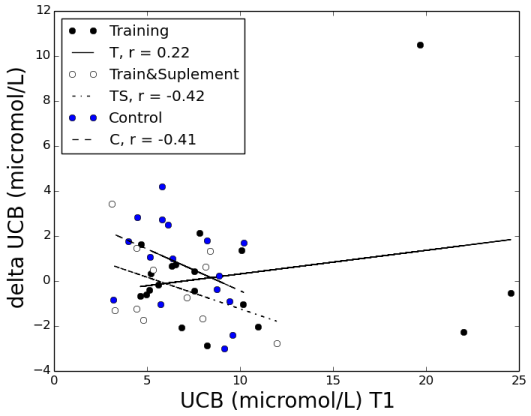


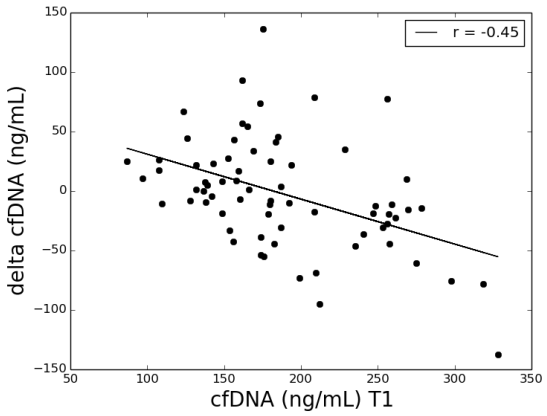
Figure 2. Paired-differences between pre-and post-intervention values for the main parameters. Each orange dot represent a value pre-intervention and green dots are 6-months post-intervention. Bold black line represents the average change. Only cell-free DNA in the TS group exhibited a significant decrease ($p = 0.009$, paired t-test).

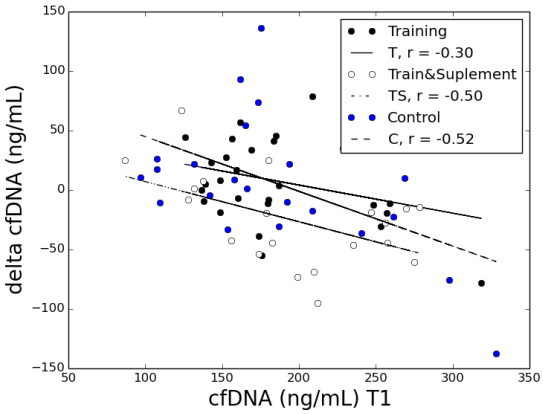

r = -0.72
delta TL (kb)
TL (kb) T1


Training
T, r = -0.74
Train&Suplement
TS, r = -0.77
Control
C, r = -0.55
delta TL (kb)
TL (kb) T1


r = 0.05
delta UCB (micromol/L)
UCB (micromol/L) T1


Training
T, r = 0.22
Train&Suplement
TS, r = -0.42
Control
C, r = -0.41
delta UCB (micromol/L)
UCB (micromol/L) T1


r = -0.45
delta cfDNA (ng/mL)
cfDNA (ng/mL) T1


Training
T, r = -0.30
Train&Suplement
TS, r = -0.50
Control
C, r = -0.52
delta cfDNA (ng/mL)
cfDNA (ng/mL) T1

A **B**

Figure 3. Scatter plot depicting correlations in the main variables at baseline to the respective 6-month change: (a) entire study population (TL, $p < 0.001$; UCB, non-significant; cfDNA, $p < 0.001$). (b) divided by intervention group (TL: T and TS group: $p < 0.001$, C group: $p = 0.011$; UCB: no group reached significance; cfDNA: T group n.s., TS: $p = 0.025$, C: $p = 0.012$).

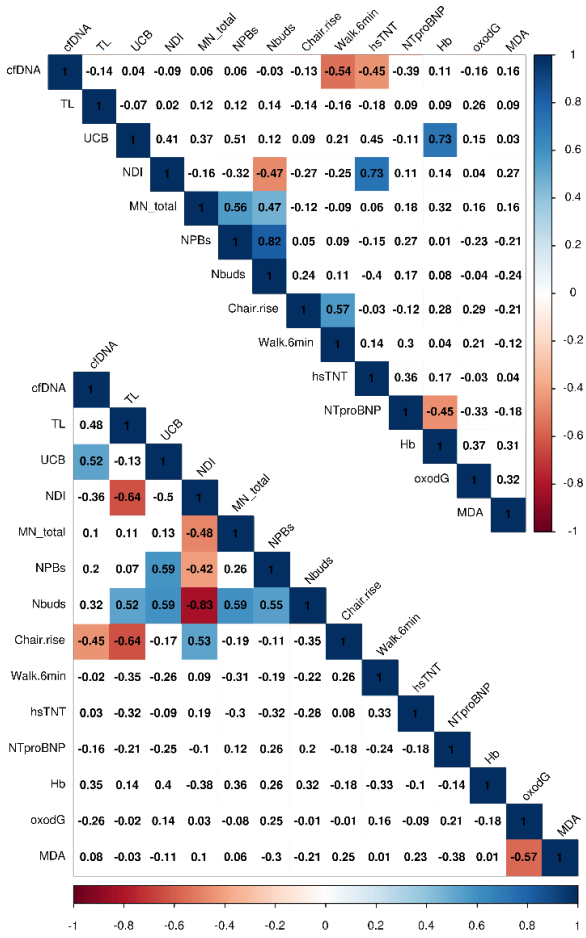
Correlations after six months exercise training

We next aimed to investigate which parameters exhibit a similar pattern with regards to negative or positive change after 6 months intervention, using a Spearman correlation matrix. The correlation matrices stratified by intervention groups are depicted in Figure 4. We briefly describe the most relevant correlations.

Changes in telomere length and cfDNA did not correlate to each other in any of the intervention groups. An increase in cfDNA was associated with decreased chair rise repetitions in the CT and RTS groups, whereas a deterioration of the 6min walking test was accompanied by an increase in cfDNA in the RT group only. Longer telomeres were associated with an improvement in the chair rise test in the RTS group but with a decrease in the TS group ($\rho = 0.65$, $p = 0.005$ and $\rho = -0.64$, $p = 0.01$).

An increase in UCB in the CT group correlated strongly with the increase in blood hemoglobin ($\rho = 0.73$, $p = 0.002$). In the RT group, UCB concentration increase correlated with an increase in both bridges ($\rho = 0.59$, $p = 0.02$) and buds ($\rho = 0.59$, $p = 0.019$). In the same group telomere length shortening was accompanied by an increase in intracellular chromosomal damage, such as formation of buds ($\rho = 0.52$, $p = 0.037$) and a decrease in nuclear division index ($\rho = -0.64$, $p = 0.007$).

A positive correlation between the observed changes in UCB and cfDNA was evident in the RT group only ($r = 0.538$, $p = 0.032$). An increase in UCB was correlated with an increase in DNA damage parameters, especially NPBs, in both training groups (RT group: $r = -0.576$, $p = 0.024$; RTS group: $r = -0.611$, $p = 0.060$).


cfDNA TL UCB NDI MN_total NPBs Nbuds Chair.rise Walk.6min hsTNT NTproBNP Hb oxodG MDA
cfDNA 1 -0.14 0.04 -0.09 0.06 0.06 -0.03 -0.13 -0.54 -0.45 -0.39 0.11 -0.16 0.16
TL 1 -0.07 0.02 0.12 0.12 0.14 -0.14 -0.16 -0.18 0.09 0.09 0.26 0.09
UCB 1 0.41 0.37 0.51 0.12 0.09 0.21 0.45 -0.11 0.73 0.15 0.03
NDI 1 -0.16 -0.32 -0.47 -0.27 -0.25 0.73 0.11 0.14 0.04 0.27
MN_total 1 0.56 0.47 -0.12 -0.09 0.06 0.18 0.32 0.16 0.16
NPBs 1 0.82 0.05 0.09 -0.15 0.27 0.01 -0.23 -0.21
Nbuds 1 0.24 0.11 -0.4 0.17 0.08 -0.04 -0.24
Chair.rise 1 0.57 -0.03 -0.12 0.28 0.29 -0.21
Walk.6min 1 0.14 0.3 0.04 0.21 -0.12
hsTNT 1 0.36 0.17 -0.03 0.04
NTproBNP 1 -0.45 -0.33 -0.18
Hb 1 0.37 0.31
oxodG 1 0.32
MDA 1
1 0.8 0.6 0.4 0.2 0 -0.2 -0.4 -0.6 -0.8 -1
cfDNA TL UCB NDI MN_total NPBs Nbuds Chair.rise Walk.6min hsTNT NTproBNP Hb oxodG MDA
cfDNA 1
TL 0.48 1
UCB 0.52 -0.13 1
NDI -0.36 -0.64 -0.5 1
MN_total 0.1 0.11 0.13 -0.48 1
NPBs 0.2 0.07 0.59 -0.42 0.26 1
Nbuds 0.32 0.52 0.59 -0.83 0.59 0.55 1
Chair.rise -0.45 -0.64 -0.17 0.53 -0.19 -0.11 -0.35 1
Walk.6min -0.02 -0.35 -0.26 0.09 -0.31 -0.19 -0.22 0.26 1
hsTNT 0.03 -0.32 -0.09 0.19 -0.3 -0.32 -0.28 0.08 0.33 1
NTproBNP -0.16 -0.21 -0.25 -0.1 0.12 0.26 0.2 -0.18 -0.24 -0.18 1
Hb 0.35 0.14 0.4 -0.38 0.36 0.26 0.32 -0.18 -0.33 -0.1 -0.14 1
oxodG -0.26 -0.02 0.14 0.03 -0.08 0.25 -0.01 -0.01 0.16 -0.09 0.21 -0.18 1
MDA 0.08 -0.03 -0.11 0.1 0.06 -0.3 -0.21 0.25 0.01 0.23 -0.38 0.01 -0.57 1
-1 -0.8 -0.6 -0.4 -0.2 0 0.2 0.4 0.6 0.8 1

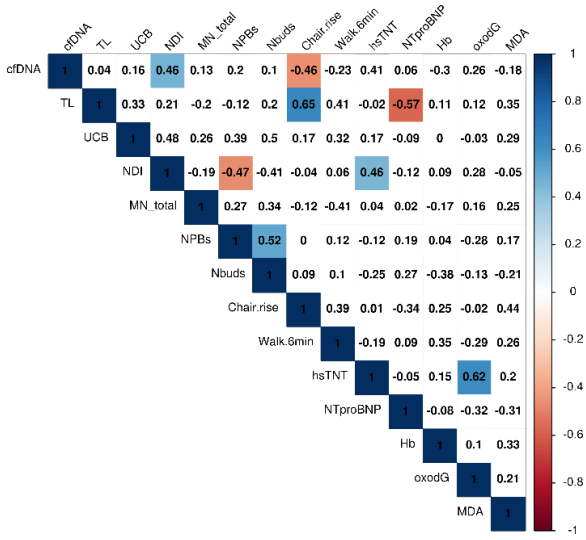

cfDNA TL UCB NDI MN_total NPBs Nbuds Chair.rise Walk.6min hsTNT NTproBNP Hb oxodG MDA
cfDNA 1 0.04 0.16 0.46 0.13 0.2 0.1 -0.46 -0.23 0.41 0.06 -0.3 0.26 -0.18
TL 1 0.33 0.21 -0.2 -0.12 0.2 0.65 0.41 -0.02 -0.57 0.11 0.12 0.35
UCB 1 0.48 0.26 0.39 0.5 0.17 0.32 0.17 -0.09 0 -0.03 0.29
NDI 1 -0.19 -0.47 -0.41 -0.04 0.06 0.46 -0.12 0.09 0.28 -0.05
MN_total 1 0.27 0.34 -0.12 -0.41 0.04 0.02 -0.17 0.16 0.25
NPBs 1 0.52 0 0.12 -0.12 0.19 0.04 -0.28 0.17
Nbuds 1 0.09 0.1 -0.25 0.27 -0.38 -0.13 -0.21
Chair.rise 1 0.39 0.01 -0.34 0.25 -0.02 0.44
Walk.6min 1 -0.19 0.09 0.35 -0.29 0.26
hsTNT 1 -0.05 0.15 0.62 0.2
NTproBNP 1 -0.08 -0.32 -0.31
Hb 1 0.1 0.33
oxodG 1 0.21
MDA 1
1 0.8 0.6 0.4 0.2 0 -0.2 -0.4 -0.6 -0.8 -1

Figure 4. Spearman correlation matrices describing relationships between changes after 6-month intervention training, stratified by intervention group. Values of Spearman ρ coefficients are given in the correspondent glyph. The glyphs are marked with colour only if they show a correlation at $P < 0.05$ level. Control group CT, n = 9-22 (upper panel); resistance training and supplementation group RTS n = 9-22 (middle); resistance training group RT, n = 10-29 (lower panel). Numerical P-values are shown in supplementary table S2.

Discussion

The present study investigated the relationship between circulating cell-free DNA, serum unconjugated bilirubin and telomere length in a predominantly female elderly population. To our knowledge, this is the first study investigating the interplay between these parameters within elderly individuals. Moreover, the novelty of these data is in linking these markers in response to a prolonged intervention involving exercise training with and without a dietary supplementation.

Telomere length and circulating cell-free DNA at baseline were not affected by age in this study population. The possible reason for this finding is the advanced age of the study participants leading to a relatively broad variance in most baseline parameters. All study participants were between 65 and 97 years of age, where the discrepancy between biological and chronological age is the greatest. Additionally, it is very plausible that individuals that have reached a more advanced age in good health have a more favourable molecular aging pattern than their slightly younger peers[30].

We hypothesized that telomere length at baseline would be inversely associated with markers of chromosomal instability and oxidative DNA damage. In contrast, we expected cell-free DNA to increase with the levels of chromosomal damage. Contrary to our hypothesis, longer telomeres were associated with increased chromosomal instability at baseline, measured by an increase in nucleoplasmtic bridges and buds. Nucleoplasmatic bridges are formed as a result of erroneous DNA repair and telomere fusion of two chromosomes [13]. This process is triggered by critical telomere shortening and uncapping. However, to our knowledge, there is no indication that nucleoplasmatic bridges formation can lead to telomere elongation. Some evidence suggests that in a case of folate deprivation nuclear buds might contain a larger amount of telomeric DNA, leading to an abnormal increase in telomeric content [31]. The present study participants indeed had an inadequate baseline level of folate [28] in erythrocytes, which might partly explain our results.

Baseline concentrations of cfDNA did not reflect the extent of DNA or chromosomal damage in PBMCs occurring simultaneously, measured by the CBMN assay end-points such as micronuclei frequencies, nucleoplasmatic bridges and buds formation. Notably,

cfDNA levels in plasma did not appear abnormally high for any of the study participants. For cfDNA integration into healthy cells [16], it is likely that much higher levels of cfDNA would be required.

There was a weak positive correlation between telomere length and UCB at baseline. This is in agreement with our recent results suggesting an occurrence of longer telomeres in individuals with Gilbert's Syndrome, a condition of mild chronic hyperbilirubinaemia [26]. Approximately 5% of our study population matched the criterion for GS diagnosis, showing increased UCB levels over the diagnostic minimum for GS. Interestingly none of the potential GS showed a tendency for short telomeres (supplementary figure 4a). However, it this setting, the group size was too small to make a statistically sound conclusion.

The relationship between UCB levels and cfDNA appears to be more complex. Even though there was no direct significant relationship between the two, the levels of cfDNA were consistently higher in individuals suspected for GS. These individuals have distinctly higher UCB levels and appear as outliers to the entire group (Supplementary Figure 4b). As we have no information on the UGT1A1 genotype of participants in the present study, we could only assume that the ones showing an increased UCB concentration indeed carry a mutation in their UGT1A1 gene which additionally slows down the excretion of circulating cfDNA entities. Another possibility is that the free UCB fraction in plasma is binding to the free DNA fraction. A study has reported that bilirubin can bind DNA in presence of Cu(II)-ions, which could promote oxidative DNA damage [32]. However, more research is needed in order to get an insight if UCB and cfDNA are directly interacting, or are merely targets of the same metabolic pathway.

The main outcomes of the Vienna Active Ageing Study related to improvement in physical fitness parameters have been described earlier [27]. Briefly, functional parameters have been found to improve over time and related to the training intervention. In addition, chromosomal damage, such as micronucleus frequencies or nucleoplasmatic bridges showed a trend to decrease in all three groups [28]. The supplementation group acquired improvements in plasma vitamin B12 and folate status in erythrocytes [28]. While acute exercise increases the concentration of cfDNA within

hours post-exercise, it is being quickly eliminated and returns to normal values within a few days [16]. However, the effect of regular moderate exercise on long-term cfDNA levels has not been reported so far. We observed a significant decrease in cfDNA levels in the RTS group after 6 months. There was no association between cfDNA and B12 or folate or the changes occurring in these parameters between the two time-points (data not shown). It is possible that there was an indirect effect of the latter two on the reduced cfDNA in plasma. As the role of circulating cfDNA is not yet well defined, we cannot exclude that the observed reduction in the training and supplementation group might not be beneficial at all as cfDNA could potentially play a role in the training adaptation.

Mean telomere length has not changed drastically throughout the course of 6 months. It has been shown previously that telomeres shorten at a rate of only about 30 bp/year which is difficult to detect with any standard telomere measurement method [33]. However, there have been reports [7] of telomere length fluctuations with time in whole blood samples, which occurs due to a shift in cell populations throughout the intervention period. Similar to the observations from *Svenson et. al,.* there was an inverse correlation between telomere length measured at baseline and the 6-month change, independently from the training intervention. These intra-individual fluctuations in blood telomere length should be considered carefully when using telomere length as a marker, especially if the measurement was performed at a single time-point.

Similarly to the outcomes at baseline, the change in measured intracellular damage parameters in the training group is closely followed by a change in TL and UCB. Additionally, and contrary to our expectations, telomere shortening correlated with higher improvement in the chair rise test. It is unclear from our results if there is any causal relationship between these parameters.

Taken together, we have shown a relationship between telomere length, unconjugated bilirubin and chromosomal anomalies in an elderly population, in the light of a lifestyle intervention. On the other hand, cfDNA showed no connections to any of the tested parameters. Perhaps, due to the very transient nature of cfDNA, a study dealing with

acute outcomes would be more appropriate. Instead, we can emphasize the potential role of UCB as a key player in age-associated cellular signalling.

Materials and Methods

Subject recruitment and sample preparation

A total of 105 institutionalized elderly individuals aged 65–98 years (both men and women), were recruited from five different senior residencies in Vienna, Austria (Curatorship of Viennese retirement homes) [11,27]. The subjects were mentally (Mini Mental State Examination ≥ 23) and physically (Short Physical Performance Battery > 4) able to participate in the study. Furthermore, they were sedentary (<1h of physical activity or exercise per week) and free of conditions contraindicated with medical training therapy or measurement of physical performance, such as cardiovascular diseases, diabetic retinopathy and regular use of cortisone-containing drugs. Regular strength training (>1×/week) in the last 6 months before the study beginning was an exclusion criterion. Written informed consent was obtained from all participants before entry, and the study was performed in accordance with the Declaration of Helsinki. This study was approved by the ethics committee of the City of Vienna (EK-11-151-0811) and registered at ClinicalTrials.gov (NCT01775111).

The study was conducted in a randomized, controlled, observer-blind design. The participants were randomly divided into three groups – cognitive training (CT), resistance training (RT), RT + protein supplement (RTS) – and matched for gender. Blood samples were taken and physical performance tests were executed before (T1 or pre), and after six months (T3 or post) of intervention.

Plasma values of liver enzymes (AST, ALT, GGT) elevated over 10% above the reference values was an additional exclusion criterion, as unconjugated bilirubin can be affected by altered liver function. This lead to exclusion of additional 4 study participants.

Blood samples were collected early morning after an overnight fast using heparin, serum and EDTA tubes (Greiner Bio-One, Kremsmunster, Austria). Peripheral blood lymphocytes were isolated using Ficoll separation tubes (Greiner Bio-One).

Study intervention design

A detailed description on the training protocol, protein and micronutrient supplementation and cognitive training are given by Franzke et. al [28]. Briefly, the resistance training groups (RT and RTS) received two weekly sessions of resistance training, conducted on two non-consecutive days and supervised by a sport scientist. Exercises were conducted using elastic bands, chairs and own body weight [27]. In the initial phase (4 weeks) one set of 15 repetitions was performed in order to learn the correct form of each exercise. From the fifth week on the intensity and volume has progressively been increased from two sets of light exercises to two sets of heavy resistance. If the participants could easily perform two sets of 15 repetitions they were told to either take more resistance or to perform a more difficult version of the exercise.

The RTS group additionally received a nutritional supplement every morning, as well as directly after each training session. Each drink supplied a total energy of 150 kcal and contained 20.7g protein (56 energy (En)%, 19.7g whey protein, 3.0g leucine, > 10g essential amino acids), 9.3g carbohydrates (25 En%, 0.8 BE), 3.0g fat (18 En%), 1.2g roughage (2 En%), 800IU (20µg) of vitamin D, 250mg calcium, vitamins C, E, B6 and B12, folic acid and magnesium (FortiFit, NUTRICIA GmbH, Vienna, Austria).

The CT group performed coordinative or cognitive tasks two times per week, equally to the RT and RTS groups in order to avoid socialization bias. Participants of all groups were instructed to maintain their regular food intake.

Chair rise test

To perform well in the chair rise test, the participants had to stand up from a chair (46 cm seat height) as often as possible within 30 s. To ensure a safe test-setting, the chair was placed against the wall. For one successful repetition, participants had to fully stand up (hip and knee fully extended) and sit back, with their arms crossed over their chest. A last-second-attempt was considered valid, if the person had covered more than 50% of the range of motion [11,27].

Handgrip strength test

To assess handgrip strength, participants performed an isometric handgrip strength test (kg) using a dynamometer. The test was conducted in a sitting position and maximal isometric contraction within 4–5 s was measured (JAMAR compatible handgrip dynamometer adapted to handle different sizes). The better result of two trials (one minute break in between) for each hand was noted [11,27].

Six minute walking test

The participants had to walk for 6 min as fast and as far as possible. The 6 minute walking test is a valid tool to evaluate aerobic endurance in the elderly. Participants were allowed to slow down and even take a short rest. Every subject performed the test separately without being disturbed by others. They had to walk back and forth on a 30 meter shuttle track and the distance covered within 6 min was registered [11,27].

Circulating cell-free DNA measurement

Circulating cell-free DNA was measured from frozen EDTA plasma using a QuantiFluor® dsDNA System (Promega), as a plate-based assay. The plasma was thawed and centrifuged for 1 min at 3000rpm, to remove all insoluble debris. Samples were measured in triplicates, according to the manufacturer's protocol. To exclude possible interferences from other plasma-derived molecules, each plasma sample was also run without addition of dsDNA dye and used as a blank for the corresponding sample.

Cytokinesis block micronucleus cytome assay

The cytokinesis block micronucleus cytome (CBMN) assay was performed according to a published protocol [34]. Cells were stimulated to undergo mitosis, using phytohaemagglutinin (PAA, Pasching, Austria) using a concentration of 1×10^6 cells/mL in culture medium. Samples were incubated at 37°C and 5% CO2. After exactly 44h, cytochalasin B (Sigma Aldrich, Vienna, Austria) was added to block cytokinesis. After exactly 72h from the start of the experiment, cells were spotted onto microscope slides, stained (Diff-Qick; Medion Diagnostics, Dudingen, Switzerland) and counted using a bright field microscope (1000-fold magnification; Olympus, Wien, Austria).

Each sample was run in duplicate and two slides of each replicate were produced. From the four resulting slides, 500 cells per slide (2000 per subject) were counted.

To assess chromosomal damage in blood lymphocytes, the frequency of MN, nucleoplasmic bridges and nuclear buds per 2000 binucleated (BN) cells was counted, as well as the number of apoptotic and necrotic cells. Furthermore, the nuclear division index (NDI) was calculated to measure cytostatic effects and the mitogenic response of lymphocytes.

DNA extraction from whole blood and concentration measurement

DNA was extracted from 100µl fresh whole blood, using the DNeasy blood and tissue mini kit (Qiagen) according to the manufacturer's instructions. Extracted DNA was stored at -20 °C.

Telomere length measurement by quantitative polimerase chain reaction (qPCR)

Telomere length was measured as described [35], with modifications. Shortly, SYBR Select Master Mix (Life Technologies) was used to amplify telomeric sequences and single copy gene (36b4). Primers were used at a final concentration of 100nM. Genomic DNA samples were diluted to a concentration of 2.5ng/uL, and 2uL were used in each reaction (5ng/reaction). 84-base oligonucleotide standards were diluted to a stock solution of 50 pg/uL. To generate a telomere standard curve, 10-fold serial dilutions of the stock solution were prepared. For the SCG standard curve, the stock solution was diluted to 0.5ng/uL, and serial dilutions were prepared thereof. All samples and standards were run in triplicate. Assays were run on a QuantStudio™ 6 Flex Real-Time PCR System (Thermo Fisher), using a 384-well block. To minimize the effect of inter-plate variability, repeated measures from the same sample were run on the same plate.

Analyses were performed at a manual threshold of 2.461 for both targets, with a qPCR efficiency ranging between 90-110%. Samples with a standard deviation exceeding 0.5 Ct were excluded from the analysis. Absolute telomere length was calculated as previously described [35].

Unconjugated bilirubin measurement by high performance liquid chromatography (HPLC)

Unconjugated bilirubin were measured from serum samples, as described previously [12], using a high-performance liquid chromatograph (Merck, Hitachi, LaChrom, Vienna, Austria) equipped with a photodiode array detector (PDA, Shimadzu,) and a Fortis C18 HPLC column (4.6 × 150 mm, 3 µm) and a phenomenex C18 HPLC guard column (4.0 × 3.0 mm). An isocratic mobile phase consisting of 0.1 M n-dioctylamine in methanol/water (95:5; v/v) and glacial acetic acid was used. Unconjugated bilirubin IX alpha (Frontier Scientific Europe, Carnforth, Lancashire, UK) served as an external standard. Sample and standard preparation and analysis were performed as previously published [12].

Biochemical parameters

High sensitive Troponin-T (hs TNT) and NP-were analyzed immediately after blood sampling at a routine laboratory (study lab GmbH, Vienna).

Oxidized nucleotides in urine

Urine samples were collected on the morning of blood samplings and stored at –20°C until further analyses. 8-oxo-7.8-dihydro-2'-deoxyguanosine (8oxodG) was measured using an ultra-performance LC and MS/MS [36]. The results were normalized to urinary creatinine concentration determined by the Jaffe reaction.

Malondialdehyde (MDA)

MDA levels were measured in plasma as described earlier [37]. Shortly, after heating (60min, 100°C) plasma samples were neutralized with methanol/NaOH, centrifuged (3min, 3000rpm) and MDA was measured using HPLC (excitation: λ = 532nm, emission: λ = 563nm, LaChrom Merck Hitachi Chromatography System, Vienna, Austria; HPLC column 125×4 mm, 5 µm; Merck, Vienna, Austria).

Statistical analysis

The sample size calculation was based on a prerequisite alpha level set at 0.05 and a power of > 0.85 using G * Power3.1.0 [38] which estimated the sample size to be 86 using

isokinetic peak torque (concentric knee extension at an angular velocity of 60°/s.; range of motion 20°–80°) as primary endpoint. Previous studies in a similarly difficult collective show a high drop-out rate of about 35–40%. Therefore, a total of about 120 subjects were included in the study [27], of which 101 were included in the present analyses at baseline.

For the baseline bivariate correlations we used Pearson and Spearman statistics to test for linear or monotonic relationship. To test for differences between pre- and post-intervention within the same group we used a paired T-test or Wilcoxon signed-rank test. Baseline differences between intervention groups were determined using a one way ANOVA and a Bonferonni correction.

Values from 6-months finishers were paired as pre- and post- intervention and divided by intervention groups. We used a pairwise exclusion. For each group the z-scores were calculated as $x - {}_0/\sigma_0$, where x is the value, ${}_0$ is the group average at baseline and σ_0 the group standard deviation at baseline. This approach corrects for any inter-group baseline differences. The 6-months difference was calculated from the z-scores for each pair of pre- and post-intervention value.

All analyses were performed using R 3.2.4. or the scipy and numpy [39] packages for Python 2.7.3. Scatter plots were generated using the matplotlib package for Python 2.7.3 [40] , the correlation matrices were generated using the corrplot package for R and the paired line plots using the ggplot2 [41] package for R. PCA and the corresponding figures in supplementary material were generated using the COVAIN toolbox for Matlab [42].

Abbreviations and units

RT = resistance training group

RTS = resistance training and supplementation group

CT = cognitive training group

TL = Telomere Length (kb)

UCB = Unconjugated Bilirubin (mol/L)

cfDNA = Circulating cell-free DNA (ng/mL)

NDI = Nuclear division index

MN = Micronuclei frequencies (per 1000 binucleated cells)

NPBs = Nucleoplasmatic bridges (per 1000 binucleated cells)

Nbuds = Nuclear buds (per 1000 binucleated cells)

hsCRP = high sensitivity C-reactive protein (mg/L)

hsTNT = high sensitivity Troponin T (ng/mL)

NT-pro-BNP = N-terminal fragment of B-type natriuretic peptide (ng/mL)

Hb = Hemoglobin (g/dL)

oxodG = 8-oxo-dGuanosine (ng/mg creatinine)

Acknowledgements

The authors want to thank Nazlisadat Seyed Khoei for establishing the cfDNA measurement method. We additionally want to thank the Curatorship of Viennese Retirement Homes and its residents for taking part in the study. This work was supported by the University of Vienna by funding the Research Platform Active Ageing and the Anniversary Fund of the Austrian National Bank (No. 14541).

Contributions

B.F., B.H-S., S.O., B.W., and K.-H.W. designed and concieved the primary study; B.F., B.H-S., S.O., and M.H. performed the A.T., B.F. designed, established, and analysed the majority of the experiments and methods; A.T. and K.H.W. prepared the DNA samples and A.T. performed the qPCR assays; A.T. performed the HPLC measurements; I.V. performed and analysed the cfDNA measurements; A.T. did the statistical analyses; K.H.W. and B.W. provided financial support; A.T. made the figures; A.T. wrote the manuscript; O.N. and M.H. assisted in writing the manuscript.

Competing financial interests

The authors declare no competing financial interests.

References

1. Richardson, A. G. & Schadt, E. E. The Role of Macromolecular Damage in Aging and Age-related Disease. *J. Gerontol. A. Biol. Sci. Med. Sci.* **69,** S28–S32 (2014).
2. Osthus, I. B. *et al.* Telomere length and long-term endurance exercise: does exercise training affect biological age? A pilot study. *PLoS One* **7,** e52769 (2012).
3. Blasco, M. A. Telomeres and human disease: ageing, cancer and beyond. *Nat Rev Genet* **6,** 611–22 (2005).
4. Der, G. *et al.* Is Telomere Length a Biomarker for Aging: Cross-Sectional Evidence from the West of Scotland? *Plos One* **7,** (2012).
5. Mather, K. A., Jorm, A. F., Parslow, R. A. & Christensen, H. Is Telomere Length a Biomarker of Aging? A Review. *J. Gerontol. A. Biol. Sci. Med. Sci.* **66A,** 202–213 (2011).
6. Aubert, G., Baerlocher, G. M., Vulto, I., Poon, S. S. & Lansdorp, P. M. Collapse of Telomere Homeostasis in Hematopoietic Cells Caused by Heterozygous Mutations in Telomerase Genes. *Plos Genet.* **8,** (2012).
7. Svenson, U. *et al.* Blood Cell Telomere Length Is a Dynamic Feature. *PLOS ONE* **6,** e21485 (2011).
8. Robertson, J. D. *et al.* Dynamics of telomere shortening in neutrophils and T lymphocytes during ageing and the relationship to skewed X chromosome inactivation patterns. *Br J Haematol* **109,** 272–9 (2000).
9. Rehkopf, D. H. *et al.* Seasonal variation of peripheral blood leukocyte telomere length in Costa Rica: A population-based observational study. *Am J Hum Biol* **26,** 367–75 (2014).
10. Wagner, K.-H.; Cameron-Smith, D.; Wessner, B.; Franzke, B. Biomarkers of Aging: From Function to Molecular Biology. *Nutrients* ***8***, 338 (2016).
11. Franzke, B. *et al.* The influence of age and aerobic fitness on chromosomal damage in Austrian institutionalised elderly. *Mutagenesis* **29,** 441–5 (2014).

12. Wallner, M. *et al.* Effects of unconjugated bilirubin on chromosomal damage in individuals with Gilbert's syndrome measured with the micronucleus cytome assay. *Mutagenesis* **27,** 731–5 (2012).
13. Fenech, M. *et al.* Molecular mechanisms of micronucleus, nucleoplasmic bridge and nuclear bud formation in mammalian and human cells. *Mutagenesis* **26,** 125–132 (2011).
14. Jahr, S. *et al.* DNA Fragments in the Blood Plasma of Cancer Patients: Quantitations and Evidence for Their Origin from Apoptotic and Necrotic Cells. *Cancer Res.* **61,** 1659–1665 (2001).
15. Gravina, S., Sedivy, J. M. & Vijg, J. The dark side of circulating nucleic acids. *Aging Cell* **15,** 398–399 (2016).
16. Breitbach, S., Tug, S. & Simon, P. Circulating cell-free DNA: an up-coming molecular marker in exercise physiology. *Sports Med* **42,** 565–86 (2012).
17. Jylhävä, J. *et al.* Aging is associated with quantitative and qualitative changes in circulating cell-free DNA: The Vitality 90+ study. *Mech. Ageing Dev.* **132,** 20–26 (2011).
18. Jylhävä, J., Jylhä, M., Lehtimäki, T., Hervonen, A. & Hurme, M. Circulating cell-free DNA is associated with mortality and inflammatory markers in nonagenarians: The Vitality 90+ Study. *Exp. Gerontol.* **47,** 372–378 (2012).
19. Jylhävä, J. *et al.* Characterization of the role of distinct plasma cell-free DNA species in age-associated inflammation and frailty. *Aging Cell* **12,** 388–397 (2013).
20. Jylhava, J. *et al.* A Genome-Wide Association Study Identifies UGT1A1 as a Regulator of Serum Cell-Free DNA in Young Adults: The Cardiovascular Risk in Young Finns Study. *Plos One* **7,** (2012).
21. Zhou, J., Tracy, T. S. & Remmel, R. P. Correlation between Bilirubin Glucuronidation and Estradiol-3-Gluronidation in the Presence of Model UDP-Glucuronosyltransferase 1A1 Substrates/Inhibitors. *Drug Metab. Dispos.* **39,** 322–329 (2011).
22. Wagner, K. H. *et al.* Looking to the horizon: the role of bilirubin in the development and prevention of age-related chronic diseases. *Clin. Sci.* **129,** 1–25 (2015).
23. Horsfall, L. J., Nazareth, I. & Petersen, I. Cardiovascular Events as a Function of

Serum Bilirubin Levels in a Large, Statin-Treated Cohort. *Circulation* **126,** 2556–2564 (2012).

24. Lin, J. P. *et al.* Association between the UGT1A1*28 allele, bilirubin levels, and coronary heart disease in the Framingham heart study. *Circulation* **114,** 1476–1481 (2006).
25. Liu, J. *et al.* Bilirubin Increases Insulin Sensitivity by Regulating Cholesterol Metabolism, Adipokines and PPARgamma Levels. *Sci Rep* **5,** 9886 (2015).
26. Tosevska, A. *et al.* Longer telomeres in chronic, moderate, unconjugated hyperbilirubinaemia: insights from a human study on Gilbert's Syndrome. *Sci. Rep.* **6,** 22300 (2016).
27. Oesen, S. *et al.* Effects of elastic band resistance training and nutritional supplementation on physical performance of institutionalised elderly - A randomized controlled trial. *Exp Gerontol* **72,** 99–108 (2015).
28. Franzke, B. *et al.* The effect of six months of elastic band resistance training, nutritional supplementation or cognitive training on chromosomal damage in institutionalized elderly. *Exp Gerontol* **65,** 16–22 (2015).
29. OMIM Entry - # 143500 - GILBERT SYNDROME. Available at: http://omim.org/entry/143500. (Accessed: 6th June 2016)
30. Franzke, B., Neubauer, O. & Wagner, K.-H. Super DNAging—New insights into DNA integrity, genome stability and telomeres in the oldest old. *Mutat. Res. Mutat. Res.* **766,** 48–57 (2015).
31. Lindberg, H. K. *et al.* Origin of nuclear buds and micronuclei in normal and folate-deprived human lymphocytes. *Mutat. Res. Mol. Mech. Mutagen.* **617,** 33–45 (2007).
32. Asad, S. F., Singh, S., Ahmad, A. & Hadi, S. M. Bilirubin/biliverdin–Cu(II) induced DNA breakage; reaction mechanism and biological significance. *Toxicol. Lett.* **131,** 181–189 (2002).
33. Daniali, L. *et al.* Telomeres shorten at equivalent rates in somatic tissues of adults. *Nat Commun* **4,** 1597 (2013).
34. Fenech, M. Cytokinesis-block micronucleus cytome assay. *Nat. Protoc.* **2,** 1084–1104 (2007).
35. O'Callaghan, N. J. & Fenech, M. A quantitative PCR method for measuring absolute

telomere length. *Biol Proced Online* **13,** 3 (2011).

36. Henriksen, T., Hillestrøm, P. R., Poulsen, H. E. & Weimann, A. Automated method for the direct analysis of 8-oxo-guanosine and 8-oxo-2′-deoxyguanosine in human urine using ultraperformance liquid chromatography and tandem mass spectrometry. *Free Radic. Biol. Med.* **47,** 629–635 (2009).
37. Ramel, A., Wagner, K. H. & Elmadfa, I. Plasma antioxidants and lipid oxidation after submaximal resistance exercise in men. *Eur J Nutr* **43,** 2–6 (2004).
38. Faul, F., Erdfelder, E., Lang, A.-G. & Buchner, A. G*Power 3: A flexible statistical power analysis program for the social, behavioral, and biomedical sciences. *Behav. Res. Methods* **39,** 175–191 (2007).
39. Walt, S. van der, Colbert, S. C. & Varoquaux, G. The NumPy Array: A Structure for Efficient Numerical Computation. *Comput. Sci. Eng.* **13,** 22–30 (2011).
40. Hunter, J. D. Matplotlib: A 2D Graphics Environment. *Comput. Sci. Eng.* **9,** 90–95 (2007).
41. H. Wickham. ggplot2: Elegant Graphics for Data Analysis. Springer-Verlag New York, 2009.
42. Sun, X. L. & Weckwerth, W. COVAIN: a toolbox for uni- and multivariate statistics, time-series and correlation network analysis and inverse estimation of the differential Jacobian from metabolomics covariance data. *Metabolomics* **8,** S81

5.1 SUPPLEMENTARY MATERIAL

Supplementary figures for "Circulating cell-free DNA, telomere length and unconjugated bilirubin in the Vienna Active Ageing Study: an exploratory analysis"

Anela Tosevska [1]*, Bernhard Franzke [1], Marlene Hofmann [3], Immina Vierheilig [2], Barbara Schober-Halper [1], Stefan Oesen [1], Oliver Neubauer [1,4], Barbara Wessner [1,3], Karl-Heinz Wagner [1, 2]*, Vienna Active Ageing Study Group (VAAS)

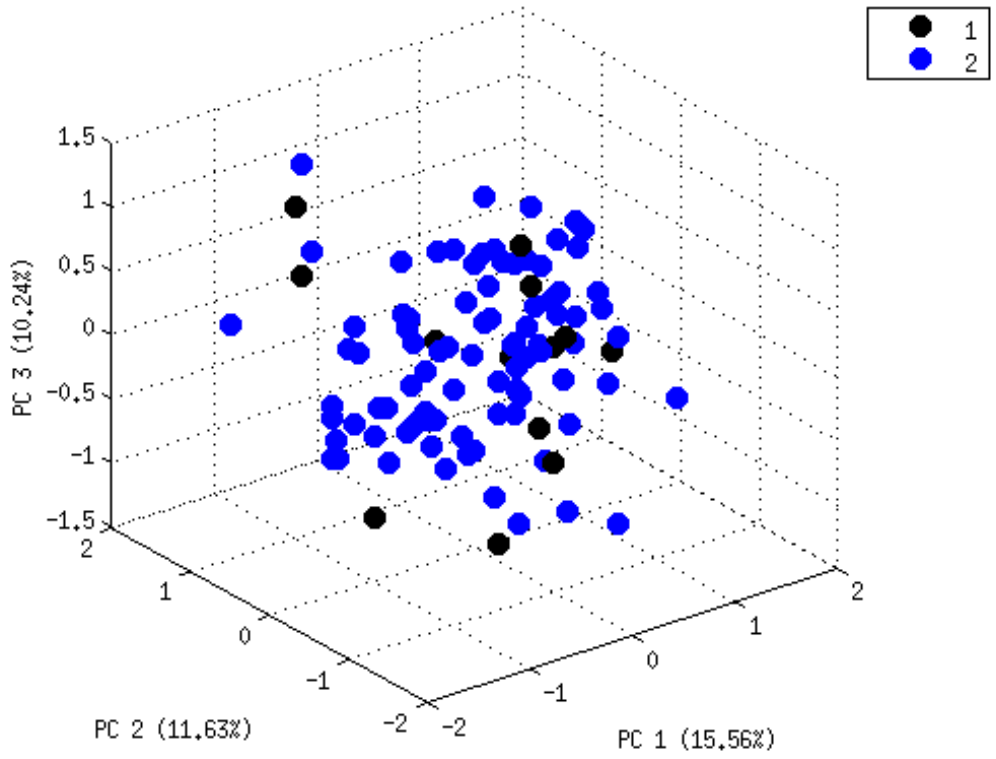
[1] Research Platform Active Ageing, University of Vienna, Althanstrasse 14, 1090, Vienna, Austria

[2] Department of Nutritional Sciences, University of Vienna, Althanstrasse 14, 1090, Vienna, Austria

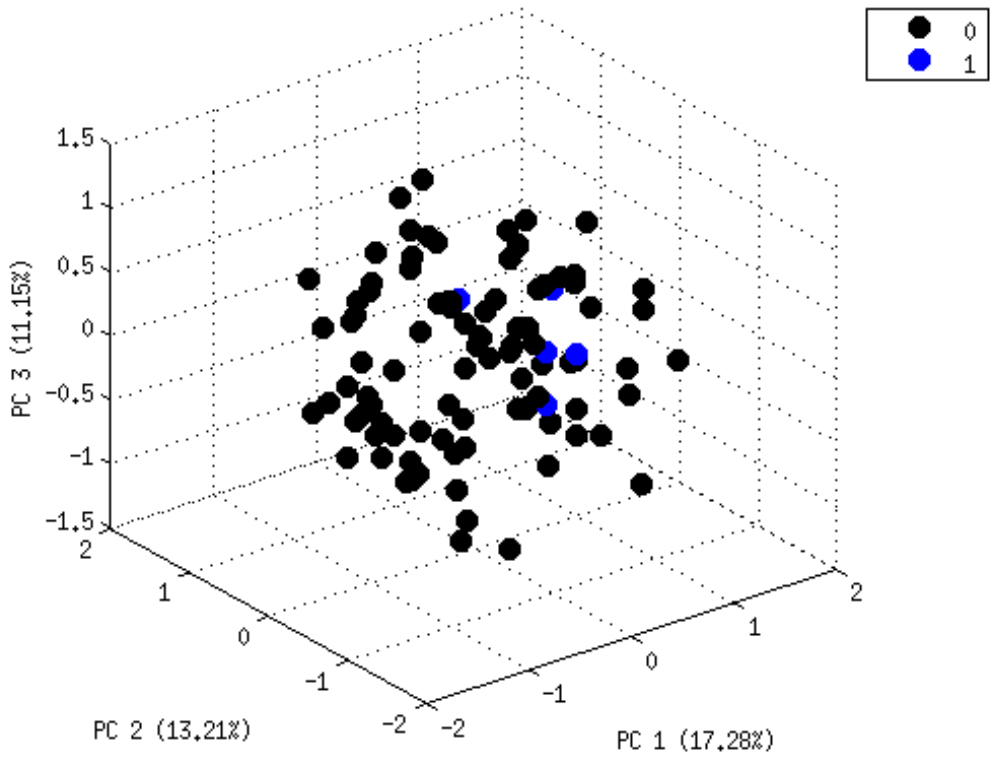
[3] Centre for Sport Science and University Sports, Department of Sport and Exercise, University of Vienna, Austria.

[4] Queensland University of Technology, Faculty of Health, School of Biomedical Sciences, Institute of Health and Biomedical Innovation (IHBI), Tissue Repair and Regeneration Group, 60 Musk Avenue, Kelvin Grove Campus, Brisbane, QLD 4059, Australia

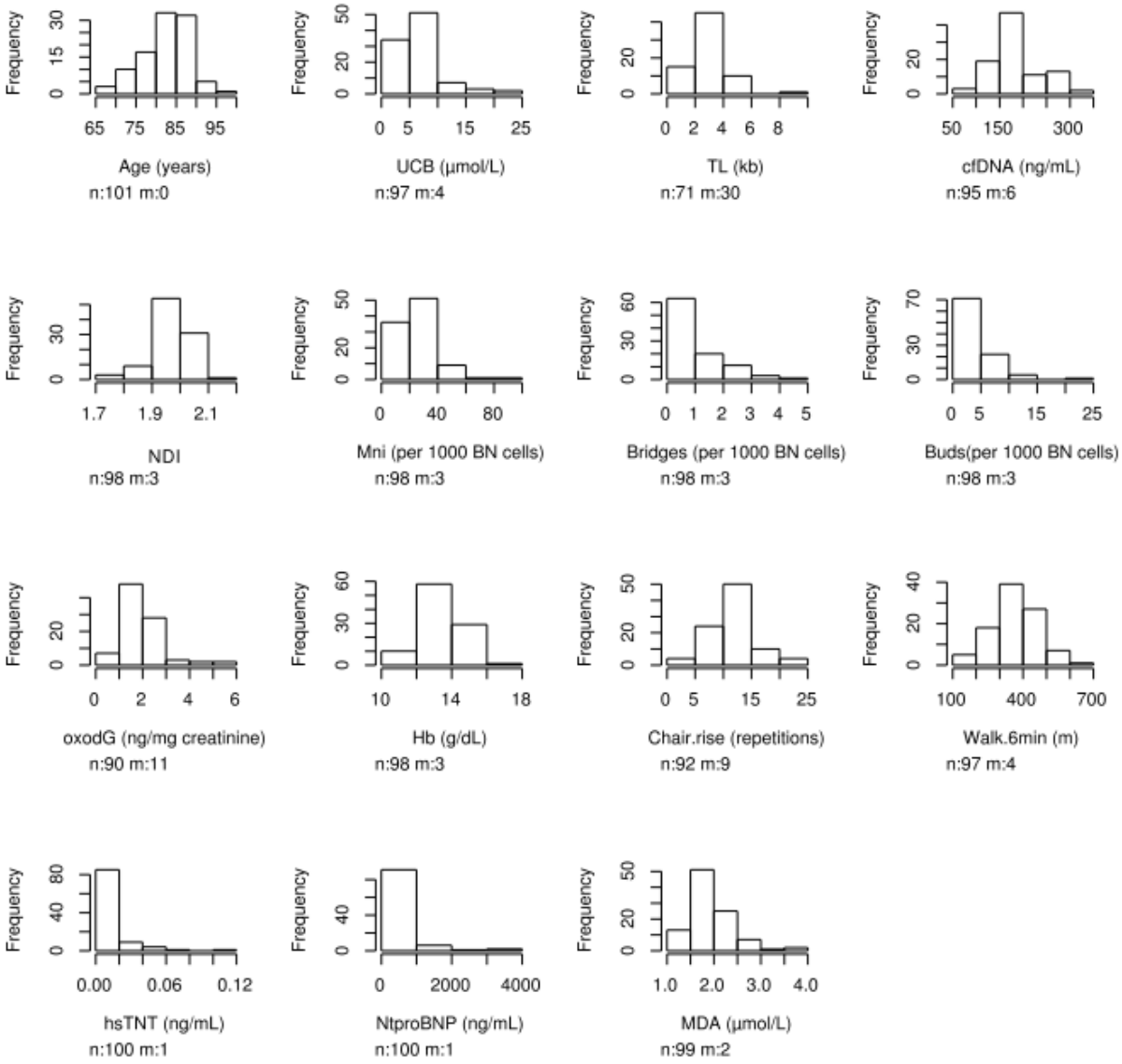
Supplementary figure S1. PCA clustering of participants in the Vienna Active Ageing Study at baseline. Black circles (1) represent males and blue (2) represent females. There is no clear distinction between the two genders using the 3 most relevant principal components.



Supplementary figure S2. PCA clustering of participants in the Vienna Active Ageing Study at baseline. Blue circles (1) represent individuals with Gilbert's Syndrome and black (0) represent normobilirubinemic individuals. There is no clear distinction between the two groups using the 3 most relevant principal components.

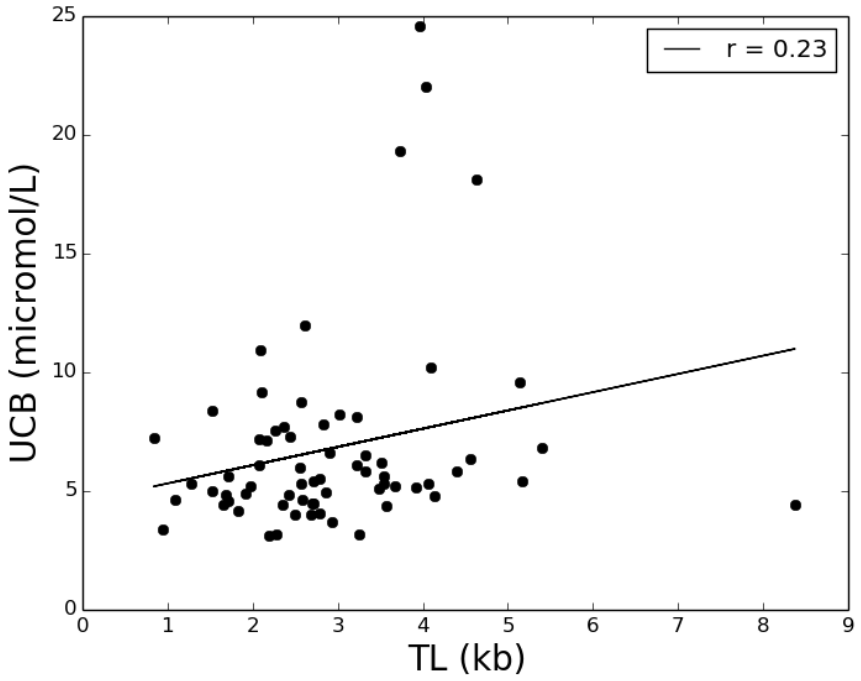


Supplementary figure S3. Histograms representing data distribution of variables at baseline.

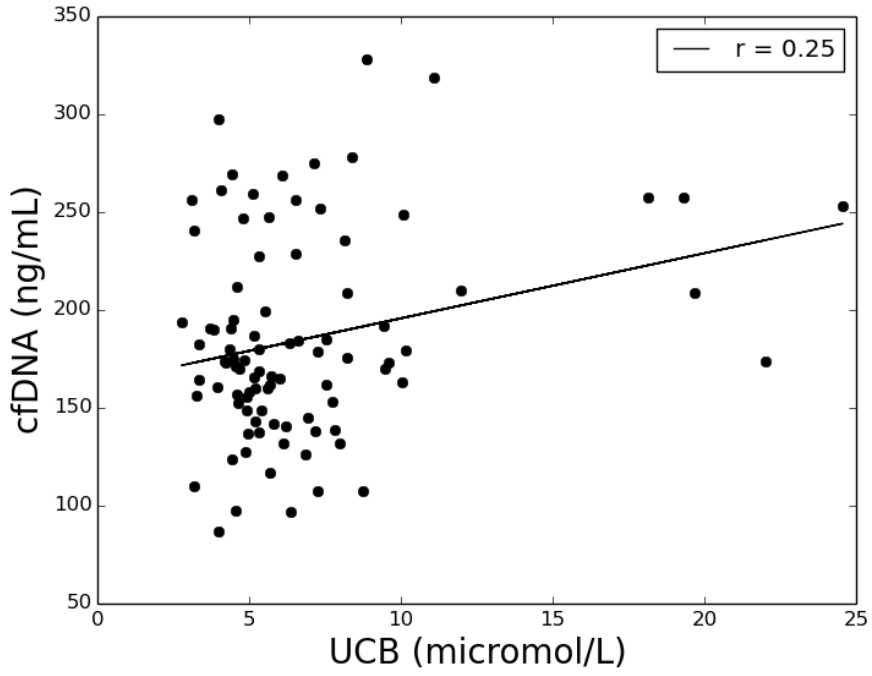


Supplementary figure 4. Scatter plots showing linear correlations at baseline between (a) Telomere length and unconjugated bilirubin, p = 0.051; (b) Unconjugated bilirubin and circulating cell-free DNA, p = 0.014.

a



b



	Age	UCB	TL	cfDNA	NDI	MN	Bridges	Buds	oxodG		Hb	Chair.rise	Walk.6min	hsTNT	NTproBNP	MDA
Age	NA	0.025	0.501	0.593	0.952	0.640	0.126	0.201	0.761	Age	0.978	0.614	0.002	0.033	0.000	0.338
UCB	0.025	NA	0.047	0.237	0.464	0.282	0.043	0.019	0.603	UCB	0.013	0.833	0.194	0.443	0.784	0.306
TL	0.501	0.047	NA	0.545	0.093	0.511	0.000	0.000	0.053	TL	0.852	0.961	0.361	0.235	0.573	0.690
cfDNA	0.593	0.237	0.545	NA	0.100	0.787	0.305	0.583	0.745	cfDNA	0.034	0.994	0.700	0.754	0.911	0.353
NDI	0.952	0.464	0.093	0.100	NA	0.963	0.003	0.488	0.433	NDI	0.296	0.030	0.013	0.184	0.272	0.515
MN	0.640	0.282	0.511	0.787	0.963	NA	0.534	0.041	0.019	MN	0.726	0.046	0.104	0.906	0.654	0.956
Bridges	0.126	0.043	0.000	0.305	0.003	0.534	NA	0.000	0.543	Bridges	0.006	0.046	0.544	0.871	0.103	0.001
Buds	0.201	0.019	0.000	0.583	0.488	0.041	0.000	NA	0.791	Buds	0.008	0.097	0.194	0.279	0.248	0.001
oxodG	0.761	0.603	0.053	0.745	0.433	0.019	0.543	0.791	NA	oxodG	0.083	0.730	0.576	0.970	0.124	0.204
Hb	0.978	0.013	0.852	0.034	0.296	0.726	0.006	0.008	0.083	Hb	NA	0.010	0.149	0.650	0.031	0.440
Chair.rise	0.614	0.833	0.961	0.994	0.030	0.046	0.046	0.097	0.730	Chair.rise	0.010	NA	0.000	0.285	0.100	0.206
Walk.6min	0.002	0.194	0.361	0.700	0.013	0.104	0.544	0.194	0.576	Walk.6min	0.149	0.000	NA	0.058	0.002	0.601
hsTNT	0.033	0.443	0.235	0.754	0.184	0.906	0.871	0.279	0.970	hsTNT	0.650	0.285	0.058	NA	0.000	0.481
NTproBNP	0.000	0.784	0.573	0.911	0.272	0.654	0.103	0.248	0.124	NTproBNP	0.031	0.100	0.002	0.000	NA	0.296
MDA	0.338	0.306	0.690	0.353	0.515	0.956	0.001	0.001	0.204	MDA	0.440	0.206	0.601	0.481	0.296	NA

Supplementary table S1. P values for Spearman correlation between variables at baseline. Raw untransformed values were used for the tests.

	cfDNA	TL	UCB	NDI	MN_total	NPBs	Nbuds	Chair.rise	Walk.6min	hsTNT	NTproBNP	Hb	oxodG	MDA
cfDNA	NA	0.586	0.887	0.722	0.811	0.822	0.909	0.602	0.014	0.038	0.074	0.639	0.502	0.487
TL	0.586	NA	0.817	0.928	0.636	0.649	0.572	0.591	0.515	0.472	0.721	0.724	0.291	0.726
UCB	0.887	0.817	NA	0.145	0.188	0.063	0.691	0.779	0.443	0.080	0.672	0.002	0.603	0.919
NDI	0.722	0.928	0.145	NA	0.481	0.142	0.027	0.280	0.298	0.000	0.626	0.559	0.882	0.234
MN_total	0.811	0.636	0.188	0.481	NA	0.007	0.026	0.631	0.705	0.785	0.419	0.159	0.506	0.498
NPBs	0.822	0.649	0.063	0.142	0.007	NA	0.000	0.852	0.712	0.514	0.225	0.972	0.342	0.350
Nbuds	0.909	0.572	0.691	0.027	0.026	0.000	NA	0.339	0.668	0.067	0.458	0.740	0.864	0.289
Chair.rise	0.602	0.591	0.779	0.280	0.631	0.852	0.339	NA	0.008	0.891	0.595	0.224	0.219	0.346
Walk.6min	0.014	0.515	0.443	0.298	0.705	0.712	0.668	0.008	NA	0.532	0.180	0.850	0.337	0.601
hsTNT	0.038	0.472	0.080	0.000	0.785	0.514	0.067	0.891	0.532	NA	0.077	0.416	0.890	0.865
NTproBNP	0.074	0.721	0.672	0.626	0.419	0.225	0.458	0.595	0.180	0.077	NA	0.027	0.133	0.398
Hb	0.639	0.724	0.002	0.559	0.159	0.972	0.740	0.224	0.850	0.416	0.027	NA	0.099	0.154
oxodG	0.502	0.291	0.603	0.882	0.506	0.342	0.864	0.219	0.337	0.890	0.133	0.099	NA	0.145
MDA	0.487	0.726	0.919	0.234	0.498	0.350	0.289	0.346	0.601	0.865	0.398	0.154	0.145	NA

Training and Supplementation (RTS)

	cfDNA	TL	UCB	NDI	MN.total	NPBs	Nbuds	Chair.rise	Walk.6min	hsTNT	NTproBNP	Hb	oxodG	MDA
cfDNA	NA	0.874	0.631	0.047	0.596	0.412	0.681	0.048	0.329	0.076	0.791	0.201	0.278	0.450
TL	0.874	NA	0.381	0.422	0.439	0.644	0.439	0.005	0.088	0.935	0.013	0.678	0.639	0.155
UCB	0.631	0.381	NA	0.162	0.467	0.262	0.143	0.642	0.340	0.617	0.790	0.989	0.934	0.385
NDI	0.047	0.422	0.162	NA	0.431	0.038	0.074	0.870	0.789	0.043	0.622	0.708	0.250	0.821
MN.total	0.596	0.439	0.467	0.431	NA	0.245	0.147	0.632	0.075	0.869	0.925	0.461	0.521	0.290
NPBs	0.412	0.644	0.262	0.038	0.245	NA	0.019	0.993	0.600	0.617	0.422	0.867	0.238	0.483
Nbuds	0.681	0.439	0.143	0.074	0.147	0.019	NA	0.704	0.667	0.282	0.242	0.097	0.588	0.365
Chair.rise	0.048	0.005	0.642	0.870	0.632	0.993	0.704	NA	0.077	0.981	0.130	0.270	0.947	0.053
Walk.6min	0.329	0.088	0.340	0.789	0.075	0.600	0.667	0.077	NA	0.396	0.682	0.113	0.199	0.258
hsTNT	0.076	0.935	0.617	0.043	0.869	0.617	0.282	0.981	0.396	NA	0.833	0.510	0.003	0.385
NTproBNP	0.791	0.013	0.790	0.622	0.925	0.422	0.242	0.130	0.682	0.833	NA	0.721	0.160	0.167
Hb	0.201	0.678	0.989	0.708	0.461	0.867	0.097	0.270	0.113	0.510	0.721	NA	0.662	0.148
oxodG	0.278	0.639	0.934	0.250	0.521	0.238	0.588	0.947	0.199	0.003	0.160	0.662	NA	0.385
MDA	0.450	0.155	0.385	0.821	0.290	0.483	0.365	0.053	0.258	0.385	0.167	0.148	0.385	NA

Training (RT)

	cfDNA	TL	UCB	NDI	MN.total	NPBs	Nbuds	Chair.rise	Walk.6min	hsTNT	NTproBNP	Hb	oxodG	MDA
cfDNA	NA	0.060	0.039	0.079	0.641	0.342	0.124	0.032	0.924	0.888	0.431	0.110	0.251	0.701
TL	0.060	NA	0.726	0.008	0.680	0.810	0.037	0.011	0.206	0.189	0.392	0.619	0.950	0.914
UCB	0.039	0.726	NA	0.056	0.648	0.021	0.020	0.533	0.339	0.720	0.321	0.198	0.630	0.696
NDI	0.079	0.008	0.056	NA	0.013	0.033	0.000	0.012	0.673	0.347	0.618	0.103	0.901	0.647
MN.total	0.641	0.680	0.648	0.013	NA	0.192	0.001	0.394	0.155	0.138	0.574	0.120	0.748	0.774
NPBs	0.342	0.810	0.021	0.033	0.192	NA	0.004	0.631	0.394	0.116	0.204	0.270	0.284	0.149
Nbuds	0.124	0.037	0.020	0.000	0.001	0.004	NA	0.110	0.324	0.170	0.327	0.173	0.980	0.319
Chair.rise	0.032	0.011	0.533	0.012	0.394	0.631	0.110	NA	0.217	0.701	0.401	0.456	0.964	0.248
Walk.6min	0.924	0.206	0.339	0.673	0.155	0.394	0.324	0.217	NA	0.102	0.248	0.159	0.505	0.960
hsTNT	0.888	0.189	0.720	0.347	0.138	0.116	0.170	0.701	0.102	NA	0.361	0.641	0.670	0.255
NTproBNP	0.431	0.392	0.321	0.618	0.574	0.204	0.327	0.401	0.248	0.361	NA	0.530	0.342	0.052
Hb	0.110	0.619	0.198	0.103	0.120	0.270	0.173	0.456	0.159	0.641	0.530	NA	0.477	0.951
oxodG	0.251	0.950	0.630	0.901	0.748	0.284	0.980	0.964	0.505	0.670	0.342	0.477	NA	0.007
MDA	0.701	0.914	0.696	0.647	0.774	0.149	0.319	0.248	0.960	0.255	0.052	0.951	0.007	NA

Supplementary table S2. P values for Spearman correlation between 6-moths-changes divided by intervention groups. Values were transformed into z-scores according to the baseline mean in for each intervention group and the difference between paired z-scores were used for the tests.

Part III

CONCLUSION

6

CONCLUDING REMARKS

This work provides new directions for bilirubin research by identifying a relationship between moderate benign hyperbilirubinaemia and telomere length. GS provides a good model for investigating the effects of bilirubin in humans without the need for an intervention trial. The first publication in chapter 3, describes the BiliHealth study, a case-control study in GS, where we could observe a difference in average telomere length in PBMCs in mildly hyperbilirubinaemic cases compared to normobilirubinaemic individuals [Tosevska et al., 2016]. This is an important step towards unraveling the mechanisms behind the observed beneficial effects of bilirubin in age-related diseases. As the observed difference was more pronounced with advanced age, a telomere-protective effect of increased UCB concentration can be suggested.

Under the assumption that UCB acts as a telomere-protective agent, we looked at several potential protective mechanisms. The most compelling one, and in line with previous findings, is that UCB can reduce the mitotic aging in cells by modulating their proliferation. This is particularly important in the light of excessive oxidative stress. While UCB is itself a potential pro-oxidant at extremely high concentrations, we could show that it does not trigger ROS formation nor it affects cell cycle and apoptosis at concentrations that mimic the physiological range in humans (1-17.1 µmol/l). In contrast, treating cells with hydrogen peroxide did cause shifts in the cell cycle towards the G2 phase. Whether these cells eventually undergo mitosis or cell-cycle arrest could not be determined.

A direct antioxidant effect of UCB is another potential mechanism for direct telomere protection. If oxidative stress causes increased damage to telomeres, this would eventually lead to excessive telomere shortening, whereas UCB, acts as a very potent free radical scavenger. From chapter 3 we could see a positive association between telomere length in PBMCs and antioxidant capacity of serum measured by the ferric reducing ability of plasma (FRAP) assay. As increased UCB leads to a remarkably increased serum antioxidant capacity, we could easily assume that UCB protects telomeres from accelerated attrition by antagonizing the intracellular build-up of free radicals or preventing them from entering the intracellular space. Indeed, our in vitro data in chapter 4 show a potential of UCB, which was added to the culture media, to minimize the adverse effects of exposure to oxidative stress.

In chapter 5 we looked at a more general population of elderly individuals and the interactions between telomere length and UCB in this age group. The prevalence of GS in this cohort was 5%, which is within the expected range of 3-10% in the general population. As estimation of GS prevalence and bilirubin measurement were only part of a secondary analyses, the power of identifying statistically meaningful differences in this small group was very low. Nonetheless, individuals with high serum UCB had consistently longer telomeres, within a narrow telomere length distribution, compared to the non-affected individuals in this cohort.

In addition to UCB, telomere length in this cohort was associated with an increase in chromosomal damage markers such as the formation of nucleoplasmatic bridges and nuclear buds. These anomalies occur due to telomere-telomere fusion in unprotected telomeres, or excessive amplification of DNA, respectively. Hence, we must observe the results of this study with caution as the method used for telomere length assessment rather measures telomere content in the entire sample. The increased telomere content could originate from destabilized chromosomes. An assay looking at single telomeres in cells could complement our results and clarify whether the longer telomeres in hyperbilirubinaemia are not just a side effect from increased chromosomal instability.

Overall, the interpretation of these results needs to be taken with caution as: (1) telomere length was estimated in PBMCs which are known to exhibit telomerase activity; (2) we estimated only the average length of telomeres in a mixed cell population, which does not give any information on single cells and single telomeres. What is yet not clear is whether GS individuals have longer telomeres at very young age. Our study results suggested that this is likely not the case, as subjects younger than 35 years of age did not show a significant difference in telomere length. On the other hand, Gunn rat liver tissue coming from relatively young rats could clearly show a difference in telomere length. We cannot exclude that this can be organism- or tissue-specific. Moreover, the Gunn rats have up to 500-fold higher UCB levels compared to their normobilirubinaemic counterparts. In humans this ratio is much lower and does not exceed 20-fold. Other differences between the models such as telomerase expression for instance, also need to be considered.

6.1 FUTURE PROSPECTS

By now it is clear that telomeres are dynamic features and do not change linearly through time. Hence, to establish if there is a real effect of bilirubin on telomere length, a longitudinal approach is essential. Since following human subjects over their lifetime is an extremely challenging study design, animal studies could assist in the pursuit of challenges that remain. The Gunn rat has provided an extensive level of understanding of underlying processes in organs and tissues affected by hyperbilirubinaemia.

However, apart from the many parallels with the human GS condition, this model has the disadvantage that it does not have any residual UGT1A1 activity, thus is a more suitable model for Crigler-Najjar Syndrome rather than GS. A transgenic humanized mouse model of GS has been developed for this reason, in order to provide a more accurate model of moderate UGT1A1 impairment [Fujiwara et al., 2010]. This mouse model could be used in further studies, and followed from birth throughout its natural lifespan in order to establish a causal effect of UCB on telomere length and maintenance. Moreover, this model could provide the opportunity to sample other tissues and organs, which would be important for disease assessment. Ultimately, if a causal relationship between UCB and telomere maintenance is established, one can aim to identify the key players in the interaction. Whether UCB would directly act at telomeres as an ROS scavenger, or is involved in cellular signalling, is yet to be determined.

BIBLIOGRAPHY

Sanjiv B Amin and Angelo A Lamola. Newborn jaundice technologies: unbound bilirubin and bilirubin binding capacity in neonates. In *Seminars in perinatology*, volume 35, pages 134–140. Elsevier, 2011.

Daniel W Belsky, Avshalom Caspi, Renate Houts, Harvey J Cohen, David L Corcoran, Andrea Danese, HonaLee Harrington, Salomon Israel, Morgan E Levine, Jonathan D Schaefer, et al. Quantification of biological aging in young adults. *Proceedings of the National Academy of Sciences*, 112(30):E4104–E4110, 2015.

MC Benton, RA Lea, D Macartney-Coxson, C Bellis, MA Carless, JE Curran, M Hanna, D Eccles, GK Chambers, J Blangero, et al. Serum bilirubin concentration is modified by UGT1A1 haplotypes and influences risk of Type-2 diabetes in the norfolk island genetic isolate. *BMC genetics*, 16(1):1, 2015.

Lu-Qin Bian, Rong-Zhen Li, Zheng-Yun Zhang, Yan-Ji Jin, Hyung-Wook Kang, Zhen-Zhu Fang, Youn-Soo Park, and Yoon-Ho Choi. Effects of total bilirubin on the prevalence of osteoporosis in postmenopausal women without potential liver disease. *Journal of bone and mineral metabolism*, 31(6):637–643, 2013.

Elizabeth H Blackburn and Joseph G Gall. A tandemly repeated sequence at the termini of the extrachromosomal ribosomal RNA genes in tetrahymena. *Journal of molecular biology*, 120(1):33–53, 1978.

Elizabeth H Blackburn, Carol W Greider, and Jack W Szostak. Telomeres and telomerase: the path from maize, tetrahymena and yeast to human cancer and aging. *Nature medicine*, 12(10):1133–1138, 2006.

Ai-Ching Boon, Clare L Hawkins, Kavita Bisht, Jeff S Coombes, Bhavisha Bakrania, Karl-Heinz Wagner, and Andrew C Bulmer. Reduced circulating oxidized LDL is associated with hypocholesterolemia and enhanced thiol status in Gilbert syndrome. *Free Radical Biology and Medicine*, 52(10):2120–2127, 2012.

Rolf Brodersen. Bilirubin. solubility and interaction with albumin and phospholipid. *Journal of Biological Chemistry*, 254(7):2364–2369, 1979.

Andrew C Bulmer, Joanne T Blanchfield, Istvan Toth, Robert G Fassett, and Jeff S Coombes. Improved resistance to serum oxidation in Gilbert's syndrome: a mechanism for cardiovascular protection. *Atherosclerosis*, 199(2):390–396, 2008.

Richard M Cawthon. Telomere measurement by quantitative PCR. *Nucleic acids research*, 30(10):e47–e47, 2002.

Richard M Cawthon. Telomere length measurement by a novel monochrome multiplex quantitative PCR method. *Nucleic acids research*, 37(3):e21–e21, 2009.

Jane-Jane Chen. Regulation of protein synthesis by the heme-regulated eIF2α kinase: relevance to anemias. *Blood*, 109(7):2693–2699, 2007.

Ilaria Chiodi and Chiara Mondello. Telomere-independent functions of telomerase in nuclei, cytoplasm, and mitochondria. *Frontiers in oncology*, 2:133, 2012.

Namita Roy Chowdhury and Jayanta Roy Chowdhury. Disorders of bilirubin metabolism. *The Liver: Biology and Pathobiology, Fifth Edition*, pages 251–256, 2001.

Alberto Ciccia and Stephen J Elledge. The DNA damage response: making it safe to play with knives. *Molecular cell*, 40(2):179–204, 2010.

Lee C Claridge, Matthew J Armstrong, Caroline Booth, and Paramjit S Gill. Gilbert's syndrome. *BMJ*, 342(9):d2293, 2011.

Elisa Coluzzi, Monica Colamartino, Renata Cozzi, Stefano Leone, Carlo Meneghini, Nathan O'Callaghan, and Antonella Sgura. Oxidative stress induces persistent telomeric DNA damage responsible for nuclear morphology change in mammalian cells. *PloS one*, 9(10):e110963, 2014.

Marcus S Cooke, Mark D Evans, Miral Dizdaroglu, and Joseph Lunec. Oxidative DNA damage: mechanisms, mutation, and disease. *The FASEB Journal*, 17(10):1195–1214, 2003.

Emilio Cusanelli and Pascal Chartrand. Telomeric repeat-containing RNA TERRA: a noncoding RNA connecting telomere biology to genome integrity. *Frontiers in genetics*, 6:143–143, 2014.

Titia De Lange. Shelterin: the protein complex that shapes and safeguards human telomeres. *Genes & development*, 19(18):2100–2110, 2005.

Serkalem Demissie, Daniel Levy, Emelia J Benjamin, L Adrienne Cupples, Jeffery P Gardner, A Herbert, Masayuki Kimura, Martin G Larson, James B Meigs, John F Keaney, et al. Insulin resistance, oxidative stress, hypertension, and leukocyte telomere length in men from the framingham heart study. *Aging cell*, 5(4):325–330, 2006.

Robert L Dilley and Roger A Greenberg. Alternative telomere maintenance and cancer. *Trends in cancer*, 1(2):145–156, 2015.

Mitch J Duncan, Christopher E Kline, Corneel Vandelanotte, Charli Sargent, Naomi L Rogers, and Lee Di Milia. Cross-sectional associations between multiple lifestyle behaviors and health-related quality of life in the 10,000 steps cohort. *PloS one*, 9(4): e94184, 2014.

Nora Fernandez-Jimenez, Ainara Castellanos-Rubio, Leticia Plaza-Izurieta, Galder Gutierrez, Iñaki Irastorza, Luis Castaño, Juan Carlos Vitoria, and Jose Ramon Bilbao. Accuracy in copy number calling by qPCR and PRT: a matter of DNA. *PLoS One*, 6(12):e28910, 2011.

Annette L Fitzpatrick, Richard A Kronmal, Jeffrey P Gardner, Bruce M Psaty, Nancy S Jenny, Russell P Tracy, Jeremy Walston, Masyuki Kimura, and Abraham Aviv. Leukocyte telomere length and cardiovascular disease in the cardiovascular health study. *American Journal of epidemiology*, 165(1):14–21, 2007.

Robert S Franco. Measurement of red cell lifespan and aging. *Transfusion Medicine and Hemotherapy*, 39(5):302–307, 2012.

Bernhard Franzke, Barbara Halper, Marlene Hofmann, Stefan Oesen, Heidemarie Peherstorfer, Klemens Krejci, Birgit Koller, Karin Geider, Andreas Baierl, Anela Tosevska, et al. The influence of age and aerobic fitness on chromosomal damage in austrian institutionalised elderly. *Mutagenesis*, 29(6):441–445, 2014.

Ryoichi Fujiwara, Nghia Nguyen, Shujuan Chen, and Robert H Tukey. Developmental hyperbilirubinemia and cns toxicity in mice humanized with the udp glucuronosyltransferase 1 (UGT1) locus. *Proceedings of the National Academy of Sciences*, 107(11): 5024–5029, 2010.

Francesca S Gazzaniga and Elizabeth H Blackburn. An antiapoptotic role for telomerase RNA in human immune cells independent of telomere integrity or telomerase enzymatic activity. *Blood*, 124(25):3675–3684, 2014.

Elisa Gobbini, Camilla Trovesi, Corinne Cassani, and Maria Pia Longhese. Telomere uncapping at the crossroad between cell cycle arrest and carcinogenesis. *Molecular & Cellular Oncology*, 1(1):e29901, 2014.

Janett Göhring, Nick Fulcher, Jaroslaw Jacak, and Karel Riha. Telotool: a new tool for telomere length measurement from terminal restriction fragment analysis with improved probe intensity correction. *Nucleic acids research*, page gkt1315, 2013.

Carol W Greider. Telomerase activity, cell proliferation, and cancer. *Proceedings of the National Academy of Sciences*, 95(1):90–92, 1998.

Annemien Haveman-Nies, Lisette CPGM de Groot, and Wija A van Staveren. Dietary quality, lifestyle factors and healthy ageing in europe: the seneca study. *Age and ageing*, 32(4):427–434, 2003.

Philip C Haycock, Emma E Heydon, Stephen Kaptoge, Adam S Butterworth, Alex Thompson, and Peter Willeit. Leucocyte telomere length and risk of cardiovascular disease: systematic review and meta-analysis. 2014.

Ilka U Heinemann, Martina Jahn, and Dieter Jahn. The biochemistry of heme biosynthesis. *Archives of biochemistry and biophysics*, 474(2):238–251, 2008.

Thomas Hofmann, Stefanie Klenow, Anke Borowicki, Chris IR Gill, Beatrice L Pool-Zobel, and Michael Glei. Gene expression profiles in human peripheral blood mononuclear cells as biomarkers for nutritional in vitro and in vivo investigations. *Genes & nutrition*, 5(4):309–319, 2010.

Brody Holohan, Woodring E Wright, and Jerry W Shay. Telomeropathies: An emerging spectrum disorder. *The Journal of cell biology*, 205(3):289–299, 2014.

Laura J Horsfall, Greta Rait, Kate Walters, Dallas M Swallow, Stephen P Pereira, Irwin Nazareth, and Irene Petersen. Serum bilirubin and risk of respiratory disease and death. *Jama*, 305(7):691–697, 2011.

Laura J Horsfall, Irwin Nazareth, and Irene Petersen. Cardiovascular events as a function of serum bilirubin levels in a large statin-treated cohort. *Circulation*, pages CIRCULATIONAHA–112, 2012.

Laura J Horsfall, Irwin Nazareth, Stephen P Pereira, and Irene Petersen. Gilbert's syndrome and the risk of death: A population-based cohort study. *Journal of gastroenterology and hepatology*, 28(10):1643–1647, 2013.

J. D. Hunter. Matplotlib: A 2D graphics environment. *Computing In Science & Engineering*, 9(3):90–95, 2007.

Jergen Jacobsen and Rolf Brodersen. Albumin-bilirubin binding mechanism. *Journal of Biological Chemistry*, 258(10):6319–6326, 1983.

Min Kyoung Jeon, Jong-Baeck Lim, and Gyun Min Lee. Development of a serum-free medium for in vitro expansion of human cytotoxic t lymphocytes using a statistical design. *BMC biotechnology*, 10(1):1, 2010.

Chang Hee Jung, Min Jung Lee, Yu Mi Kang, Jenie Yoonoo Hwang, Jung Eun Jang, Jaechan Leem, Joong-Yeol Park, Hong-Kyu Kim, and Woo Je Lee. Higher serum bilirubin level as a protective factor for the development of diabetes in healthy korean men: A 4year retrospective longitudinal study. *Metabolism*, 63(1):87–93, 2014.

Masayuki Kimura, Rivka C Stone, Steven C Hunt, Joan Skurnick, Xiaobin Lu, Xiaojian Cao, Calvin B Harley, and Abraham Aviv. Measurement of telomere length by the southern blot analysis of terminal restriction fragment lengths. *Nature protocols*, 5(9): 1596–1607, 2010.

Patricia A Kruk, Nicholas J Rampino, and Vilhelm A Bohr. DNA damage and repair in telomeres: relation to aging. *Proceedings of the National Academy of Sciences*, 92(1): 258–262, 1995.

Doreen Kuhlow, Simone Florian, Guido von Figura, Sandra Weimer, Nadja Schulz, Klaus J Petzke, Kim Zarse, AF Pfeiffer, K Lenhard Rudolph, and Michael Ristow. Telomerase deficiency impairs glucose metabolism and insulin secretion. *Aging (Albany NY)*, 2(10):650–8, 2010.

Min-Sun Kwak, Donghee Kim, Goh Eun Chung, Seung Joo Kang, Min Jung Park, Yoon Jun Kim, Jung-Hwan Yoon, and Hyo-Suk Lee. Serum bilirubin levels are inversely associated with nonalcoholic fatty liver disease. *Clinical and molecular hepatology*, 18(4):383–390, 2012.

Martin Lacko, Hennie MJ Roelofs, Rene HM Te Morsche, Adri C Voogd, Michel B Oude Ophuis, Wilbert HM Peters, and Johannes J Manni. Genetic polymorphism in the conjugating enzyme UGT1A1 and the risk of head and neck cancer. *International Journal of Cancer*, 127(12):2815–2821, 2010.

Angelo A Lamola and Marie Russo. Fluorescence excitation spectrum of bilirubin in blood: a model for the action spectrum for phototherapy of neonatal jaundice. *Photochemistry and photobiology*, 90(2):294–296, 2014.

Michael Z Levy, Richard C Allsopp, A Bruce Futcher, Carol W Greider, and Calvin B Harley. Telomere end-replication problem and cell aging. *Journal of molecular biology*, 225(4):951–960, 1992.

Carlos López-Otín, Maria A Blasco, Linda Partridge, Manuel Serrano, and Guido Kroemer. The hallmarks of aging. *Cell*, 153(6):1194–1217, 2013.

Lingeng Lu, Chong Zhang, Gongjian Zhu, Melinda Irwin, Harvey Risch, Guido Menato, Marco Mitidieri, Dionyssios Katsaros, and Herbert Yu. Telomerase expression and telomere length in breast cancer and their associations with adjuvant treatment and disease outcome. *Breast Cancer Research*, 13(3):1, 2011.

Hongxia Ma, Ziyuan Zhou, Sheng Wei, Zhensheng Liu, Karen A Pooley, Alison M Dunning, Ulrika Svenson, Göran Roos, H Dean Hosgood III, Min Shen, et al. Shortened telomere length is associated with increased risk of cancer: a meta-analysis. *PloS one*, 6(6):e20466, 2011.

Vanessa Marchesi. Risk factors: Short telomeres: association with cancer survival and risk. *Nature Reviews Clinical Oncology*, 10(5):247–247, 2013.

Paula Martínez and María A Blasco. Telomeric and extra-telomeric roles for telomerase and the telomere-binding proteins. *Nature Reviews Cancer*, 11(3):161–176, 2011.

Antony F McDonagh. Photolysis and photoisomerization of bilirubin in serum specimens exposed to room lighting. *Clinica Chimica Acta*, 393(2):130, 2008.

Allan J McLean and David G Le Couteur. Aging biology and geriatric clinical pharmacology. *Pharmacological reviews*, 56(2):163–184, 2004.

Finny Monickaraj, Sankaramoorthy Aravind, Pichamoorthy Nandhini, Paramasivam Prabu, Chandrakumar Sathishkumar, Viswanathan Mohan, and Muthuswamy Balasubramanyam. Accelerated fat cell aging links oxidative stress and insulin resistance in adipocytes. *Journal of biosciences*, 38(1):113–122, 2013.

Alison J Montpetit, Areej A Alhareeri, Marty Montpetit, Angela R Starkweather, Lynne W Elmore, Kristin Filler, Lathika Mohanraj, Candace W Burton, Victoria S Menzies, Debra E Lyon, et al. Telomere length: a review of methods for measurement. *Nursing research*, 63(4):289, 2014.

Richard G Morgan, Stephen J Ives, Lisa A Lesniewski, Richard M Cawthon, Robert HI Andtbacka, R Dirk Noyes, Russell S Richardson, and Anthony J Donato. Age-related telomere uncapping is associated with cellular senescence and inflammation independent of telomere shortening in human arteries. *American Journal of Physiology-Heart and Circulatory Physiology*, 305(2):H251–H258, 2013.

Meltem Muftuoglu, Heng Kuan Wong, Syed Z Imam, David M Wilson, Vilhelm A Bohr, and Patricia L Opresko. Telomere repeat binding factor 2 interacts with base excision repair proteins and stimulates DNA synthesis by DNA polymeraseβ. *Cancer research*, 66(1):113–124, 2006.

Nathan O'Callaghan, Natalie Baack, Razinah Sharif, and Michael Fenech. A qPCR-based assay to quantify oxidized guanine and other FPG-sensitive base lesions within telomeric DNA. *Biotechniques*, 51(6):403–411, 2011.

Nathan J O'Callaghan and Michael Fenech. A quantitative PCR method for measuring absolute telomere length. *Biological procedures online*, 13(1):1, 2011.

Keizo Ohnaka, Suminori Kono, Toyoshi Inoguchi, Guang Yin, Makiko Morita, Masahiro Adachi, Hisaya Kawate, and Ryoichi Takayanagi. Inverse associations of serum bilirubin with high sensitivity c-reactive protein, glycated hemoglobin, and prevalence of Type 2 diabetes in middle-aged and elderly japanese men and women. *Diabetes research and clinical practice*, 88(1):103–110, 2010.

Patricia L Opresko, Jinshui Fan, Shamika Danzy, David M Wilson, and Vilhelm A Bohr. Oxidative damage in telomeric DNA disrupts recognition by TRF1 and TRF2. *Nucleic acids research*, 33(4):1230–1239, 2005.

Jacintha N O'Sullivan, Jennifer C Finley, Rosa-ana Risques, Wen-Tang Shen, Katherine A Gollahon, and Peter S Rabinovitch. Quantitative fluorescence in situ hybridization (QFISH) of telomere lengths in tissue and cells. *Current Protocols in Cytometry*, pages 12–6, 2005.

Jong-Seok Park, Eunju Nam, Hye-Kyeong Lee, Mi Hee Lim, and Hyun-Woo Rhee. In cellulo mapping of subcellular localized bilirubin. *ACS chemical biology*, 2016.

Fuhua Peng, Xuhui Deng, Yang Yu, Xiaohong Chen, Liping Shen, Xiufeng Zhong, Wei Qiu, Ying Jiang, Jie Zhang, and Xueqiang Hu. Serum bilirubin concentrations and multiple sclerosis. *Journal of Clinical Neuroscience*, 18(10):1355–1359, 2011.

Arlan G Richardson and Eric E Schadt. The role of macromolecular damage in aging and age-related disease. *The Journals of Gerontology Series A: Biological Sciences and Medical Sciences*, 69(Suppl 1):S28–S32, 2014.

Jérôme D Robin, Andrew T Ludlow, Kimberly Batten, Frédérique Magdinier, Guido Stadler, Kathyrin R Wagner, Jerry W Shay, and Woodring E Wright. Telomere position effect: regulation of gene expression with progressive telomere shortening over long distances. *Genes & development*, 28(22):2464–2476, 2014.

Stefan W Ryter and Rex M Tyrrell. The heme synthesis and degradation pathways: role in oxidant sensitivity: heme oxygenase has both pro-and antioxidant properties. *Free Radical Biology and Medicine*, 28(2):289–309, 2000.

Sharon A Savage and Blanche P Alter. Dyskeratosis congenita. *Hematology/oncology clinics of North America*, 23(2):215–231, 2009.

Harvey A Schwertner and Libor Vítek. Gilbert syndrome, UGT1A1* 28 allele, and cardiovascular disease risk: possible protective effects and therapeutic applications of bilirubin. *Atherosclerosis*, 198(1):1–11, 2008.

Harvey A Schwertner, William G Jackson, and Gil Tolan. Association of low serum concentration of bilirubin with increased risk of coronary artery disease. *Clinical chemistry*, 40(1):18–23, 1994.

Jurgen Seppen and Piter Bosma. Bilirubin, the gold within. *Circulation*, pages CIRCULATIONAHA–112, 2012.

Jerry W Shay and Woodring E Wright. Role of telomeres and telomerase in cancer. In *Seminars in cancer biology*, volume 21, pages 349–353. Elsevier, 2011.

Roland Stocker, Yorihiro Yamamoto, Antony F McDonagh, Alexander N Glazer, and Bruce N Ames. Bilirubin is an antioxidant of possible physiological importance. *Science*, 235(4792):1043–1046, 1987.

Irina Strazhesko, Olga Tkacheva, Sergey Boytsov, Dariga Akasheva, Ekaterina Dudinskaya, Vladimir Vygodin, Dmitry Skvortsov, and Peter Nilsson. Association of insulin resistance, arterial stiffness and telomere length in adults free of cardiovascular diseases. *PloS one*, 10(8):e0136676, 2015.

Keiko Suzuki, Pinaki Bose, Rebecca YY Leong-Quong, Donald J Fujita, and Karl Riabowol. Reap: A two minute cell fractionation method. *BMC research notes*, 3(1):294, 2010.

Susan JJ Swiggers, Marianne A Kuijpers, Maartje JM de Cort, H Berna Beverloo, and JMJM Zijlmans. Critically short telomeres in acute myeloid leukemia with loss or gain of parts of chromosomes. *Genes, Chromosomes and Cancer*, 45(3):247–256, 2006.

R Testa, F Olivieri, C Sirolla, L Spazzafumo, MR Rippo, M Marra, AR Bonfigli, A Ceriello, R Antonicelli, C Franceschi, et al. Leukocyte telomere length is associated with complications of Type 2 diabetes mellitus. *Diabetic Medicine*, 28(11):1388–1394, 2011.

Philip Thomas, Nathan J O'Callaghan, and Michael Fenech. Telomere length in white blood cells, buccal cells and brain tissue and its variation with ageing and alzheimer's disease. *Mechanisms of ageing and development*, 129(4):183–190, 2008.

Anela Tosevska, Christine Moelzer, Marlies Wallner, Milan Janosec, Ursula Schwarz, Carina Kern, Rodrig Marculescu, Daniel Doberer, Wolfram Weckwerth, and Karl-Heinz Wagner. Longer telomeres in chronic, moderate, unconjugated hyperbilirubinaemia: insights from a human study on Gilbert's syndrome. *Scientific reports*, 6, 2016.

Stefan Van Der Walt, S Chris Colbert, and Gael Varoquaux. The numpy array: a structure for efficient numerical computation. *Computing in Science & Engineering*, 13(2): 22–30, 2011.

Ramiro E Verdun and Jan Karlseder. Replication and protection of telomeres. *Nature*, 447(7147):924–931, 2007.

Libor Vitek, Milan Jirsa, Marie Brodanova, Milan Kalab, Zdenek Marecek, Vilem Danzig, Ladislav Novotny, and Petr Kotal. Gilbert syndrome and ischemic heart disease: a protective effect of elevated bilirubin levels. *Atherosclerosis*, 160(2):449–456, 2002.

Libor Vitek, Michaela Novotna, Martin Lenicek, Ladislav Novotny, Jitka Eberova, Jan Petrasek, and Milan Jirsa. Serum bilirubin levels and UGT1A1 promoter variations in patients with schizophrenia. *Psychiatry research*, 178(2):449–450, 2010.

Karl-Heinz Wagner, Marlies Wallner, Christine Molzer, Silvia Gazzin, Andrew Cameron Bulmer, Claudio Tiribelli, and Libor Vitek. Looking to the horizon: the role of bilirubin in the development and prevention of age-related chronic diseases. *Clinical Science*, 129(1):1–25, 2015.

Marlies Wallner, Andrew C Bulmer, Christine Mölzer, Elisabeth Müllner, Rodrig Marculescu, Daniel Doberer, Michael Wolzt, Oswald F Wagner, and Karl-Heinz Wagner. Haem catabolism: a novel modulator of inflammation in Gilbert's syndrome. *European journal of clinical investigation*, 43(9):912–919, 2013.

Kyle M Walsh, Veryan Codd, Ivan V Smirnov, Terri Rice, Paul A Decker, Helen M Hansen, Thomas Kollmeyer, Matthew L Kosel, Annette M Molinaro, Lucie S McCoy, et al. Variants near tert and terc influencing telomere length are associated with high-grade glioma risk. *Nature genetics*, 46(7):731–735, 2014.

Zhilong Wang, David B Rhee, Jian Lu, Christina T Bohr, Fang Zhou, Haritha Vallabhaneni, Nadja C de Souza-Pinto, and Yie Liu. Characterization of oxidative guanine damage and repair in mammalian telomeres. *PLoS Genet*, 6(5):e1000951, 2010.

Jon F Watchko and Claudio Tiribelli. Bilirubin-induced neurologic damage-mechanisms and management approaches. *New England Journal of Medicine*, 369 (21):2021–2030, 2013.

Nan-ping Weng. Regulation of telomerase expression in human lymphocytes. In *Springer seminars in immunopathology*, volume 24, pages 23–33. Springer, 2002.

Peter Willeit, Julia Raschenberger, Emma E Heydon, Sotirios Tsimikas, Margot Haun, Agnes Mayr, Siegfried Weger, Joseph L Witztum, Adam S Butterworth, Johann Willeit, et al. Leucocyte telomere length and risk of Type 2 diabetes mellitus: new prospective cohort study and literature-based meta-analysis. *PloS one*, 9(11):e112483, 2014.

Chenan Zhang, Jennifer A Doherty, Stephen Burgess, Rayjean J Hung, Sara Lindström, Peter Kraft, Jian Gong, Christopher I Amos, Thomas A Sellers, Alvaro NA Monteiro, et al. Genetic determinants of telomere length and risk of common cancers: a mendelian randomization study. *Human molecular genetics*, 24(18):5356–5366, 2015.

Jinying Zhao, Yun Zhu, Jue Lin, Tet Matsuguchi, Elizabeth Blackburn, Ying Zhang, Shelley A Cole, Lyle G Best, Elisa T Lee, and Barbara V Howard. Short leukocyte telomere length predicts risk of diabetes in american indians: the strong heart family study. *Diabetes*, 63(1):354–362, 2014.

COLOPHON

This document was typeset using the typographical look-and-feel `classicthesis` developed by André Miede. The style was inspired by Robert Bringhurst's seminal book on typography "*The Elements of Typographic Style*". `classicthesis` is available for both LaTeX and LyX:

http://code.google.com/p/classicthesis/

Happy users of `classicthesis` usually send a real postcard to the author, a collection of postcards received so far is featured here:

http://postcards.miede.de/

Final Version as of July 19, 2016 (`classicthesis` version 0.70).